Pathways for kidney triglyceride accumulation

Diego A. Scerbo

Submitted in partial fulfillment of the requirements for the degree of Doctor of Philosophy under the Executive Committee of the Graduate School of Arts and Sciences

COLUMBIA UNIVERSITY

2018

Kidney triglyceride accumulation in the fasted mouse is dependent upon serum free fatty acids and Krüppel-Like Factor 5 role in diabetic inflammation

Diego A. Scerbo

Abstract

Lipid accumulation is a pathological feature of every type of kidney injury. However, despite this striking histological feature, physiological accumulation of lipids in the kidney is poorly understood. We studied whether the accumulation of lipids in the fasted kidney is derived from lipoproteins or non-esterified fatty acids (NEFAs). Increasing circulating NEFAs using a beta adrenergic receptor agonist caused a 15-fold greater accumulation of lipid in the kidney, while mice with reduced NEFAs due to adipose tissue deficiency of adipose triglyceride lipase had reduced renal triglycerides. Fasting-induced kidney lipid accumulation was not affected by inhibition of lipoprotein lipase (LpL) with poloxamer 407 or by use of mice with induced genetic LpL deletion. Despite the increase in CD36 expression with fasting, genetic loss of CD36 did not alter fatty acid uptake or triglyceride accumulation. Our data demonstrate that fasting-induced triglyceride accumulation in the kidney correlates with the plasma concentrations of NEFAs but is not due to uptake of lipoprotein lipids and does not involve the fatty acid transporter CD36.

A second project was initiated to assess how diabetes causes increased systemic inflammation. Calgranulins S100A8 and S100A9 circulating levels are increased during diabetes and might instigate a sterile inflammatory response in the innate immune system. To determine whether krüppel-like factor 5 (KLF5) regulates S100A8 and S100A9 during hyperglycemia; we generated myeloid-specific KLF5 knockout mice (MKK) and found these mice had no change in circulating monocytes and neutrophils. We isolated neutrophils from these mice and found that S100A8 and S100A9 expression was not changed. We found similar null results when these mice were made diabetic. We conclude that this line of myeloid-deficient KLF5 knockout mice

do not have changes in S100A8 or S100A9 expression or in the numbers of circulating white cells.

Table of Contents

List of Figures

List of Tables

Abbreviations

Apo	apolipoprotein
ATGL	adipose tissue triglyceride lipase
ATRA	all-*trans* retinoic acid
BM	bone marrow
CD36	cluster of differentiation 36
CE	cholesteryl ester
CKD	chronic kidney disease
CM	chylomicron
CMP	common myeloid progenitor
DAMP	damage associated molecular pattern
Dnep	diabetic nephropathy
DNL	*de novo* lipogenesis
ESRD	end-stage renal disease
FAO	fatty acid oxidation
FATP	Fatty acid transport protein
GFR	glomerular filtration rate
GMP	granulocyte-macrophage progenitor
HDL	high-density lipoprotein
HSPC	hematopoietic stem/progenitor cell
KLF	krüppel-like factor
LCFA	long-chain fatty acid
LD	lipid droplet
LDL	low-density lipoprotein
LpL	Lipoprotein Lipase
MKK	myeloid-specific *Klf5* knockout
MTP	microsomal triglyceride transfer protein
NEFA	non-esterified fatty acid
NepS	nephrotic syndrome
P407	poloxamer 407
PPAR	peroxisome proliferator-activated receptor
RAGE	receptor for advanced glycosylation end-products
STZ	streptozotocin
T1D	type 1 diabetes
T2D	type 2 diabetes
TG	triglyceride
TLR	toll-like receptor
VLDL	very low-density lipoprotein

Chapter 1: Lipid Metabolism

1.1 Introduction

Fatty acids are crucial molecules necessary for nearly all cell functions including membrane structure, intracellular signaling, and energy production. A fatty acid is a carboxylic acid bound to an aliphatic backbone. The degree of saturation and length of the aliphatic backbone can alter the function of fatty acids. Hydrophobic by nature, fatty acids must be bound to carrier molecules in order to be transported in the blood stream or in the cytoplasm of cells. Once transported within the cell, fatty acids take a number of paths. To name a few, they can be shuttled to the mitochondria to be used to generate ATP, act as cofactors for transcription, or become esterified to glycerol and stored in lipid droplets (LDs).

1.2 Fatty Acid Transport

Fatty acids circulate in the blood stream either bound to albumin or esterified into triglyceride (TG) and contained in lipoproteins. Serum albumin is a globular protein produced by the liver and maintains oncotic pressure. Albumin binds both hydrophilic molecules such as cations and hydrophobic molecules such as fatty acids, steroid hormones, and hemin (1).

Fatty acids also circulate in the blood while esterified to glycerol; three fatty acids are included in one TG molecule. Very low-density lipoproteins (VLDL) and chylomicrons (CM) are TG-rich lipoproteins synthesized in hepatocytes and enterocytes, respectively. Microsomal TG transfer protein (MTP) is essential for the formation of these lipoprotein particles (2). MTP binds to either ApoB48 (CM) or ApoB100 (VLDL) and transfers TGs to the nascent particle. Further modification to the nascent particle occurs *via* the additions of apolipoprotein E (ApoE), apolipoprotein CI and cholesteryl esters (CE). VLDL and CM gain apolipoprotein C-II (apoC-II)

in the circulation as they mature. ApoC-II is a required co-factor for activation of lipoprotein lipase (LpL) (3). LpL is synthesized as a monomer by parenchymal cells and transported to the surface of endothelial cells by glycosylphosphatidylinositol-anchored high-density lipoprotein-binding protein-1 (GPIHBP-1) (4). LpL is anchored to the endothelial surface by both GPIHBP-1 and heparan sulfate proteoglycans (5) (6). LpL is critical for TG clearance in the plasma. Familial LpL deficiency presents with severe hypertriglyceridemia causing lipemic plasma (7). LpL is regulated post-transcriptionally in many tissues. LpL is reported to be inhibited by apolipoprotein C-III (ApoC-III) (8), which can be found attached to TG-rich lipoproteins (9). Though inhibition of ApoC-III clears TG from the plasma, it may not be through LpL. Gordts *et al.* demonstrate Apo-CIII inhibits low-density lipoprotein receptor (LDLR) and LDL-like protein-1 (LRP-1) clearance of lipoproteins in the liver. In mice lacking both LDLR and LRP-1, antisense oligonucleotides targeting ApoC-III did not lower TG in the plasma (10). In order to function properly, LpL must form a homodimer in a head-to-tail fashion (11). Angiopoietin-like proteins (ANGPTL)-3,4, and 8 inhibit LpL, presumably by breaking the homodimer, which LpL requires to function (12) and by promoting intracellular degradation of LpL in the ER (13).

VLDL and CM particles are rid of their TG in the plasma by LpL and cholesterol ester transfer protein (CETP). CETP is a circulating enzyme that swaps TG for CE with high-density lipoproteins (HDL) and LDL. As VLDL loses TG and gains CE it turns into an intermediate density lipoprotein (IDL) and LDL. LDL is cleared from the circulation by binding to LDLR on hepatocytes *via* ApoB contained within the particle (14). The LDLR is regulated at the transcriptional level by sterol-regulatory element binding protein-2 (SREBP 2) (15) (16). A circulating protein called proprotein convertase subtilism/kexin type 9 (PCSK9) that is secreted by the small intestine and liver, binds to LDLR and initiates its intracellular degradation of the

protein (17). Although the proteins and lipids of all lipoproteins are susceptible to oxidative damage, oxidatively modified LDL (ox-LDL) is of particular interest because of its atherogenic properties (18). However, "ox-LDL" is a broad generalization of a heterogeneous population of particles, of which may have dissimilar physiologic properties (19).

After hydrolysis, fatty acids are freed from the lipoprotein and must be transported into the cell. This process may or may not require the assistance of a surface membrane receptor. In cases where it does not, fatty acids can diffuse through the membrane to the cytoplasm in a phenomenon called "flip-flop" (20). This may be the case for when the concentration of fatty acids is very high. When fatty acid concentration is low, a transporter is necessary. Several proteins have been reported to transport fatty acids across the cell surface including cluster of differentiation (CD) 36 (21) (22), plasma membrane fatty acid binding protein (FABPpm) (23), and the family of fatty acid binding proteins/ solute carrier family 27 A (FATP/SLC27A) (24). CD36 is a transmembrane scavenger receptor which binds a number of factors including ox-LDL (25), thrombospondin (26), collagen types I and IV (27) and long-chain fatty acids (LCFA) (28). The role of CD36 as a fatty acid transporter in a number of tissues such as heart, skeletal muscle and adipose tissue is highlighted in total body CD36 knockout studies (29) (30). CD36 null mice have a two-thirds decrease in fatty acid uptake and utilization in these tissues. Conversly, mice that overexpress CD36 in their skeletal muscle have increased rates of fatty acid oxidation during contractions (31). FATPs are a family of LCFAs transporters consisting of six other isoforms. FATPs share a large degree of sequence homology to long-chain acyl CoA synthetase 1 (ACSL1) (32). FATP1 and FATP4 have acyl-CoA synthetase as well as transport activity. (33) (34). FABPpm (also referred to as liver or L-FABP) was reported to transport LCFA to the nucleus when overexpressed in L-cells (35), as well as transferring fatty acyl CoAs to nuclear

transcription factors (36). This family of transporters also traffics fatty acids within the cytoplasm of the cell (35).

1.3 Fatty Acid Oxidation

Fatty acids enter the cell and are trapped by binding to coenzyme A (CoA). ACSLs form a thioester bond between a fatty acid and a CoA molecule using ATP to create fatty acyl-CoA. Once trapped in the cytoplasm fatty acyl-CoAs can be processed in downstream reactions. Fatty acyl-CoAs enter the mitochondria through the carnitine shuttle. This process requires the addition of carnitine to fatty acyl-CoAs by carnitine palmitoyltransferase I (CPT1), located on the mitochondrial outer membrane. Indeed, patients with CPT1 deficiency have an increased carnitine:palmitoylcarnitine ratio in the serum and low circulating ketones (37). Acyl-carnitine is transferred across the inner membrane of the mitochondria *via* a translocase called carnitine-acylcarnitine translocase/solute carrier family 25 member 20 (CACT/SLC25A20). Once across, CPTII, located on the inner membrane catalyzes the reverse reaction of CPT1, by reattaching CoA in place of carnitine to again form fatty acyl-CoA. In the mitochondria, β-oxidation cleaves fatty acyl-CoA to acetyl-CoAs that then enter the citric acid cycle/Krebs cycle. The citric acid cycle generates reducing agents, NADH and $FADH_2$, which delivers high-energy electrons to the electron transport chain. Intermediates of the citric acid cycle are used in other cellular processes as well. For example, α-ketoglutarate is generated from isocitrate oxidation and is the substrate for the synthesis of non-essential amino acids. Alanine transaminase converts α-ketoglutarate and alanine to glutamate. Glutamate is then converted to glutamine. Glutamine itself is a component and precursor for almost every other macromolecule. The electron transport chain uses the energy of electrons generated from NADH and $FADH_2$ to transport protons into the

intermembrane space of the mitochondria. These protons then flow down their gradient *via* an ATP synthase to generate ATP by coupling inorganic phosphate to ADP.

1.4 *De Novo* Synthesis of fatty acids

Fatty acids can be synthesized from carbohydrate-derived acetyl-CoA, in what is known as *de novo* lipogenesis (DNL). Glucose and fructose are highly lipogenic substrates and provide the two-carbon substrate needed for DNL (38). This process begins by the formation of malonyl-CoA by acetyl-CoA carboxylase (ACC), a multifunctional rate-limiting enzyme (39). Fatty acid synthetase (FAS) is a network of enzymes that elongates fatty acids until they reach 16-18 carbons in length (40). DNL is regulated transcriptionally by SREBP1-c and carbohydrate response element binding protein (ChREBP). SREBP1-c is, in turn, transcriptionally regulated by the liver X receptor/retinoid X receptor (LXR/RXR) and insulin (41). SREBPs exist as a precursor protein in the ER. This protein is cleaved by SREBP cleaving-activating protein, when sterols are present. Once cleaved, SREBP translocates to the Golgi apparatus and undergoes another round or proteolytic cleavages before translocating to the nucleus. ChREBP is activated by an influx of glucose into the cell (42) and binds to carbohydrate response element, upstream of FAS and ACC promoters (43) (44). After synthesis, palmitate can undergo a number of modifications, most notably elongation and desaturation. Elongation occurs in similar fashion to DNL, however it occurs in the membranes of the endoplasmic reticulum (ER) and produces stearic acid. Monounsaturated fatty acids are produced by stearoyl-CoA desaturase (SCD), which introduces a double bond between C-9 and C-10 of stearic acid to generate oleic acid.

De novo synthesized fatty acids (as well as those obtained extracellularly) are stored by being esterified with a glycerol molecule forming monoacyl-glycerols, diacylglycerols, and TGs that are stored in LDs. In most tissues, save for enterocytes, TG synthesis begins with glycerol-3-

phosphate gaining a fatty acyl-CoA to form lysophosphatidic acid (LPA), catalyzed by glycerol-3-phosphate acyltransferase. LPA is a potent signaling molecule, notably for its mitogenic effects on cells (45). The enzyme 1-acylglycerol-3phosphate O-acyltransferase adds another fatty acyl-CoA to LPA to form phosphatidic acid (PA), which is a precursor to many phospholipid species as well as diacylglycerol (DAG). DAG is synthesized from PA following removal of a phosphate by phosphatidic acid phosphatase. DAG is a potent intracellular second massager, activating protein kinase C (PKC) (46). DAG is converted to TG by the addition of the final fatty acyl-CoA by diacylglycerol acyl transferase 1 and 2 (DGAT1 and DGAT2). Phospholipids serve as an additional building block for TG synthesis. In enterocytes, monoacylglycerol is derived from hydrolysis of dietary TG by pancreatic lipase and is taken up by enterocytes with the aid of bile salts (47). Thus, enterocytes bypass several steps in TG synthesis by using monoacylglycerol as an initial molecule. DAG is synthesized from monoacylglycerol *via* addition of a fatty acyl-CoA by monoacylglycerol acyltransferase, which is then converted to TG by DGAT 1 and 2. Synthesized TG in enterocytes are then packaged into CM and released into the circulation.

TG and CE are stored in LDs within the cells. LDs are not inert storage vesicles, but an active participant cellular metabolism. Proteins are studded on the surface of LDs, most notable are perilipins (PLINs) (48). Phosphorylation of the perilipin proteins allows intracellular lipases, such as hormone sensitive lipase (HSL) and adipose triglyceride lipase (ATGL) to access TG in LDs for hydrolysis. As the name suggests, HSL is activated by hormones such as catecholamines and adrenocorticotropic hormone and is inhibited by insulin (49). Catecholamines cause a downstream signaling cascade leading to phosphorylation of HSL by protein kinase A (PKA) ATGL is transcriptionally downregulated by insulin and is transactivated by peroxisome proliferator-activated receptor (PPAR) γ in adipocytes (50).

1.5 Regulation of fatty acid metabolism by PPARs

PPARs are members of nuclear receptors superfamily. They are transcription factors that regulate many genes involved in lipid metabolism (51). Conversely, PPARs themselves require lipids and lipid derivatives to active gene expression (52). While PPARs play a role in many other cellular functions, their role in lipid metabolism will be discussed here. There are three PPARs; PPARα, PPARβ/δ, and PPARγ (of which there are three alternative splicing variants, γ1, γ2, and γ3). PPARs heterodimerize with RXR and bind PPAR response elements on DNA promoters of numerous genes (52).

PPARα is highly expressed in oxidative tissues such the heart, brown adipose tissue, liver and kidney (53). PPARα controls the transcription of many genes required for FAO including *Cpt1a* and *Acox* (12) as well as genes related to the transport of fatty acids such as *Cd36* and *Lpl*. (54,55). The role of PPARα has been extensively characterized in the liver and the heart (56). *Ppara* $^{-/-}$ mice have increased TG, long chain acyl-carnitines, and non-esterified fatty acids (NEFAs) in their livers, as well as decreased glycogen and free carnitine (12). Due to its role in fatty acid catabolism, PPARα is an attractive drug target for dyslipidemia. Fibrates constitute a class of drugs that exert their function by activating PPARα. Fibrates raise plasma HDL and lower plasma VLDL in humans (57).

PPARβ/δ similarly controls FAO in peripheral tissues such as skeletal muscle and adipose tissue (58). Over expression of PPARβ/δ in skeletal muscle caused an increase in fatty acid utilization and more type-1 muscle fibers (59). Cardiomyocyte specific deletion of PPARβ/δ leads to impaired ability of the heart to oxidize palmitate (60).

PPARγ is essential for adipocyte differentiation as well as lipid storage and lipolysis (61) in these cells (62). As a result, mice lacking PPARγ in adipocytes are protected from diet-

induced obesity and insulin resistance (63). PPARγ controls the transcription of perilipins (64), which are critical for the structure and function of LDs. PPARγ also drives the transcription of glycerol kinase (65), a key enzyme in the esterification process of fatty acids to a glycerol backbone and ATGL (61). Thiazolidinediones are PPARγ agonist compounds used as anti-diabetic drugs (66). Due to PPARγ role of increasing storage of fatty acids in adipose tissue, diabetic patients have reduced serum TG and increased glucose utilization by tissues−lowering serum glucose (67). Pan-PPAR agonists, those that activate all or more multiple PPARs, have been explored for therapeutic benefit. Bezafibrate, a pan agonist, ameliorates cardiomyopathy in a mouse model of Barth syndrome (68). Bavachinin lowers glucose without inducing weight gain or liver toxicity in obese mice (69). Bavachinin also worked synergistically with thiazolidinediones and fibrates to lower glucose and plasma TG in *db/db* mice (69).

1.6 Lipotoxicity

Lipotoxicity occurs when non-adipose tissues are unable to properly store lipids, causing buildup of toxic lipid species. (70) These lipid metabolites include NEFAs, free cholesterol, ceramides, and DAGs. Lipotoxicity is liable for a number of diseases and organ dysfunction such as non-alcoholic fatty liver disease, insulin resistance in muscle, cardiac dysfunction, and kidney dysfunction (71-74).

NEFAs, particularly saturated fatty acids, are damaging to cells (75). Specifically, cells incubated with saturated fatty acids undergo apoptotic death (76). On the other hand, cells incubated with unsaturated fatty acids accumulate TG without decreased viability. SCD 1 is the enzyme that converts saturated fatty acids to monounsaturated fatty acids. *Scd-1*$^{-/-}$ mice put on a methionine-choline deficient diet accumulate less TG in their livers, but are more prone to liver injury (77), likely due to an increase in intracellular saturated fatty acids. The mechanisms by

which saturated NEFAs induce apoptosis are not entirely clear. ER-stress is induced in β-cells incubated with saturated fatty acids (78). It is worth noting that unsaturated fatty acids have also been shown to be toxic. Oleic acid is cytotoxic to cardiomyoctes when lipolysis from lipid droplets is stimulated in these cells (79). NEFAs may also cause an upregulation of death receptors such as Fas and TRAIL receptor 5 (80) (81). NEFAs are also susceptible to lipid peroxidation by free radicals. As all membranes of cells are made of fatty acids, lipid oxidation products can severely complicate the integrity of cells. Glutathione peroxidase 4 reduces lipid hydroperoxides to alcohols, and its absence is embryonically lethal in mice (82). While NEFAs are toxic to cells, these molecules are also building blocks for potent signaling lipids. NEFAs can cause an increase in cellular lipid intermediates such as ceramides and DAGs, which cause cellular dysfunction at high intracellular concentrations (83) (84) (85).

Ceramides are composed of a sphingosine and a fatty acid and predominantly constitute a component of the cellular membrane. Ceramides can be made *de novo* in the ER from palmitate and serine as the preliminary building blocks. Sphingosine is synthesized from palmitoyl CoA and a serine amino acid by serine palmitoyl transferase (SPT) (86). Ceramide synthase then combines sphingosine to a fatty acyl CoA to create a ceramide molecule. However, a majority of cellular ceramides come from the salvage pathway (87). The salvage pathway utilizes sphingosine released from the lysosome, which is then trapped by ceramide synthase (87). Targeting of the *de novo* pathway of ceramide synthesis has reversed lipotoxicity in tissues. In a dilated lipotoxic cardiomyopathy model, treatment with the SPT inhibitor myriocin, improved systolic function and prolonged survival rates (88). The exact mechanism by which ceramides induce apoptosis is not clear. Ceramides may induce apoptosis by increasing cytochrome c release from the mitochondria (89). Additionally, mitochondrial dysfunction and impaired fatty

acid oxidation (FAO) only exacerbate lipid accumulation and lipotoxicity. Ceramides also cause insulin resistance by interfering with JAK/STAT signaling—increasing suppressor of cytokine signaling 3 in adipose tissue (90) (91).

DAG is generated as a metabolite of TG synthesis and from cleavage of phosphatidylinositol 4,5 bisphosphate, along with inositol triphosphate (IP3). IP3 opens Ca^{2+} channels on the mitochondrial membrane and ER and DAG activates PKC. Upon Ca^{2+} binding PKC translocates to the membrane and phosphorylates insulin receptor substrate 1, thereby inactivating it (92) and preventing GLUT4 translocation to the cell membrane (93). Therefore, a high amount of intracellular DAG can result in systemic insulin resistance. One method to increase intracellular DAG levels is *via* deletion of DGATs. Though *Dgat1*$^{-/-}$ animals are healthy and resistant to obesity, heart-specific *Dgat1* null mice have increased DAG in their hearts and severe heart failure (94). This cardiac phenotype could be treated with glucagon-like peptide-1 (GLP-1) agonists, which reduced cardiomyocyte DAG and improved cardiac function (94). The extent to which DAG contributes to insulin resistance in humans is not clear. It may be that certain DAG species are more prone to causing insulin resistance than others. DAGs composed of saturated fatty acids or in a 1,2-DAG conformation are more prone to cause insulin resistance than other subspecies (95) (96). There are two isoforms DGAT, 1 and 2, and research suggests DGAT1 preferentially adds fatty acyl molecules in the 1,2-DAG position (97).

Chapter 2: Physiology, Metabolism, and Disease in the Kidney

2.1 Kidney Anatomy & Physiology

The kidney is a bean-shaped organ, which controls numerous homeostatic biological functions, including electrolyte and fluid balance, regulating blood pH, and blood pressure (98) The kidney is also an endocrine organ producing calcitriol (vitamin D3), erythropoietin, and renin (99). While comprising only 3% of one's total mass, the kidney is richly supplied with blood, receiving up to a fifth of the cardiac output. This is essential for its principal function of filtering blood. Much of what is filtered is reabsorbed and what is not is released as waste. The efficiency of the filtration apparatus in the kidney is called the glomerular filtration rate (GFR). The functional unit of this filtration system is called the nephron and each nephron is segmented into specialized areas.

Blood enters the kidney through the afferent arteriole and travels through the glomerulus before exiting and re-entering the circulation through the efferent arteriole. The glomerulus (Figure 1) is found within Bowman's capsule, a sac that collects glomerular filtrate. The glomerulus is a network of cell types that creates a sieving mechanism in the kidney. The endothelial cells are perforated with fenestrae. These fenestrae are lined by a negatively charged glycocalyx, which repel large, polar molecules. Enfolded around the endothelial cells are podocytes. These cells have long foot processes that inter-digitate, forming filtration slits. Mesangial cells are contractile intra-and extra-glomerular cells, which contract and change the shape of the glomerulus—adjusting the rate at which the glomerulus filters. GFR is the volume of fluid that enters Bowman's capsule per unit time. The hydrostatic pressure of the afferent and efferent arterioles, as well as the other cell types mentioned, are crucial in determining the GFR (98). The pathophysiology of glomerular injury is characterized by sclerosis of the thin

capillaries, proliferation of mesangial cells, and podocyte effacement of endothelial cells (100). The compromised filtration apparatus causes a dramatic drop in GFR, which manifests clinically as proteinuria. A GFR of 60 mL/min per 1·73 m^2 for more than three months is considered chronic kidney injury (CKD) (101).

After the filtrate is drained into Bowman's capsule, it enters the proximal tubule (Figure 2). The cells of the proximal tubule are polarized epithelial cells with a luminal brush boarder. The proximal tubule epithelial cells reabsorb a majority of what is filtered through by the glomerulus such as Na^+, K^+, PO_4^{3+}, citrate, amino acids and glucose. Nearly all the glucose filtered through the glomerulus is taken up by the proximal tubules via he sodium/glucose co-transporter 2 (SGLT2). Using secondary active transport, SGLT2 transports Na+ and glucose into the cell. A Na^+/K^+ pump drives Na^+ out of the cell and glucose leaves the cell and enters the bloodstream via the glucose transporter GLUT2. SGLT2 is a pharmacological target to lower plasma glucose for diabetic patients (102). By inhibiting this transporter, glucose is not reabsorbed but leaked out in the urine, thus lowering plasma glucose. The filtrate proceeds to the descending loop of Henle. The loop of Henle creates a concentration gradient in the medulla. This gradient becomes more permeable to water and the filtrate becomes more concentrated the further it descends downward—aiding in the reabsorption of water. The ascending loop of Henle is not permeable to water but permeable to ions. This allows for the reabsorption of ions from the filtrate in order to diluting it. The filtrate moves to the distal tubules, a portion of which is a specialized Na^+ sensing cell called the macula densa. These cells communicate to local smooth muscle cells, which release renin and also control vasodilation or constriction of the afferent arteriole. The distal tubules participate in calcium homeostasis by reabsorbing Ca^{2+} in the presence of parathyroid hormone. Finally, the filtrate moves down the collecting ducts. The

collecting duct connects the nephron to the ureter and is responsive to aldosterone and vasopressin which allows for the regulation of total body blood pressure (103). Like the loop of Henle, the collecting ducts descend the medulla and osmotic gradient, which allows for the reabsorption of water from the renal filtrate (104).

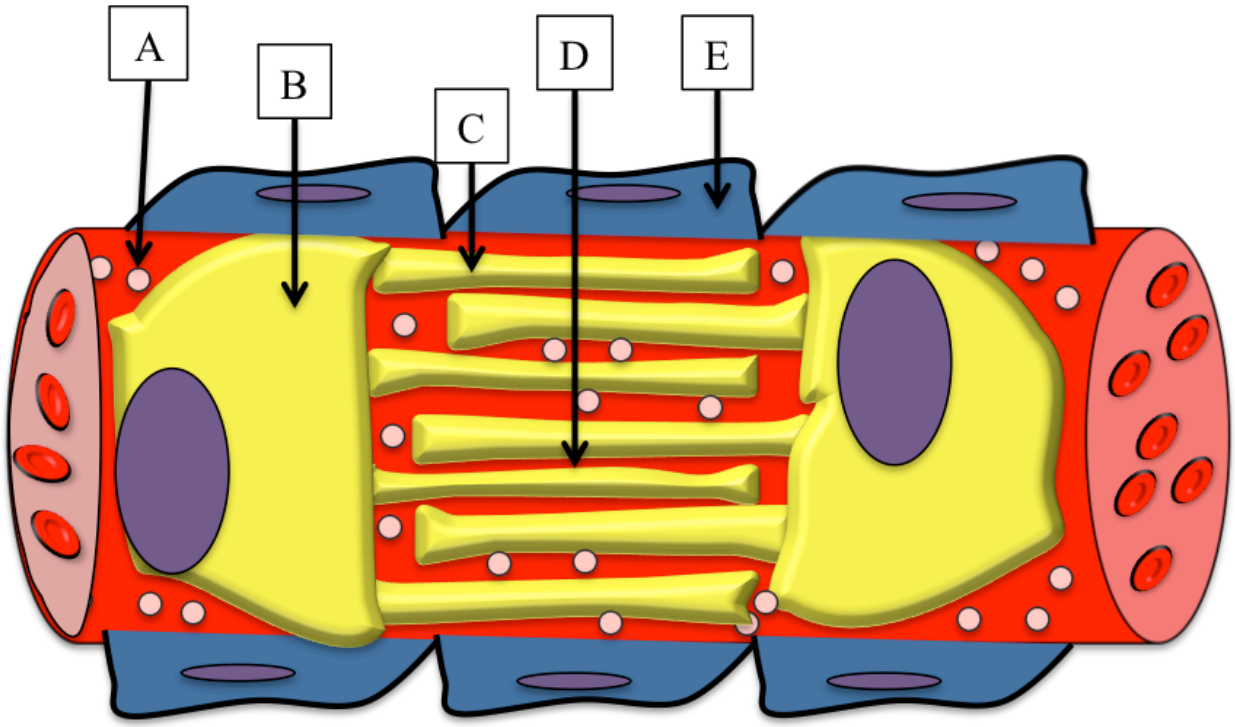

Figure 1. Sieving mechanism of the glomerulus is an intricate network of multiple cell types

The glomerulus is a network of cell types that creates a sieving mechanism in the kidney. These include fenestrated endothelial cells lined with a glycocalyx and podocytes that exclude large polar molecules from passing through the filtrate. Weaved within the glomerular capillaries are mesangial cells which contract to control the flow of filtrate in glomeruli.(A) fenestrae, (B) podocytes, (C) podocyte foot processes, (D) filtration slits (E) mesangial cells.

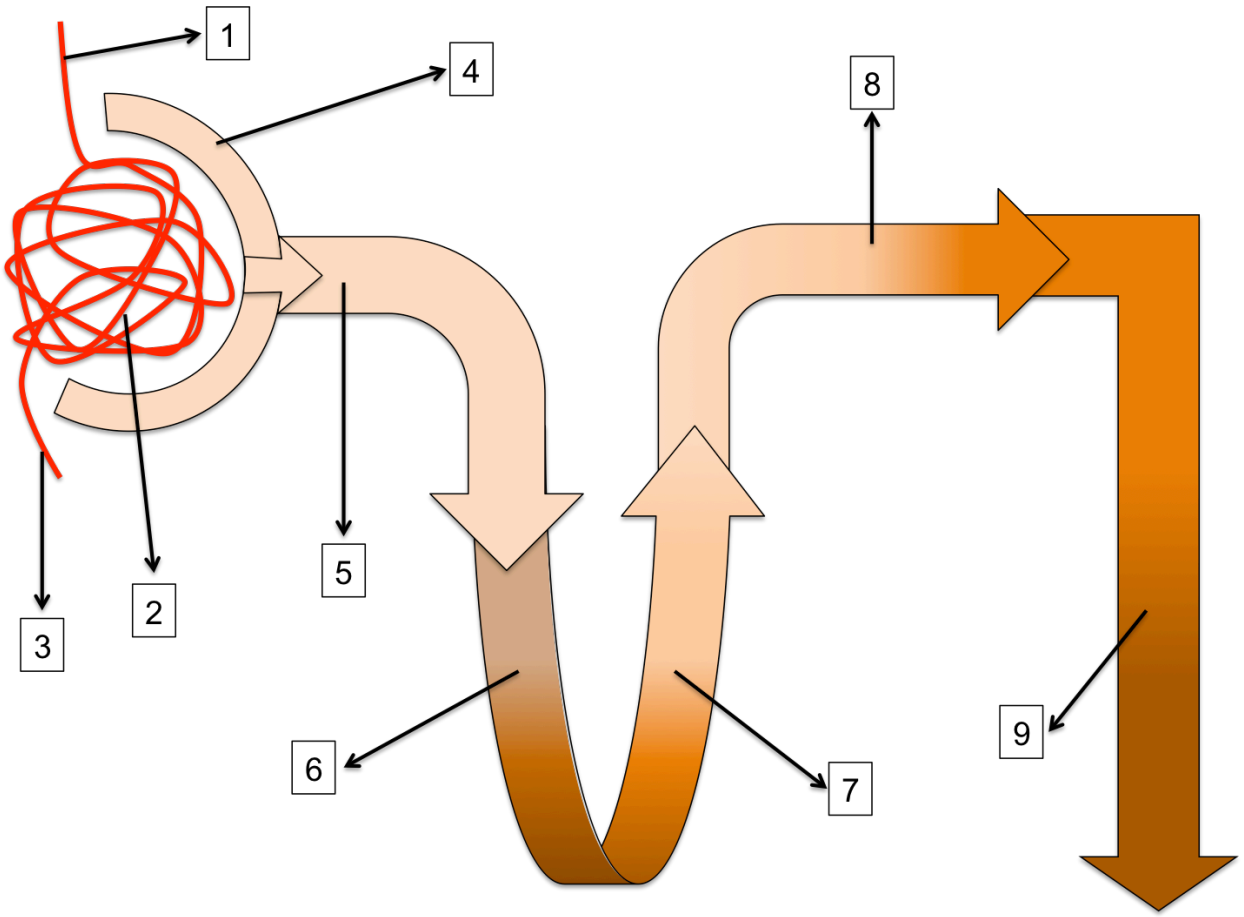

Figure 2. Segments and filtrate concentration along the nephron

The nephron is the functional unit of the kidney. Each segment contains specialized cell-types for the reabsorption of water and nutrients as well as the production of hormones. Arrows indicate flow of filtrate; while the gradient conveys concentration of the filtrate (darker color indicates higher concentration of ions). (1) afferent arteriole, (2) glomerulus, (3) efferent arteriole, (4) Bowman's Capsule, (5) proximal tubules, (6) descending loop of Henle, (7) ascending loop of Henle, (8) distal tubules, (9) collecting ducts.

2.2 Diabetic Kidney Disease

Nephrotic syndrome (NepS) describes a condition in which the kidney can no longer properly filter blood due to damage to the glomerulus (105). NepS is defined as when one presents with proteinuria, hypoalbuminurea/edema, and hyperlipidemia (106). NepS is either due to primary causes, such as genetic glomerulopathies and injuries that damage the glomerulus or secondary causes that result in renal injury. Secondary causes are brought on by systemic insults such as hepatitis B/C, HIV or lupus. NepS progresses to CKD and eventually end-stage renal disease (ESRD), which requires dialysis or kidney transplant (Figure 3). Currently, diabetes mellitus (DM) is the most common cause of NepS and ESRD in developed countries and is known as diabetic nephropathy (DNep) (107), for which there is currently no cure. About one fifth of patients with DM go on to develop DNep (108), but it is not known why some DM patients go on to develop DNep and other do not. Nonetheless, current therapies aim to slow the progress of DNep to ESRD in patients. Patients with DNep suffer from a trifecta of hypertension, hyperglycemia, and hyperlipidemia.

Currently, the most effective drugs for DNep block the renin-angiotensin system, such as angiotensin-converting enzyme inhibitors (ACEi) or angiotensin II type 1-receptor blockers (ARBs). These drugs slow the rate of GFR decline in rodents and humans (109). Clinical trials have shown that ACEi is renoprotective if patients with diabetes take them before the onset of renal decline. The Bergamo Nephrologic Diabetes Complications Trial (BENEDICT) showed that type 2 diabetes (T2D) patients with hypertension but without proteinuria given ACEi halved their risk of albuminuria after four years compared to non-ACEi therapy (110).

Microvascular complications of DNep are facilitated by chronic hyperglycemia. Patients with DM and DNep are advised to properly manage their glucose levels. Hyperglycemia has

been shown to cause sclerosis of the glomerulus, activation of the renin-angiotensin-aldosterone system in the kidney, and effacement of podocytes (111). Thus glycemic control of patients with DM has been explored as a therapeutic intervention aiming to slow or prevent ESRD. Several clinical trials show a significant reduction in albuminuria in patients with DM who were on aggressive glycemic control regiments (112). However, there was no evidence that intensive glucose management reduced risk for ESRD (111). Still though, the Kidney Disease Outcomes Quality Initiative recommends in their 2012 guidelines an HbA1C ≤7% in patients with DNep (113).

A relatively new class of glucose lowering drugs has been developed. This class of drugs inhibits SGLT2, which is expressed on the luminal surface of proximal tubule epithelial cells. The proximal tubule reabsorbs 180g glucose/day through SGLT2. Drugs that inhibit SGLT2 allow glucose to pass through the urine. Patients with T2D that were given SGLT2 inhibitors had a reduction in albuminuria and a slower decline of GFR (111). SGLT2 inhibitors are not used in patients who already have CKD or reduced renal function as these drugs have been shown to initially lower GFR through renal hemodynamic effects (114) However, research in animal models suggests that reducing the hyperfiltration in and intraglomerular pressure is beneficial for overall kidney function (115).

Dyslipidemia is highly associated with cardiovascular disease and patients with diabetic renal disease are at higher risk for cardiovascular disease than those with DM alone (116). Dyslipidemia is characterized by hypertriglyceridemia, low and poorly functioning HDL, and increased small dense LDL levels (117). Table 1 describes associations between the dyslipidemia and progress of CKD as well as possible causes. These data suggest that cholesterol-lowering techniques should be effective in preventing or slowing the progress of CKD. However, the

benefit of statins in preventing ESRD is not clear. A meta-analysis of 57 randomized clinical trials shows statin therapy does not reduce the risk for kidney failure events in adults but may reduce proteinuria and rate of eGFR decline (118). A second meta-analysis found that although treatment with statins did not slow the progression of ESRD, it did lower the rates of death (119). More research needs to be done to understand the role cholesterol plays in kidney pathogenesis and whether it can be targeted for treatment of CKD.

Figure 3. Nephrotic Syndrome leads to dyslipidemia

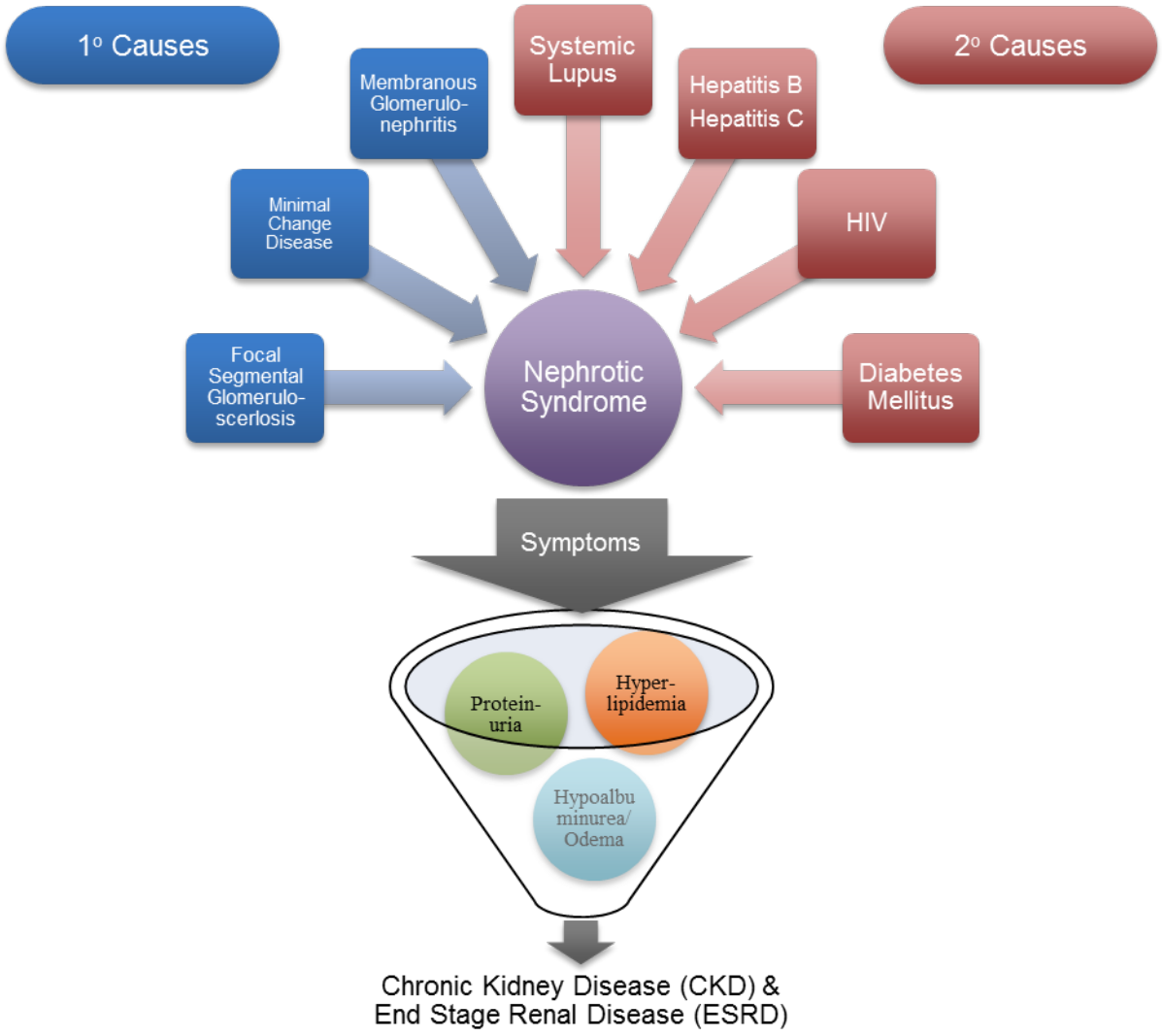

Table 1. Association between dyslipidemia and CKD

Lipoprotein	Evidence for Renal Injury	Ref	Cause(s) of Dyslipidemia	Ref
Hyperlipidemia	In humans, hypertriglyceridemia is a risk factor associated with an increased risk of progression of CKD	(120)	Decreased LpL activity and GPIHBP1 protein; increased Angptl4 Increase VLDL production by liver Downregulation of VLDL in skeletal muscle and adipose tissue	(121) (122) (120) (123) (124)
Hypercholesterolemia	*ApoE*$^{-/-}$ mice develop morphological and pathological hallmarks of kidney injury Dietary cholesterol cause glomerulosclerosis in the kidney in rodents; reversible with low cholesterol diet	(125) (126) (127) (128,129)	Upregulation of PCSK9 and increased degradation of LDL receptor protein (IDOL) Decrease in hepatic LDLR	(130) (131)
Dysfunction HDL particles	Inverse correlation between plasma HDL in CKD and cardiovascular events African American patients with HDL associated protein, APOL1 risk alleles progress to CKD more quickly.	(132) (133)	CE-poor HDL particles from systemic upregulation of ACAT and decreased serum LCAT APOL1 mutation causes HDL dysfunctional	(134) (135) (136)

2.3 Kidney Lipid Metabolism and Lipotoxicity in Health and Disease

The association of lipid accumulation and injury in the kidney is not a new notion, but has recently gained more attention. Kimmelstiel and Wilson, in their seminal work, described lipoid deposits during DNep (137). Rudolf Vichow lectured on "fatty degeneration" as a stage of glomerulonephritis—a primary cause of NepS. Multiple animal models of kidney injury and DNep, present with TG accumulation in the kidney tubules and glomeruli (138). Questions as to the cause and origin of lipid in the kidney during injury remain unanswered.

2.3.1 *De Novo* lipogenesis. Murine kidneys express both *Apob* and *Mttp*, and knockdown of *Apob* by antisense oligonucleotides increased fasting-induced lipid accumulation (139). These data suggest the kidney can release lipoproteins though the reason is unknown. One theory suggests this is a remnant of evolution from egg laying ancestors. In chickens, estrogen causes the liver to produce a modified VLDL targeted to the yolk (VLDLy). The kidney, however, continues to produce normal VLDL—suggesting that the kidney (and other extra-hepatic tissues such as the intestines) contributes TG-containing lipoproteins for lipid delivery to other tissues (140). Kidney lipoprotein formation may have also evolved as a mechanism to regulate excess intracellular lipid accumulation. Mice given a 0.12% cholesterol diet have increased expression of ApoB in the kidney (127). When mice were switched to a 0% cholesterol diet, ApoB protein in the kidney decreased (127). If the kidney is able to synthesize lipoproteins like the liver, it is plausible the kidney may be able to synthesize TG as well.

DNL is a major contributor to liver lipotoxicity and non-alcoholic fatty liver disease (42). It has been suggested that the same pathway contributes to kidney dysfunction. Obese *db/db* mice had more TG in their kidneys and developed glomerulosclerosis, tubulointerstitial fibrosis and proteinuria (141). These mice also had an increase in renal SREBP1 and SREBP-2, as well

as their downstream targets, *Acc* and *Fasn* (141). Similarly, rats made diabetic with streptozotocin (STZ) had an increase in SREBP-1 protein and lipid accumulation around the glomeruli (142). Upon treatment with insulin, this was reversed (142). *Srebp-1c*$^{-/-}$ given a HFD accumulated less TG in their kidney, less glomerulosclerosis and express less fibrosis related genes such as plasminogen activator inhibitor-1, vascular endothelial growth factor, type IV collagen and fibronectin (143). These data suggest that DNL may play a major role in lipid accumulation in mice during metabolic syndrome. It is not clear whether this is true in humans. The human kidney does not contain a very high amount of *FASN*, the rate-limiting enzyme in DNL (144). When compared to normal kidney samples, mRNA levels of *de novo* lipogenesis genes are lower in DNep samples, despite containing more lipid (145). However, FAO genes such as *PPARA* and *CPT1* are positively correlated with GFR in the kidney (145).

2.3.2 Fatty acid oxidation. The kidney is one of the most energy consuming tissues in the body, with approximately two-thirds of its oxidative substrate provided by fatty acids (146). Excess fatty acid in the cell is esterified to form TG and stored in LDs (139). While the entire kidney can utilize fatty acids, the cortex and the epithelial tubule cells depend primarily on FAO for ATP (138). The cortex has very little glycolytic capacity compared to the medulla (147). Oxidative metabolism genes in the tubule cells of the kidney are under transcriptional control of the PPARs, specifically PPARα (148).

Decreased PPARα expression and protein levels are a common phenomenon in kidney injury (145) (149-152). Analysis of kidney samples obtained from 95 CKD patients found that FAO related genes, such as CPT1 and acyl-CoA oxidase, were downregulated compared to controls (152). Overexpression of *Ppargc1a* or treatment with fenofibrate, a PPARα agonist, mitigated tubulointerstitial fibrosis and lipid accumulation in mice with acute renal injury (152).

Though PPARα is a regulator of FAO in the kidney, other hypotheses as to its role in renal fibrosis are present. Diabetic mice given fenofibrate had reduced Wnt signaling in the kidney, thus, decreasing fibrosis of the tubules (153). Diabetic *Ppara*$^{-/-}$ mice expressed more NADPH oxidase-4 compared with diabetic wild-type mice, suggesting that the inhibitory effect of PPARα on Wnt signaling may be due to its antioxidant activity (153). During kidney injury, an immune response is triggered in order to repair the area. Fenofibrate was shown to attenuate inflammation and fibrosis by suppressing nuclear factor-kappa-light-chain-enhancer of activated B cells (NF-κB) and transforming growth factor-beta 1 (TGF-β1) in kidneys of Zucker diabetic rats (154). TGF-β1, while also being a pro-fibrotic factor, also suppresses FAO (152). These data suggest it is difficult to tease out the exact role PPARα is playing in preventing fibrosis in the kidney. Though PPARα is renoprotective in animal models, more research is needed to determine its efficacy for patients with CKD (155). However, Ang II receptor blocker, irbesartan, has been shown to activate PPARα and increase PPARα signaling in the kidney (156). Thus, this class of drug may be an effective way of targeting PPAR in the kidney.

2.3.3 Fatty Acid Uptake. The source of fatty acids for kidney oxidation and the mechanism by which fatty acids are taken up is not fully understood. Fatty acids are either transported on albumin or sequestered in TG containing lipoproteins. Albumin passes through the glomerulus, albeit very little. Thus, the tubule cells are exposed to fatty acids on the luminal and basal lateral face. Albumin is taken up on the luminal surface by LDL-receptor related protein 2 (LRP2) also known as megalin. Indeed, when ligand binding to megalin was inhibited, less ^{125}I-BSA was taken up by rat kidney tubules (157). Compromised glomerular filtration may lead to increased lipid-loaded albumin uptake on the luminal face of the kidney, causing lipotoxity in the tubule (158). On the apical side, there several known LCFA transport proteins

expressed in the kidney, such as CD36 and FATPs, as well as lipoprotein transport proteins like VLDL receptor. LpL can take fatty acids from lipoproteins via TG hydrolysis. The kidney has high LpL expression and activity making it comparable to the heart (159). LpL activity in the kidney is nutrient dependent—being lower in the postprandial state (159). Lipid not oxidized by the kidney is stored in small LDs in the kidney (139).

A common manner by which TG can accumulate in tissues is by taking up more fatty acid than can be oxidized or used structurally. Fatty acids can enter the cell by diffusing through the membrane or *via* a cell surface receptor. A common LCFA in tissues is CD36. During DNep in humans, *CD36* is upregulated almost three-fold (145), suggesting that the observed TG accumulation in the kidney may be accounted for by increased FA uptake. During kidney injury, the barrier of the glomerulus is compromised allowing albumin and other proteins to flow through. Albumin triggers *Cd36* expression in the kidney (160). CD36 mediates uptake of albumin in proteinuria nephropathies (161). High glucose has also been shown to increase *Cd36* expression of proximal tubule cells *in vitro*, *via* AKT-PPARγ signaling (162). Hyperglycemia in concert with hyperlipidemia induces renal disease more than either alone (163). GLP-1 agonists have been shown to have a protective role in animal models of DNep. However, outcome data for patients with CKD or ESRD is lacking (164) (165).

CD36 is an attractive target for tackling renal disease. CD36 binds oxLDL and causes a downstream pro-inflammatory and pro-fibrogenic signal cascade (166). CD36 and Na^+/K^+-ATPase-a1 form a pro-inflammatory loop in the kidney during a high fat western-diet (167). By deleting *Cd36* in ApoE null background, mice were protected from kidney damage during a western diet (167). Blocking CD36 with an Apo-A1 mimetic prevented CKD in mice, but this effect was not seen in CD36 null mice (168). Similarly, CD36 null mice on a HFD did not

present with the same amount of glomerular damage or tubular fibrosis as wild-type mice. (169). Thus CD36, and by extension, lipid uptake, seems an important feature in the progression of renal disease.

From the research presented, it is clear there is no consensus in which way lipid accumulates in the kidney during injury or CKD. The three major mechanisms, DNL, decreased FAO, and increased fatty acid import are summarized in Figure 4.

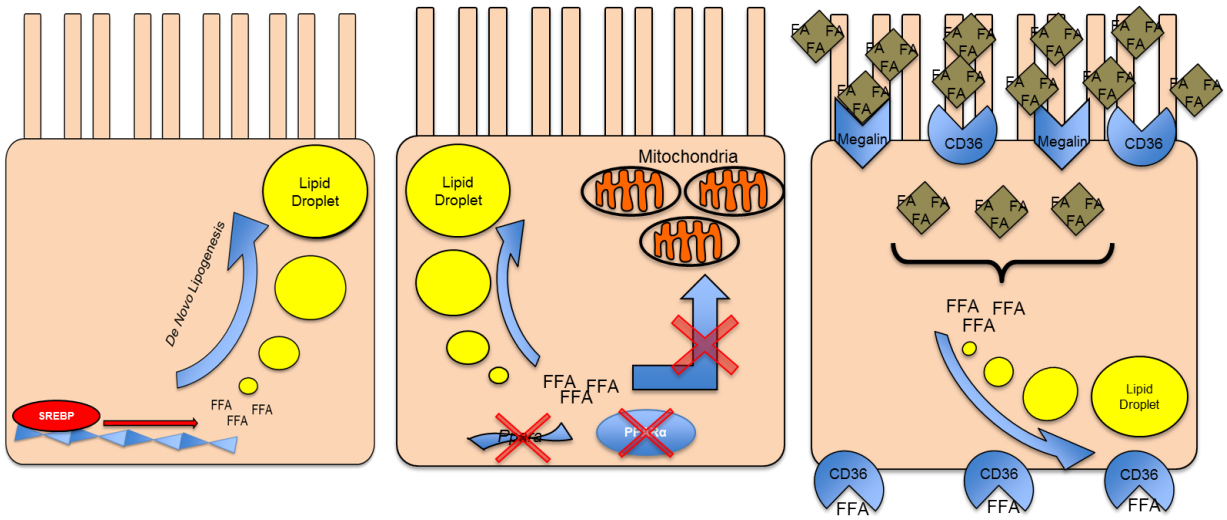

Figure 4. Summary of mechanisms of lipid accumulation in the kidney during injury

Triglyceride accumulation in the kidney involves increased synthesis, decreased oxidation, or increased uptake. There are several theories available as to how the kidney accumulates triglyceride during injury. A) *De novo* lipogenesis mediated by sterol-regulatory element binding protein (SREBP). B) Decreased fatty acid oxidation (FAO) due to decrease in PPARα protein and mRNA. C) Increase in uptake of albumin-bound NEFA from the luminal surface by megalin and CD36 or NEFA uptake by CD36 from the basolateral surface.

Chapter 3: Kidney triglyceride accumulation in the fasted mouse is dependent upon serum free fatty acids.

This chapter has been published in the Journal of Lipid Research (170).

Diego Scerbo, Ni-Huiping Son, Alaa Sirwi, Lixia Zeng, Kelli M. Sas, Vincenza Cifarelli, Gabriele Schoiswohl, Lesley-Ann Huggins, Namrata Gumaste, Yunying Hu, Subramaniam Pennathur, Nada A. Abumrad, Erin E. Kershaw, M. Mahmood Hussain, Katalin Susztak, Ira J. Goldberg

3.1 Abstract

Lipid accumulation is a pathological feature of every type of kidney injury. Despite this striking histological feature, physiological accumulation of lipids in the kidney is poorly understood. We studied whether the accumulation of lipids in the fasted kidney are derived from lipoproteins or non-esterified fatty acids (NEFAs). With overnight fasting, kidneys accumulated triglyceride but had reduced levels of ceramide and glycosphingolipid species. Fasting led to a nearly 5-fold increase in kidney uptake of plasma [^{14}C]oleic acid. Increasing circulating NEFAs using a beta adrenergic receptor agonist caused a 15-fold greater accumulation of lipid in the kidney, while mice with reduced NEFAs due to adipose tissue deficiency of adipose triglyceride lipase had reduced triglycerides. *Cd36* mRNA increased 2-fold, and *Angptl4*, an LpL inhibitor, increased 10-fold. Fasting-induced kidney lipid accumulation was not affected by inhibition of LpL with poloxamer 407 or by use of mice with induced genetic LpL deletion. Despite the increase in CD36 expression with fasting, genetic loss of CD36 did not alter fatty acid uptake or triglyceride accumulation. Our data demonstrate that fasting-induced triglyceride accumulation in the kidney

correlates with the plasma concentrations of NEFAs, but is not due to uptake of lipoprotein lipids and does not involve the fatty acid transporter CD36.

3.2 Introduction

The kidney is one of the most energy consuming tissues in the body with approximately two-thirds of its oxidative substrate provided by fatty acids (146). Excess fatty acid in the cell is esterified to form triglyceride and stored in LDs. While the entire kidney can utilize fatty acids, the cortex and the epithelial tubule cells depend on fatty acid oxidation (FAO) for ATP (138).

The cortex is also the site of large accumulations of neutral lipids during kidney disease and injury (138). Pathways that contribute to lipid accumulation in the kidney are not well established. Some studies suggest that during obesity, diabetes, and aging, an increase in the sterol regulatory element proteins (SREBPs) leads to greater *de novo* fatty acid synthesis, which drives lipid accumulation and decreases renal function (141-143,171). Other studies have shown that renal failure causes decreased FAO (152,172), which could independently increase lipid accumulation.

Multiple pathways are dysregulated in chronic kidney disease (CKD)—making this issue difficult to study. On the other hand, neutral lipid accumulation also occurs during fasting (139). In many tissues such as the heart, muscle, and adipose tissue, lipoprotein lipase (LpL) and cluster of differentiation (CD) 36 are necessary for proper transport of fatty acids into the tissues (173,174). LpL is synthesized by parenchymal cells and translocates to the endothelial surface where it hydrolyses very-low density lipoprotein (VLDL) and chylomicron TGs to produce non-esterified fatty acids (NEFAs). NEFAs can then either diffuse through the membrane in a process called “flip-flop” (175) or transfer across the membrane by a saturable receptor-mediated process

(176). CD36 has been postulated to mediate active transport of NEFAs into cells (177). Like the heart, skeletal muscle, and adipose tissue, the kidney robustly expresses both LpL and CD36 (178,179). However, in an unbiased assessment of renal genes in mice with diabetic kidney disease, *Cd36* was reduced; as were other genes associated with renal fatty acid oxidation (180). This suggests that FAO and lipid uptake into the kidney are coordinately regulated.

In the current study, we first determined NEFA uptake into the kidney during fasting and then modulated plasma NEFA levels and assessed whether this altered kidney TG accumulation. We then tested whether TG-rich lipoproteins or NEFAs were the source of kidney TG stores. In addition, we tested how kidney CD36 and LpL were affected by fasting and whether these known moderators of TG metabolism affect fasting-induced lipid accumulation in the kidney. Please note that figures and all references to them presented in section 3.4.2 were not published in the original article.

3.3 Material and Methods

3.3.1 Animal Studies: We used 10-16 week-old male and female C57BL/6 mice, *Cd36*$^{-/-}$ mice,(29) floxed *Lpl* mice (*Lpl*$^{fl/fl}$), i*Lpl*$^{-/-}$ mice, floxed *Mttp* (*Mttp*$^{fl/fl}$) and liver-specific *Mttp* knockout mice (*L-Mttp*$^{-/-}$), and adipocyte specific *Atgl* knockout mice (AAKO) (181,182). Mice were raised on a normal chow diet. Littermates were used as controls for all studies. The NYULMC, Washington University, SUNY Downstate, and U. Pittsburgh Institutional Animal Care and Use Committees approved all procedures. Mice of each genotype were divided into two groups; one group was fasted 16 hours overnight and the other was allowed to feed *ad libitum* for the same time period. All mice were then euthanized with a lethal injection of 100mg/kg ketamine and 10 mg/kg xylazine. Animals were dissected open then perfused by cardiac

puncture in the heart with 5 mL of PBS until liver and kidneys blanched. Tissues were dissected out, snap frozen in liquid nitrogen and stored at -80^{o}C for further use. Kidneys were also bisected and embedded into Tissue-Tek OCT compound (Sakura) for oil-red O histology.

Poloxamer 407 (P407) was prepared in PBS as previously described (183). Mice were injected intraperitoneal with 1mg/g bodyweight of P407 and then fasted for 16 h. Control mice were injected with an equivalent volume of PBS.

i*Lpl*$^{-/-}$ animals were generated as described previously (184). Briefly, β-actin-driven tamoxifen-inducible-Cre (Mer/Cre/Mer) transgenic mice were crossed with LpL flanked loxP sites mice to obtain the β-*actin-MerCreMer*/*Lpl*$^{fl/fl}$ offspring, designated inducible-*Lpl*$^{-/-}$ (i*Lpl*$^{-/-}$). The i*Lpl*$^{-/-}$ mice were given an intraperitoneal injection of 1 mg of 4-hydroxytamoxifen (Sigma) in peanut oil for five consecutive days.

β_3-adrenergic receptor agonist CL 316,243 (Sigma) was dissolved in PBS and injected into C57BL/6 mice at 1mg/kg at two time points (2pm and 6pm) (185). The mice were allowed to feed *ad libitum* and sacrificed the following morning.

MTTP was inhibited using BMS-212122 (MTTPi) as previously described (186). Briefly, the MTTPi was diluted in DMSO and given to mice orally at a dose of 1mg/kg bodyweight for seven consecutive days. Control mice were given an equivalent volume of DMSO. After the final dose, mice were divided into two groups and either fasted overnight for 16 h or allowed access to food *ad libitum* and sacrificed.

3.3.2 Measurement of Plasma Lipids and Glucose: 100 μL of blood were drawn from each animal and then centrifuged at 10,000 rpm on a table top centrifuge for 10 min to obtain plasma. Plasma was used to measure TGs and NEFA using Thermo Scientific Infinity assay (Thermo Scientific) and Wako NEFA kit, respectively. Glucose was measured from whole blood

using a One Touch Ultra 2™ glucometer. TG-rich lipoproteins (density < 1.006 g/ml) were separated by sequential density ultracentrifugation of plasma in a TLA100 rotor as described in Kako Y *et al.* (187).

3.3.3 Lipid Extraction and Measurement: The lipid extraction protocol was adapted from the Folch method (188) and modified slightly from Trent *et al.* (173). Briefly, approximately 100mg of tissue was homogenized in 500 µL of ice-cold PBS using stainless steel beads for 30s in a bead beater homogenizer. From each sample, 50 µL were removed for protein analysis, and 1.5 milliliters of 2:1 chloroform: methanol was added to the rest of the homogenate in a glass test tube. Samples were then centrifuged for 10 min at 3,000 rpm at 4^{o}C. The lower organic phase was separated with glass Pasteur pipette and blown dry with nitrogen gas. The dried lipid was then dissolved with 500 µL of 2% Triton X-100 in chloroform, further dried, and then dissolved in double distilled water. The sample of tissue lysate put aside was used to assay protein content using Bradford reagent (Bio-Rad) following manufactures instructions. Using the tissue lipid extract, assays for TG were performed using previously described assay for plasma lipid. Lipid measurements were normalized to protein content of each sample or milligram of tissue weight.

3.3.4 *In vivo* NEFA Uptake: NEFA uptake was assessed in C57BL/6 mice either fasted 16 h overnight or allowed access to food *ad libitum* for the same time and in *Cd36*$^{-/-}$ and *Cd36*$^{fl/fl}$ fasted 16 h overnight. [1-^{14}C]oleic acid (PerkinElmer Life Sciences) was complexed to 0.6% fatty acid-free BSA (Sigma). Mice were injected intravenously with 1.5x10^{6} cpm of [1-^{14}C]oleic acid-BSA and blood was collected at 0.5, 2, and 5 min after injection after which the mice were sacrificed. Plasma was collected as previously described. The body cavity was perfused with 5 mL of PBS by cardiac puncture and tissues were extracted. Tissues were homogenized in 1 mL

of PBS and radioactive counts were measured using a LS 6500 multipurpose scintillation counter (Beckman Coulter). For C57BL/6 mice, radioactivity per gram tissue was normalized to average plasma NEFA levels in either the fed or fasted group. For *Cd36*$^{-/-}$ and *Cd36*$^{fl/fl}$, radioactivity per gram tissue was normalized to 2 min plasma cpm counts.

3.3.5 Renal Gene Expression: Total RNA was purified from approximately a 50 mg piece of kidney cortex using TRIzol reagent (Invitrogen) according to the instructions of the manufacturer. cDNA was synthesized using Verso cDNA Kit (Thermo Scientific) and quantitative real-time PCR were performed with Power SYBR Green PCR Master Mix (Life Technologies) using a Quant Studio 7 Flex analyzer (Life Technologies). Genes of interest were normalized against 18s rRNA. Primer sequences are listed in Table 2.

Table 2. Primer sequences of genes analyzed for quantitative PCR

Gene	Orientation	Sequence
Aox	forward	CAGGAAGAGCAAGGAAGTGG
	reverse	GACATCTGAGCCCCTGTGAT
Cpt1a	forward	CATGTCAAGCCAGACGAAGA
	reverse	TGGTAGGAGAGCAGCACCTT
Acsl1	reverse	CTTGAACCCCTTCTGGATCA
	forward	TGACCTCTCCATGCAGTCAG
Angptl4	forward	AGCAGAGATACCTATCAAAGCAGAA
	reverse	AGTCATCTCACAGTTGACCAAAAAT
Atgl	forward	CGCCTTGCTGAGAATCACCAT
	reverse	AGTGAGTGGCTGGTGAAAGGT
Cd36	forward	TGTGTTTGGAGGCATTCTCA
	reverse	TGGGTTTTGCACATCAAAGA
Fatp2	forward	ATGCCGTGTCCGTCTTTTAC
	reverse	GACCTGTGGTTCCCGAAGTA
Hsl	forward	ACACAAATCCCGCTATG
	reverse	CTCGTTGCGTTTGTAGT
Lpl	forward	GCTGGTGGGAAATGATGTG
	reverse	TGGACGTTGTCTAGGGGGTA
18s rRNA	forward	CCATCCAATCGGTAGTAGCG
	reverse	GTAACCCGTTGAACCCCATT
Srebp1c	forward	GGAGCCATGGATTGCACATT
	reverse	GGCCCGGGAAGTCACTGT
Vldlr	forward	TGACGCAGACTGTTCAGACC
	reverse	GCCGTGGATACAGCTACCAT
Fasn	forward	TTGCTGGCACTACAGAATGC
	reverse	AACAGCCTCAGAGCGACAAT
Dgat1	forward	GTGCACAAGTGGTGCATCAG
	reverse	CAGTGGGATCTGAGCCATCA
Dgat2	forward	CTGTCACCTGGCTCAACAGA
	reverse	TATCAGCCAGCAGTCTGTGC
Plin2	forward	CTACGACGACACCGAT
	reverse	CATTGCGGAATACGGAG
Plin5	forward	GTGATCAGACAGCTCAGGACCCT
	reverse	CGATTCACCACATTCTGCTGG

3.3.6 RNA Sequencing: Raw sequencing data were received in FASTQ format and mapped against the hg19 human reference genome using Tophat 2.0.9. The resulting BAM alignment files were processed using the HTSeq 0.6.1 python framework and respective hg19 GTF gene annotation, obtained from the UCSC database. Differentially expressed genes (DEG)

were identified using Bioconductor package DESeq2 (3.2), which analyzes RNA sequencing data based on a negative binomial distribution model. To control for false discovery rate (FDR), resulting values were adjusted using the Benjamini and Hochberg method. Ingenuity Pathway Analysis was then performed on the DEG in order to determine top canonical pathways being altered. Genes with an adjusted p-value <0.05 were determined to be differentially expressed. Heat map was created in Microsoft Excel, normalizing all samples to the fed group and expressing the values as fold change.

3.3.7 Lipidomics: Long-chain fatty acyl-CoAs, acyl carnitines, and ceramides were analyzed by targeted metabolomics as previously described (189-191). Briefly, approximately 20 mg renal cortex was homogenized and extracted with cold 8:1:1 methanol:chloroform:water containing known amounts of C17:0 acyl-CoA (Sigma-Aldrich,), isotope-labeled carnitines (Cambridge Isotope Laboratories), and C17:0 and C25:0 ceramide (Avanti Polar Lipids) internal standards. An equal volume from each tissue sample was combined to generate a pool sample to monitor analytical variability. Ceramides were extracted following the method of Bligh and Dyer (192) and the organic layer was dried under vacuum and resuspended in 60:40 acetonitrile:isopropanol. As an additional control, a mixture of seven standard ceramide compounds was simultaneously extracted and analyzed. Acyl-CoAs, acyl carnitines, and ceramides were quantified by liquid chromatography-electrospray ionization-tandem mass spectrometry (LC/ESI-MS/MS) in the multiple reaction monitoring (MRM) mode using an Agilent 6410 triple quadrupole MS system equipped with an Agilent 1200 LC system. Concentrations were calculated by ratios of peak areas of samples to known concentrations of internal standards. Data were normalized to tissue weight. All solvents were LC-MS grade (Sigma Aldrich).

3.3.8 Histology: Frozen sections were cut to 10 μM, air dried, fixed with 4% paraformaldehyde and washed with double distilled water. Sections were rinsed with 60% isopropanol and stained with freshly prepared oil red O for 15 min and rinsed again with 60% isopropanol. Sections were then in modified Mayer's Hematoxylin for 1 min and washed with distilled water. Slides were then mounted with cover slips using glycerin jelly. Images were taken using a Leica SCN400F Whole Slide Scanner.

3.3.9 Statistics: Data are expressed as mean ± SD. Data was analyzed by the use of unpaired Student's *t*-test or two-way ANOVA Tukey's multiple comparison tests.

3.4 Results

3.4.1 FAO increases along with triglyceride accumulation in the kidney after a fast. To study lipid accumulation in the kidney, we used an overnight fast as a TG accumulation model (139). After an overnight fast, plasma glucose in both male and female mice decreased by nearly half, while TGs and cholesterol were not significantly altered (Figure 5A-C). NEFAs increased ~2-fold (Figure 5D). As in the heart and liver, an overnight fast induced TG accumulation in the kidney; average TG increase was ~3-fold in males and 5-fold in females (Figure 5E). This accumulation occurred primarily in the renal cortex, as shown by oil-red O staining of kidney sections (Figure 5F).

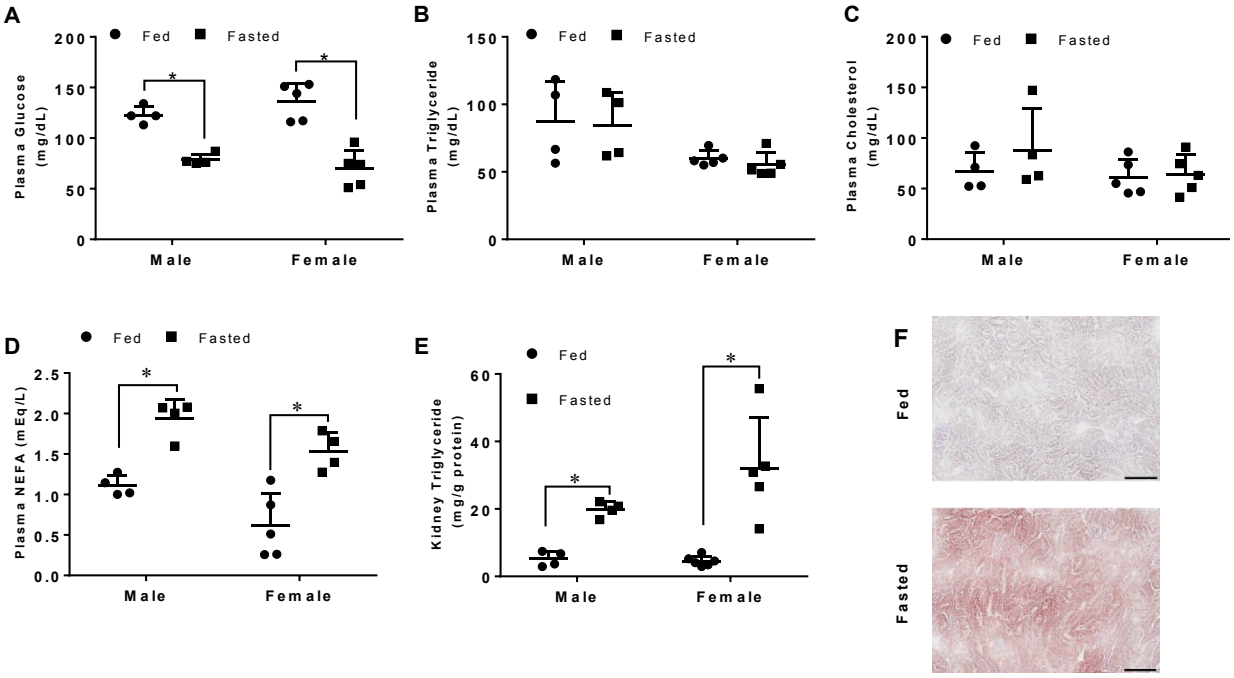

Figure 5. Kidney triglycerides increased in both male and female mice after an overnight fast

(A-E) Male and female mice were either fasted or given food *ad libitum* for 16 hs. Blood was drawn to measure glucose and plasma lipids. Lipids were extracted for intracellular triglyceride measurements. A) Plasma glucose. B) Plasma triglycerides. C) Plasma total cholesterol. D) Plasma non-esterified fatty acids (NEFAs). E) Kidney triglyceride content. F) Kidneys from male mice were formalin fixed and sectioned for oil-red O staining. Scale bar is representative of 100μM at 20X magnification. N=4-6/group. *: $p<0.05$. Results are presented as means ± SD. * indicated results compared by unpaired Student's t-test within each sex group, no significant differences were found between male and female groups using the two-way ANOVA Tukey's multiple comparison test.

To assess which lipid pathways were changed in kidneys from fasted animals, mRNAs of proteins involved in FAO, *de novo* lipid synthesis and lipid transport pathways were analyzed by RNA sequencing of whole kidney from fed and fasted mice. mRNA levels of genes that mediate *de novo* lipogenesis were decreased including fatty acid synthase (*Fasn)*, squalene epoxidase (*Sqle*), acetyl-CoA carboxylase alpha (*Acaca*), and sterol regulatory element binding transcription factor 1 (*Srebf1*) and 2 (Figure 6A). However, despite greater lipid accumulation, mRNA levels of genes involved in lipid oxidation and mitochondrial pathways were increased, including those of pyruvate dehydrogenase kinase 4 (*Pdk4*), alternative oxidase (*Aox*), carnitine palmitoyltransferase 1(*Cpt1a*), and carnitine O-acetyltransferase (*Crat*) (Figure 6A). Peroxisome proliferator-activated receptor alpha (*Ppara*) and *Ppard* were increased and *Pparg* remained unchanged (Figure 6A). Among the more oxidative portions of the kidney, PPARα is the dominantly expressed isoform (148) Ingenuity Pathway Analysis using the KEGG database showed that PPAR signaling was the most differentially regulated pathway, with 23 associated genes changed (Table 3). A majority of PPAR regulated genes were also increased after fasting (Figure 7A). In concordance with the RNA sequencing data, *Aox, Cpt1a,* and acetyl CoA synthetase long-chain 1 (*Acsl1*) were all increased ~4-fold when assessed by quantitative PCR (Figure 7B). Genes associated with lipid uptake were also assessed. *Cd36* mRNA levels increased almost 2-fold after fasting by quantitative PCR, though it did not quite reach significance. Fatty acid transport protein 2/solute carrier family member 27 member 2 (*Fatp2/Slc27A2*), a primarily intracellular enzyme that traps NEFAs by esterifying them to CoA (193), was unchanged (Figure 2C). In addition, lipoprotein receptors-LDL receptor, LDL receptor related protein 1 (*Lrp1*), *Lrp2* (megalin), and very low-density lipoprotein receptor (*Vldlr*)-remained unchanged. While *Lpl* mRNA levels were unchanged, angiopoietin-like 4

(*Angptl4*), an LpL inhibitor, was increased 9-fold. LD associated protein perilipin (*Plin*) 2 increased 20-fold and *Plin5* increased 10-fold. Intracellular lipases needed to utilize TG stored in LDs also increased; hormone sensitive lipase (*Lipe/Hsl*) mRNA increased 7-fold and adipose TG lipase (*Pnpla2/Atgl*) 2-fold. Others have reported that after a fast, both HSL and ATGL activation by phosphorylation increases in the kidney (194). Taken together, this gene expression profile suggests that despite increased mRNA levels of genes regulating FAO and decreased mRNA levels of genes mediating *de novo* lipogenesis, the kidney stores excess fatty acids in LDs during fasting. This suggests an excess of fatty acid transport into the kidney.

Table 3. Ten most significantly altered pathways in the kidney between the fed and fasted state

KEGG Pathway	p-value	Genes
PPAR signaling pathway	8.36E-08	SLC27A1, ACOX1, CPT1B, SCD2, CPT2, ACADM, EHHADH, FADS2, PCK2, ACADL, DBI, CPT1A, PCK1, CYP4A10, ACSL1, CYP27A1, HMGCS2, CYP4A31, APOC3, FABP4, ACSL4, ACAA1B, SLC27A2, ANGPTL4
Fatty acid metabolism	4.71E-06	ACOX1, CPT1B, ACAA2, ACADM, CPT2, EHHADH, ACADL, HADHA, CPT1A, HADHB, ACADVL, CYP4A10, ACSL1, CYP4A31, ACSL4, ACAA1B
Phosphatidylinositol signaling system	0.030783	PLCB4, PIK3C2G, PLCG1, INPP5K, PIK3CB, PI4KA, DGKZ, DGKH, DGKI, INPP5D, PLCB1, ITPR1
Biosynthesis of unsaturated fatty acids	1.99E-05	PECR, ACOX1, SCD2, FADS1, ACOT2, FADS2, ACOT1, ACAA1B, ACOT4, HADHA, ACOT3
Adipocytokine signaling pathway	0.034582	CPT1B, ACSL1, LEPR, IKBKG, ACSL4, PCK2, STAT3, AKT3, CPT1A, AKT2, PCK1
Arginine and proline metabolism	0.020652	SAT1, ODC1, GATM, GLUD1, ARG2, MAOB, CKMT1, DAO, NOS3, CKB
Glycine, serine and threonine metabolism	0.002628	GLYCTK, GATM, MAOB, PHGDH, GCAT, DAO, PSAT1, CBS, GLDC
Amino sugar and nucleotide sugar metabolism	0.019358	GALK1, RENBP, GNPDA1, MPI, GM8615, CMAH, UGDH, NAGK, UXS1, PMM1
Valine, leucine and isoleucine degradation	0.024859	ACAA2, DBT, ACADM, BCAT2, HMGCS2, EHHADH, ACAA1B, HADHA, HADHB
Terpenoid backbone biosynthesis	3.68E-05	DHDDS, MVD, HMGCS2, HMGCR, FDPS, MVK, IDI1, PDSS1

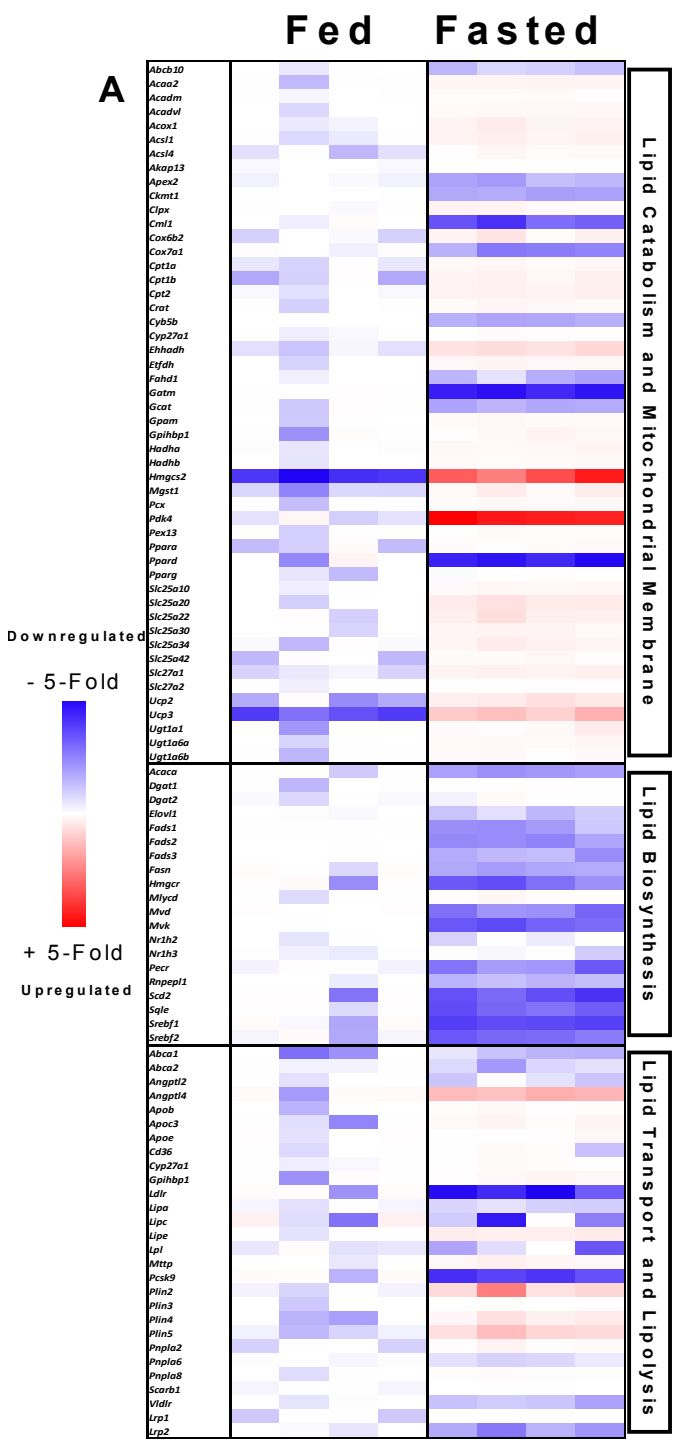

Figure 6. The kidney in the fasted state up regulates lipid oxidation genes and down regulates lipid synthesis genes

RNA sequencing of fed and fasted male kidneys. Data presented as fold change normalized to the fed group. Differentially expressed genes were identified with Bioconductor package DEseq2 (3.2) and Benjamini and Hochberg's method was used to control for false discovery rate (FDR). A) Canonical genes in pathways related to lipid metabolism and mitochondrial membranes, lipid biosynthesis and lipid transport and lipolysis.

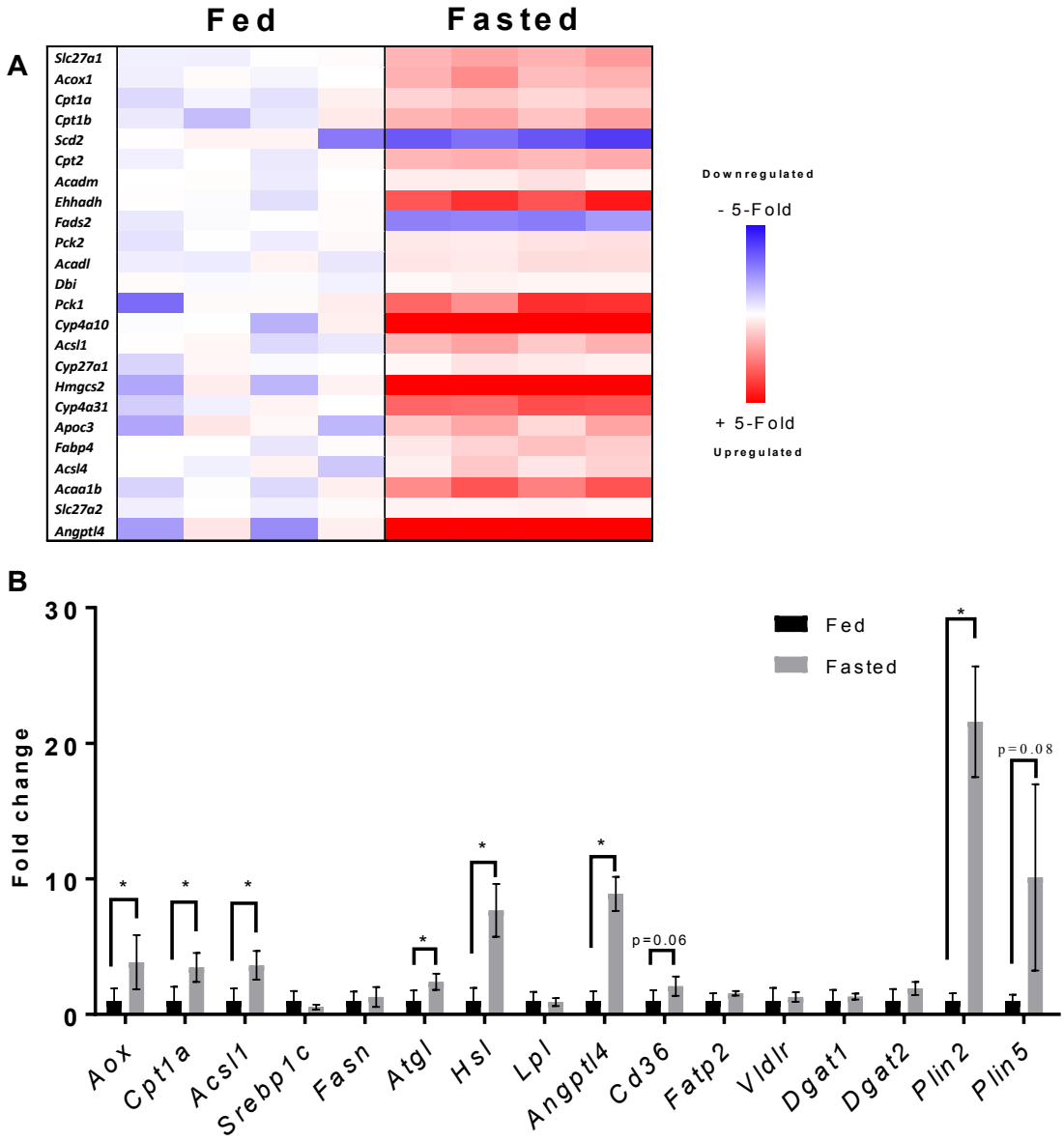

Figure 7. The kidney in the fasted state up regulates lipid oxidation genes and down regulates lipid synthesis genes (cont.)

A) Canonical genes in the PPAR pathway. B) Quantitative PCR of selected lipid metabolism genes, normalized to ribosomal 18s. Experiments were performed in male mice, N=3-5. *: $p<0.05$.Results are presented as means ± SD. Results for quantitative PCR were compared by unpaired Student's t-test.

3.4.2 Four-hour refeeding does not significantly decrease lipid accumulation accrued during fasting. Differences in arteriovenous NEFA concentrations in post-prandial rats suggest the kidney adds NEFA back to the circulation during the fed state (195). Thus, we asked whether TG accumulation in the kidney after an overnight fast would persist after 4 hours of refeeding. To test this, two groups of female mice were fasted overnight for 16 hours, with one group given food ad libitum for 4 hours after the fast. After 4-hours refeeding, these mice had a trending increase of plasma TGs (Figure 8A), a significant decrease in plasma NEFA (Figure 8B), but only a decreasing trend in kidney TG (Figure 8C) compared to mice that remained fasted. When gene expression analysis was performed (Figure 8D), we found an opposite pattern to the gene expression in Figure 7A. *Cpt1a* and *Acsl1* were decreased by 50% in the refed state compared to the fasted. Srebp1c was increased several 3-fold, while lipid droplet associated proteins such as *Atgl*, *Hsl*, and *Plin2* were all reduced in the refed state. *Angptl4* was decreased by more than 10-fold, thus suggesting an increase in LpL activity. These data suggest 4-hour refeeding causes a metabolic shift in the kidney from fasting, however TG accumulation persists, albeit much reduced.

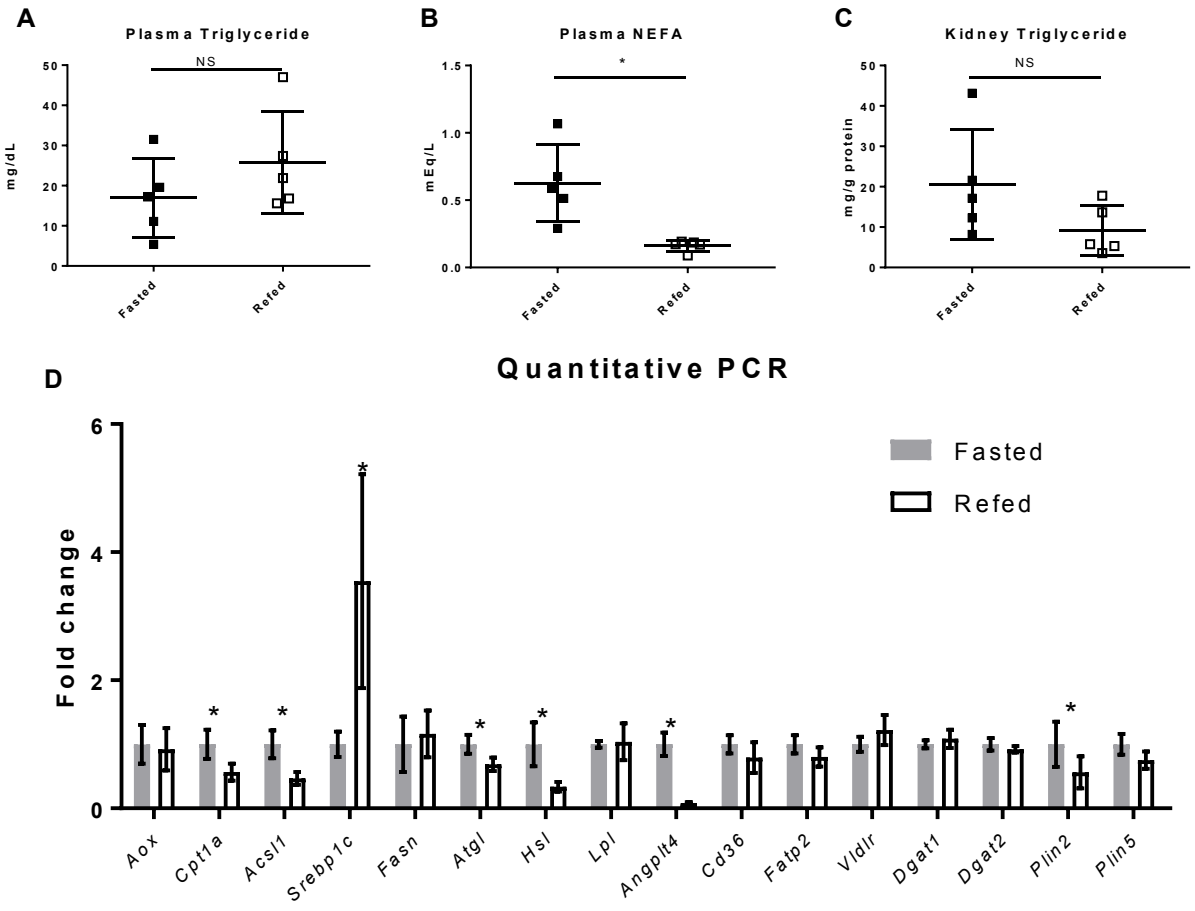

Figure 8. Four-hour refeeding does not significantly decrease lipid accumulation accrued during fasting

(A-D) 4-week old female mice were fasted for 16 hs, after which one group was refed *ad libitum* for 4 hs. Blood was drawn to measure plasma lipids. Lipids were extracted for intracellular triglyceride measurements. A) Plasma triglyceride. B) Plasma NEFA. C) Kidney triglyceride D) Quantitative PCR gene expression. N=5group. Results are presented as means ± SD. *: $p<0.05$. Statistics were performed using unpaired Student's t-test.

3.4.3 Lipidomic changes. Lipidomics was performed to analyze fatty acid species in the kidney after an overnight fast. There was an overall increase in long fatty chain acyl-CoAs (Figure 9A), although significance for changes in individual fatty acids could not be shown due to wide variation in the fasted group. Levels of the long chain acyl-carnitine C16 decreased 10-fold **(**Figure 9B). This is opposite to what was reported by Koves *et al.* (196) to happen in skeletal muscles. Additionally, a decline in long-chain ceramides and their derivatives, glycosphingolipids, in the kidney was observed after fasting (Figure 9C-D). An excess of ceramides is toxic to cells (197,198). These data suggest that in order to compensate for increased lipid oxidation, uptake of either TG-rich lipoproteins or NEFAs is increased, leading to TG but not ceramide, accumulation.

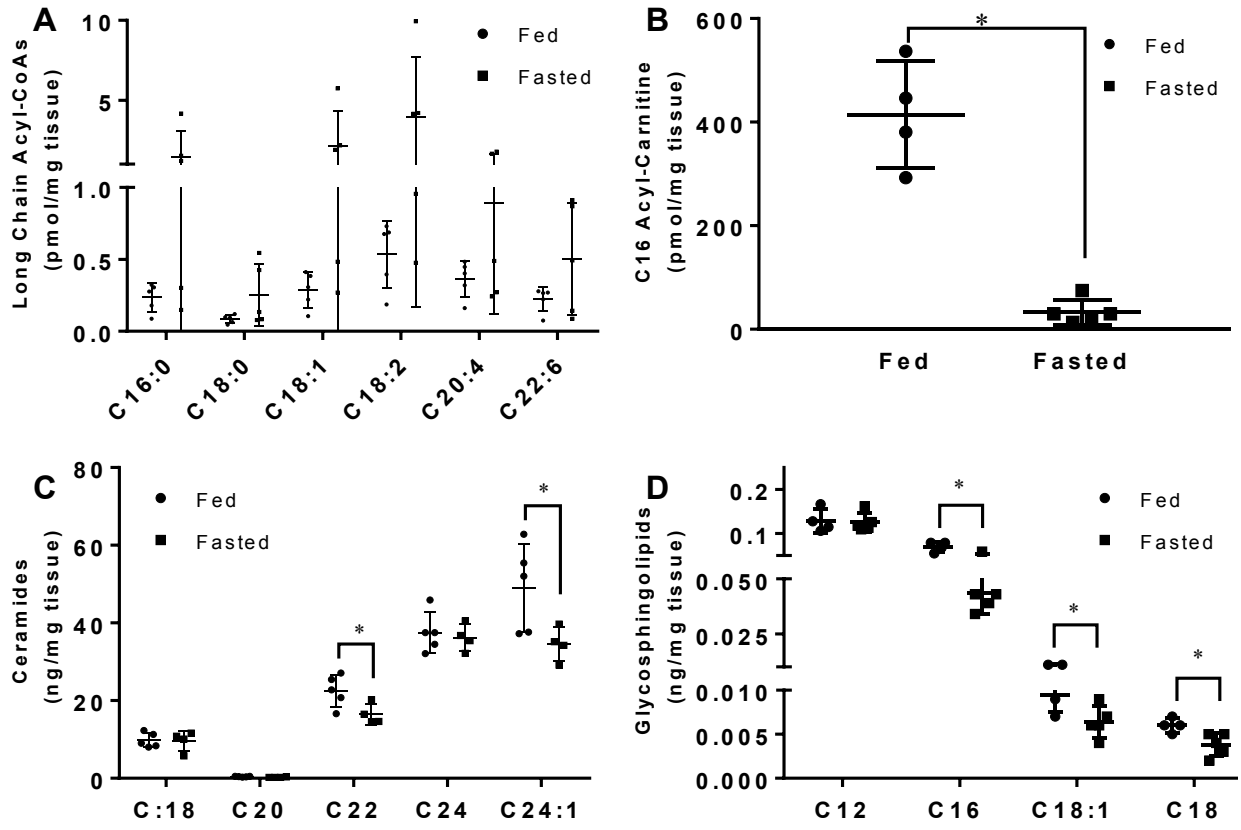

Figure 9. Ceramides and glycosphingolipids are lowered in the fasted kidney

Lipidomics were performed using liquid chromatography-electrospray ionization-tandem mass spectrometry (LC/ESI-MS/MS) on kidneys of mice that were fasted or given food *ad libitum* for 16 hs. A) Long-chain Acyl CoAs. B) C16 Acyl-Carnitine. C) Ceramides. D) Glycosphingolipids. Experiments were performed in male mice, N=4-5/group. *: $p<0.05$ Results are presented as means ± SD. Results compared using unpaired Student's t-test.

3.4.4 Lipid accumulation in the kidney is dependent on serum NEFAs. To determine whether fasting increases uptake of albumin bound NEFAs we performed an uptake study of [^{14}C]oleic acid in the fed and fasted state. After five minutes, nearly all the [^{14}C]oleic acid tracer was cleared from the circulation (Figure 10A). The liver took up a majority of fatty acids in both fed and fasted mice and accumulated more NEFAs during fasting. Similarly, kidney uptake of NEFAs was increased ~4-fold with fasting (Figure 10B).

We next tested whether altered plasma NEFA levels would lead to parallel changes in kidney TGs. To increase NEFAs in the fed state, we used a beta-adrenergic receptor agonist, CL 316, 238. Plasma NEFAs were increased 2-fold over time with two intraperitoneal injections (Figure 10C). This treatment increased kidney intracellular TG levels ~15-fold (Figure 10D); a similar TG increase was found in liver but not heart. To determine if reduced circulating fatty acid levels would reduce kidney TG after fasting, we studied mice with an adipocyte specific deletion of *Atgl* (mice are denoted AAKO*)*. As had been shown previously (182), AAKO mice have lower circulating NEFAs (Figure 11A), and unlike floxed control mice (*Atgl*$^{fl/fl}$ littermates), NEFAs decreased with fasting. Plasma TGs are also reduced in this model (Figure 11B). Mirroring the liver, the kidney also had a ~40% reduction in fasting TG content compared to fasted controls (Figure 11C). Liver TG accumulation with fasting was reduced in AAKO mice as was reported previously (182). These data demonstrate that renal TG during fasting is modulated by plasma NEFA levels.

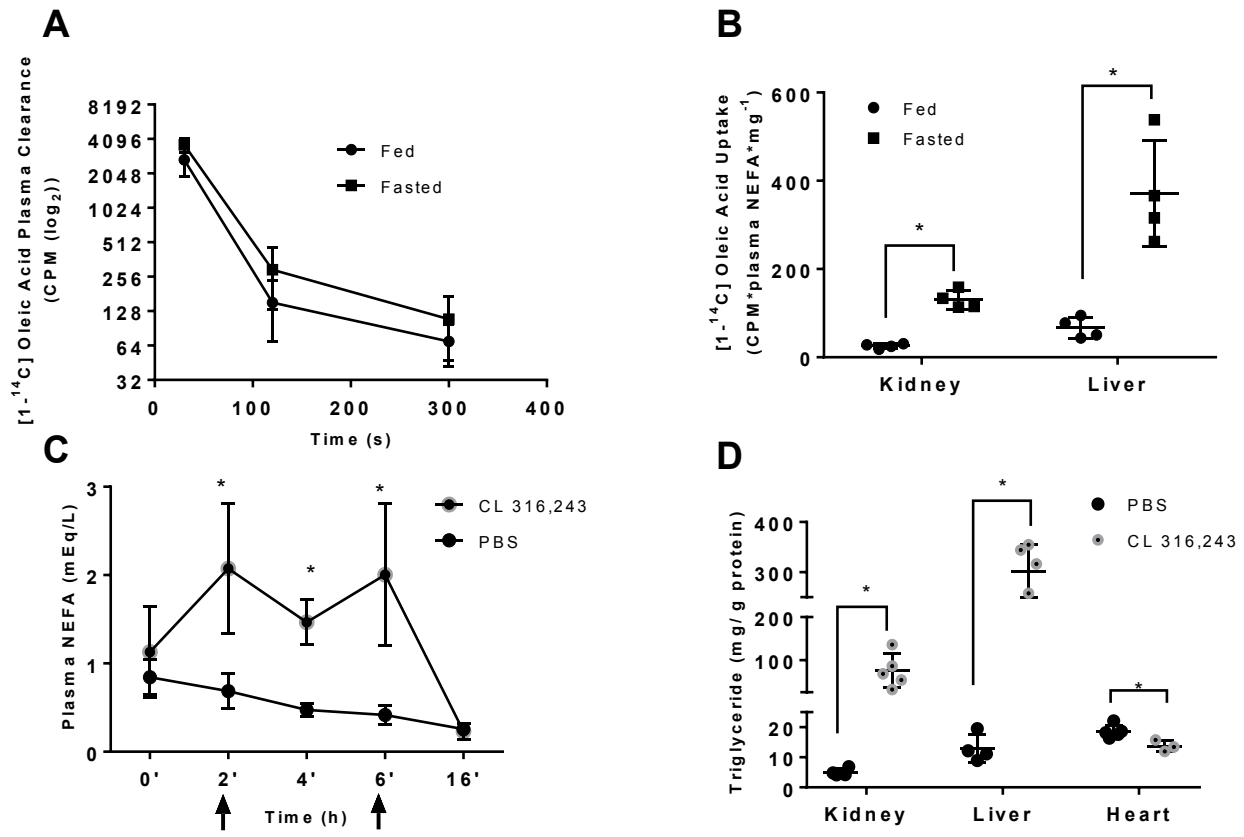

Figure 10. Plasma free fatty acids determine kidney triglyceride content

(A-B) [$^{1\text{-}14}$C]oleic acid (OA) was injected intravenously into male mice. Presence of radioactive signal was measured in plasma or tissue homogenate using a LS 6500 multipurpose scintillation counter. A) Plasma clearance of [$^{1\text{-}14}$C]OA over time. B) Liver and kidney ^{14}C label 300s after injection. Experiments were performed in male mice, N= 4-5/group. (C-D) Male mice were injected with CL 316,243 at 2 and 6-h time points, and blood samples were drawn at indicated points in order to measure NEFA concentration in the blood. Mice were sacrificed at the 16-h time point to collect tissues, N=4-5/group. C) Plasma NEFAs over time after two CL 316,243 injections (indicated by arrows). D) Tissue triglyceride content 16 hs after first injection. *: $p<0.05$ Results are presented as means ± SD. Results compared using unpaired Student's t-test.

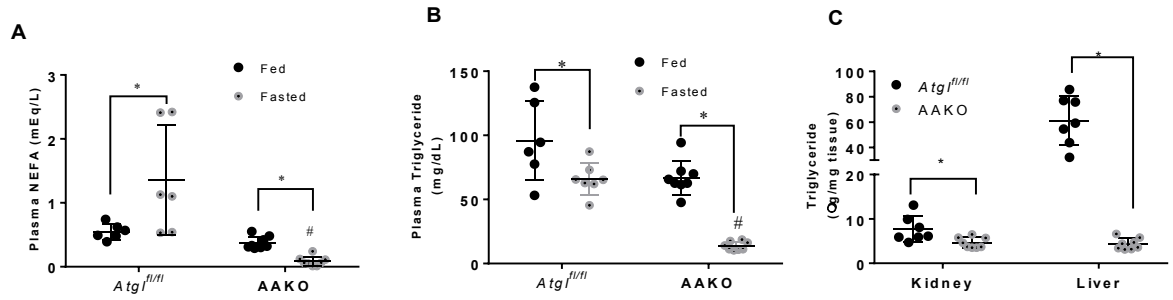

Figure 11. Plasma free fatty acids determine kidney triglyceride content (cont.)

(A-C) Female adipocyte *Atgl* knockout mice (AAKO) or littermate controls were fasted for 16 hs and sacrificed, N=6-8/group. A) Plasma NEFA and B) Triglyceride of AAKO and control mice in the fed and 16 h fasted state. C) Kidney and liver triglyceride of AAKO and control mice after a 16 h fast. *: $p<0.05$, # $p<0.05$. * indicate comparison between feeding status using unpaired Student's t-test. # Indicates comparison between genotype using the two-way ANOVA Tukey's multiple comparison test. Results are presented as means ± SD.

3.4.5 Lipid accumulation in the kidney is not dependent on CD36. We then asked whether NEFA uptake required CD36, a known fatty acid transporter highly expressed in the kidney and increased 2-fold with fasting (Figure 7B). However, uptake study of oleic acid into kidneys from *Cd36*$^{-/-}$ mice was not decreased (Figure 12A,B), and kidneys from *Cd36*$^{-/-}$ mice had the same amount of TG increase with fasting as did wild-type mice (Figure 12C) compared to Figure 5E). Thus, the kidney does not require CD36 for fasting-induced lipid accumulation.

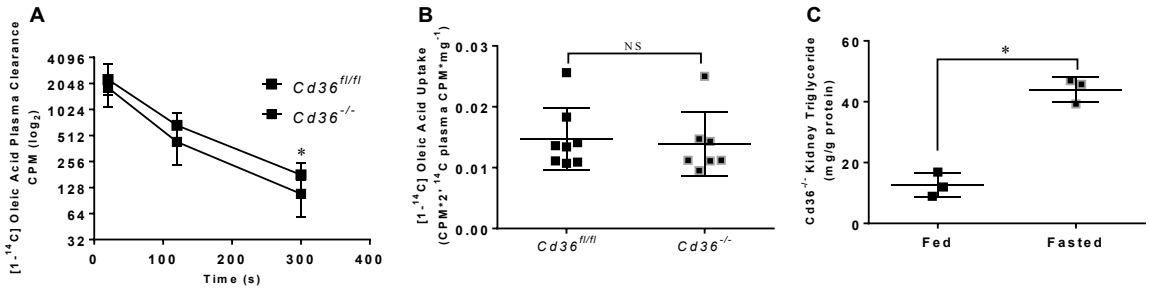

Figure 12. Kidney triglyceride accumulation do not require CD36 for transport fatty acid transport

(A-C) [$^{1\text{-}14}$C]OA was injected intravenously into male mice. Presence of radioactive signal was measured in plasma or tissue homogenate as mentioned before. A) Plasma clearance of [$^{1\text{-}14}$C]OA over time, N=8-9/group. B) OA uptake in fasted *Cd36*$^{fl/fl}$ and *Cd36*$^{-/-}$ N= 8-9/group. Kidney lipids were extracted from kidneys of *Cd36*$^{-/-}$ in the fed and fasted state using 2:1 methanol:chloroform. C) Kidney triglyceride in fed and fasted *Cd36*$^{-/-}$, N=3/group. *: $p<0.05$, # $p<0.05$. * indicates comparison between feeding status using unpaired Student's t-test. Results are presented as means ± SD.

3.4.6 Triglyceride accumulation in the kidney does not require LpL or circulating lipoproteins. LpL is required for fasting TG accumulation in the heart (173); like in the heart but not in the liver, LpL is amply expressed in the kidney (178,199). To assess whether LpL and lipoproteins are necessary for TG accumulation in the kidney, we injected mice with a surfactant compound, poloxamer 407 (P407). P407 blocks the clearance of lipoproteins from the circulation and causes lipemia (200). In our mice, TG increased from ~50 mg/dL to over 5000 mg/dL (Figure 13A). P407 also increased plasma NEFAs in both fed and fasted mice (Figure 13B), likely due to association with TG-rich lipoproteins (173). P407 did not decrease TG accumulation in the kidney after a fast, but led to a ~20% increase in TGs during the fed state (Figure 13C). Similar results were found in females (Figure 13D-F) as in males.

To further explore the role of LpL, we studied mice with a tamoxifen-inducible deletion of LpL (i$Lpl^{-/-}$) (184). We assessed the changes in renal TG accumulation before and after an overnight fast and compared them to floxed littermate ($Lpl^{fl/fl}$) controls also injected with tamoxifen. Two weeks after the final tamoxifen injections, plasma TGs increased more than 20-fold in both fed and fasted i$Lpl^{-/-}$ mice (Figure 13G). Plasma NEFAs slightly increased as well in i$Lpl^{-/-}$ mice after fasting (Figure 13H). TGs in the kidney did not decrease, but rather increased by 25% after fasting, compared to the fasting $iLpl^{fl/fl}$ group (Figure 13I). This might be due to the increased fatty acids in i$Lpl^{-/-}$ mice after fasting.

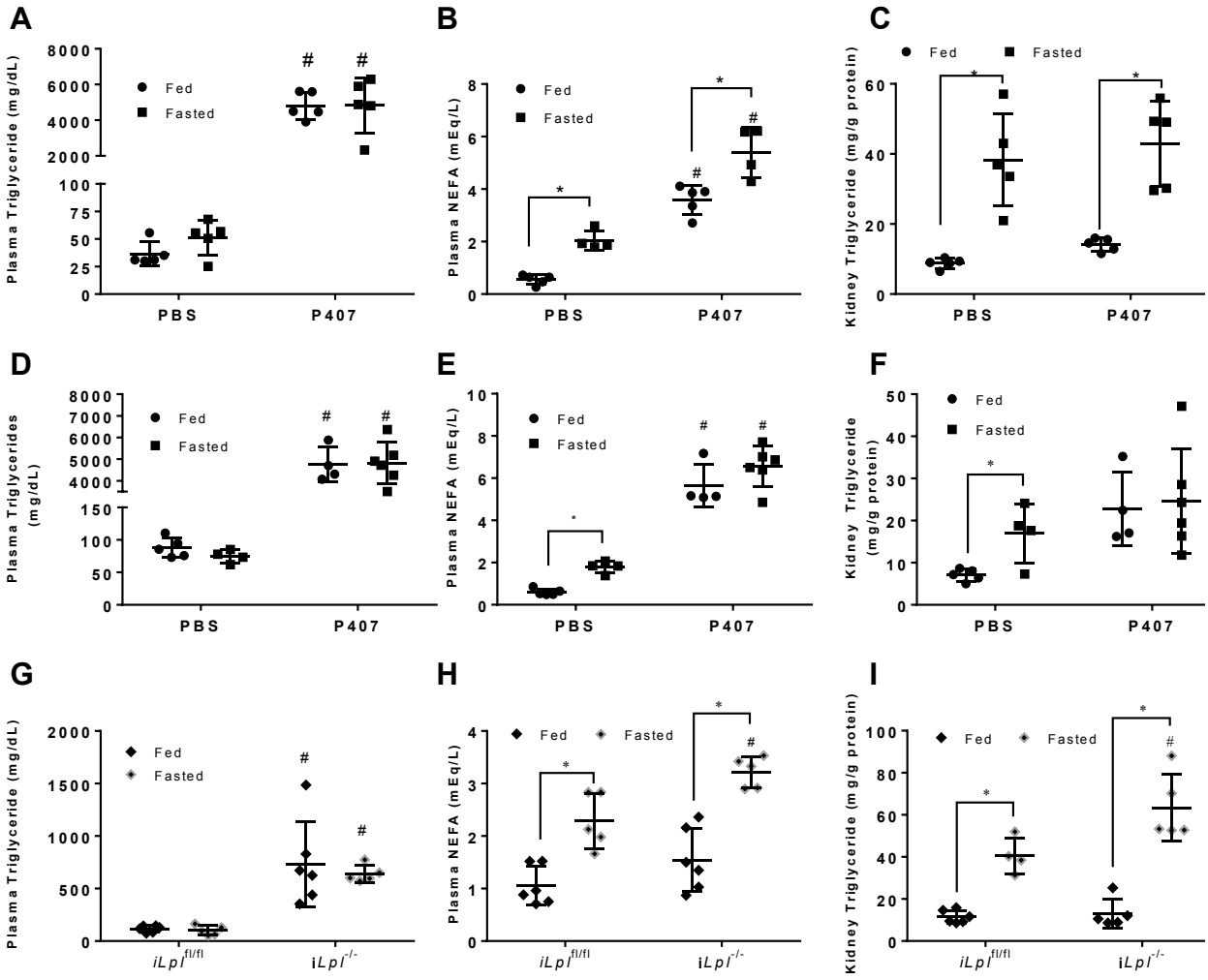

Figure 13. LpL is not required for triglyceride accumulation in the kidney

(A-C) Male mice were injected with poloxamer 407 (P407) or PBS equivalent and fasted or given food ad libitum for 16 hs (Top Panel). A) Plasma triglycerides and B) plasma NEFAs. C) Kidney triglyceride content. N= 4-5/group. (D-F) P407 repeated in females (middle panel) with same conditions as males. (G-I) Tamoxifen Inducible LpL floxed (i*Lpl*$^{fl/fl}$) and knock out (i*Lpl*$^{-/-}$) male mice were fasted or given ad libitum access to food for 16 hs. Blood was drawn for measurement of plasma lipids and kidney lipids were extracted and measured (Bottom panel). G) Plasma triglycerides and H) NEFAs. I) Triglyceride content of kidneys. N= 4-6/group. *: $p<0.05$, # $p<0.05$. * indicates comparison between feeding status using unpaired Student's t-test. #

indicates comparison between genotype or treatment using the two-way ANOVA Tukey's multiple comparison test.

We further explored whether lipoproteins are the source of fatty acids in the kidney by blocking microsomal triglyceride transfer protein (MTTP), a key regulator of lipoprotein formation in the liver and small intestines (201). After a 16 h fast, BMS-212122, a MTTP inhibitor (MTTPi), decreased plasma VLDL TGs by approximately 40% (Figure 14A). MTTPi treatment increased liver TGs (Figure 14B), but unexpectedly, the kidney TG level trended toward an increase (Figure 14B). It has been previously shown that the kidney can synthesize and secrete lipoproteins (139).

To test whether some of the effects of plasma TG reduction were masked by intra-renal MTTP inhibition, we fasted mice with a liver-specific knockdown of *Mttp* (L-*Mttp*$^{-/-}$) (202) for 16 h. Plasma TGs were decreased several fold (Figure 14C) while liver TGs in the L-*Mttp*$^{-/-}$ were increased. Fasting kidney TG levels were slightly affected by loss of *Mttp* in the liver (Figure 14D). These results suggest that circulating lipoproteins and LpL play a minimal role, if any, in lipid accumulation in the kidney during a fast.

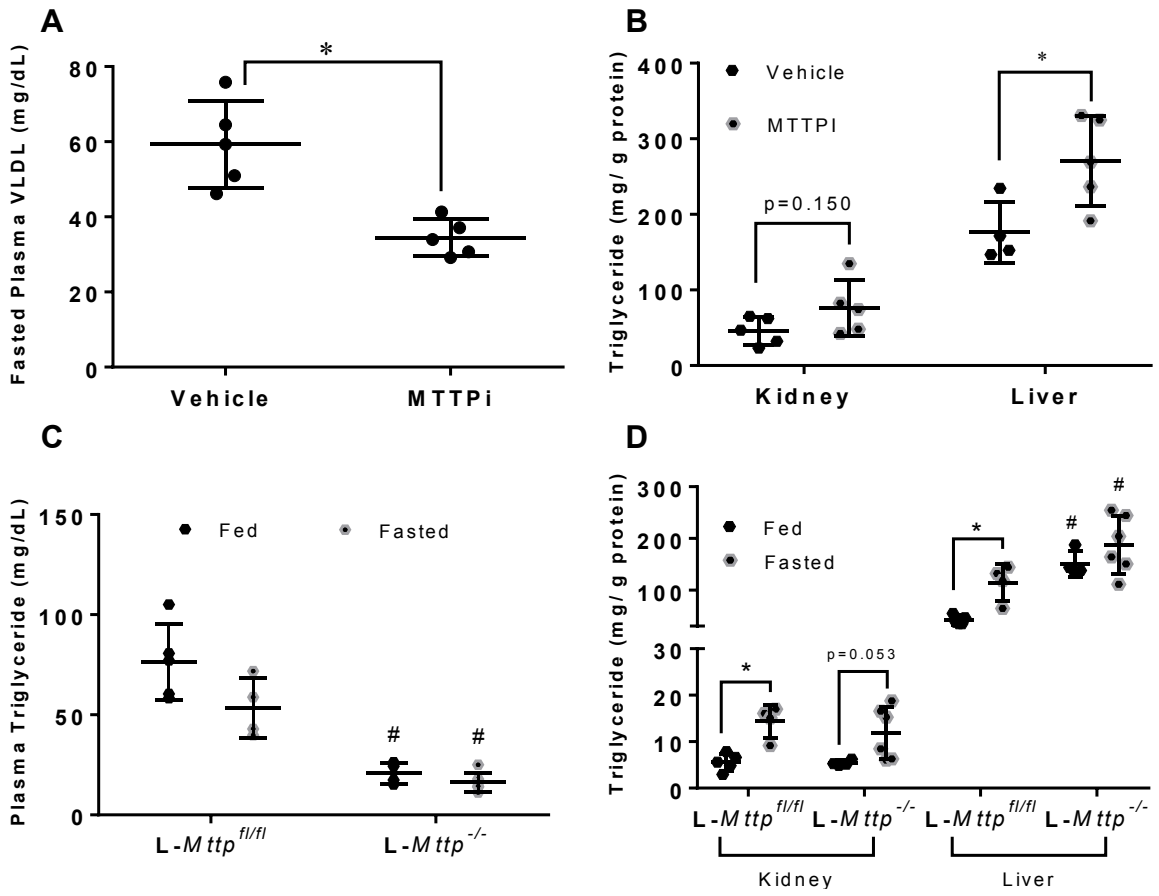

Figure 14. Triglyceride-rich lipoproteins are not a significant source of triglyceride in the kidney

(A-B) Whole body blockade of microsomal triglyceride transfer protein (MTTP) was achieved using BMS-212122 (MTTPi, N=4-5/group) given orally for seven days or vehicle (DMSO) equivalent to mice. Data obtained after a 16 h fast. A) Very-low density lipoprotein (VLDL) triglyceride levels obtained from ultracentrifugation of plasma of mice treated with MTTPi or vehicle. B) Kidney and liver triglyceride content of fasted mice treated with either MTTPi vehicle. (C-D) Liver-specific blockade of MTTP was achieved with a liver-specific knockout of MTTP (L-*Mttp*$^{-/-}$, N=4-6/group). C) Plasma triglycerides of L-*Mttp*$^{-/-}$ mice versus floxed littermate controls. D) Kidney and liver triglyceride content of L-*Mttp*$^{-/-}$ mice versus littermate controls. Experiments were performed in male mice.*: $p<0.05$, # $p<0.05$. * indicates comparison

between feeding status using unpaired Student's t-test. # indicates comparison between genotype using the two-way ANOVA Tukey's multiple comparison test.

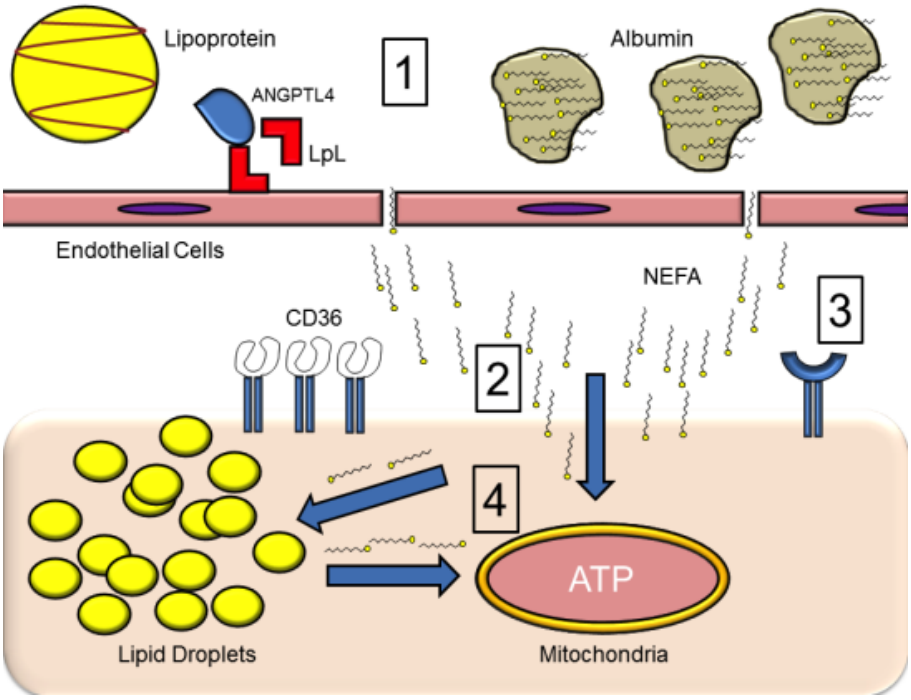

Figure 15. Triglyceride-rich lipoproteins are not a significant source of triglyceride in the kidney (cont.)

Summary figure of research data: 1) During fasting Angptl4 inhibits LpL, so that triglycerides on lipoproteins cannot be hydrolyzed, thus fatty acid loaded albumin is the primary exogenous source of fatty acids for the kidney. 2) Though CD36 is amply expressed on the kidney, it is not required for the transport of fatty acids into the kidney during fasting, which might involve non-receptor diffusion across the member. 3) Though CD36 does not appear to act as a major transporter, it does not discount that other transporters may exist. 4) Once inside the cell, fatty acid is shuttled to the mitochondria where it can be oxidized for ATP. If the rate of fatty acid flux into the cells is far greater than the cells capacity for oxidization, excess fatty acids are stored in LDs. Stored fatty acids can also be released from the LDs and oxidized.

3.4 Discussion

Lipid accumulates in the kidney cortex during diseased and non-diseased states. The source of the lipids and the mechanism(s) by which they accumulate is unclear. In addition, little information is available to determine whether lipid accumulations are pathological or physiological. In this study, we evaluated the physiologic regulation of kidney lipids during fasting and explored the roles of lipid uptake processes that are known to affect TG storage in other tissues. Unlike muscles, kidney lipid storage is not dependent on either LpL or CD36 and correlates with plasma NEFAs. Further data indicated that kidney TG accumulation was dependent on NEFAs from the plasma. Using [^{14}C]oleic acid, we showed that the kidney indeed takes up more NEFAs during a fast (Figure 10B). We further showed that increasing serum NEFA levels in the fed state with CL 315,343, a β3-adrenergic receptor agonist, markedly increased kidney TG accumulation (Figure 10C,D). At the same time, heart TGs were reduced with CL 315,343 treatment; these data are consistent with our previous studies indicating that circulating TGs and not NEFAs are the source of cardiac TG (173). Conversely, lowering circulating NEFAs using AAKO mice Figure 11B) led to reduced kidney TG (Figure 11C). Our results confirm studies which measured arterial versus venous blood and showed that the kidney takes up more fatty acid during fasting (203).

Fasting-induced lipid accumulation was associated with increased expression of genes that modulated fatty acid metabolism and TG storage and not with greater accumulation of ceramides. Upon refeeding, there was a reverse trend of metabolic genes in the kidney (Figure 8D), as well as decreased plasma NEFA (Figure 8B), however no change in kidney TGs (Figure 8C). This suggests after a fast, the kidney is slow to release TG or fatty acid uptake is curbed due to a decrease of circulating NEFAs. In many tissues, dysfunction is associated with the

accumulation of potentially toxic lipids such as ceramides. The non-pathological storage of NEFAs as TG components was suggested by an increase in the LD proteins *Plin2* and *5* (Figure 7B), This data indicates a capacity for safely storing excess TG. Following fasting, our lipidomic analysis showed a trend to an increase in fatty acyl CoAs, a decrease in C16 acyl-carnitine, and a decrease in long chain ceramides and glycosphingolipids. An increase in skeletal muscle acyl-carnitines was associated with incomplete FAO in high-fat diet fed animals (204). Therefore, the decrease in renal acyl-carnitines in the fasted state could result from more complete beta-oxidation. An increase in ceramides is associated with cellular apoptosis as well as insulin resistance (90,197,198). There is a dearth of information on the role of ceramides in kidney injury and some of what is reported is conflicting. Sas *et al*. reported that in a diabetic obesity model of kidney injury, long chain ceramides and glycosphingolipids are reduced (190). Others have reported an increase in glycosphingolipids, a product of ceramides, associated with diabetic nephropathy and mesangial expansion (205).

To achieve a global perspective on the changes in kidney lipid metabolism during fasting, we performed RNA sequencing of the kidney. Several enzymes associated with increased ceramide production were reduced. mRNA levels of sphingomyelin phosphodiesterase1 (Table 4), which is responsible for hydrolyzing sphingolipids to form ceramides in the fasted kidney, were reduced (205) and serine palmitoyltransferase subunits 1 and 2 (Table 4) that control *de novo* synthesis of ceramide, were unchanged

FAO appeared to increase with fasting, and *de novo* synthesis did not appear to increase. Though this was not measured directly, our indirect data strongly suggest this is the case. The mRNA levels of genes in the lipid synthesis pathway were down regulated, while genes in the lipid oxidation pathway, mitochondrial electron transport, and fatty acid transport were up

regulated (Figure 6A). The PPAR pathway was the most differentially regulated pathway amongst those in the KEGG database, which have been shown to regulate FAO genes (Table 3) (206). These data suggest that along with greater TG storage, the kidney is accumulating an excess supply of substrate for storage while catabolizing more lipids for energy. During fasting, many tissues burn fats rather than glucose, and like the kidney, some of these tissues also store lipids perhaps as a local energy supply to use in times of greater energy requirements (207). The gene expression profile in the kidney implies greater FAO during fasting. This differs from the heart, which also accumulates TGs during fasting, but does not show the same pattern of increased FAO genes (173).

The increase in FAO during fasting is contrary to what is reported in kidney injury. FAO-associated genes are down regulated in the kidneys of mice with folic acid-induced nephropathy as well as in humans with CKD (152). However, during early diabetic kidney disease, when eGFR is not significantly decreased, beta-oxidation is increased (190,191). Therefore, fasting and early diabetes may reflect a need for greater energy requirements by intact tubular cells in the kidney, while CKD illustrates an example of pathologic injury and lipid accumulation due to reduced lipid oxidation.

We sought to determine the transporter required for renal NEFA uptake. A logical transporter was CD36; our quantitative PCR showed an increased trend of *Cd36* mRNA levels in the kidney during the fasted state Figure 7A). CD36 is a long-chain fatty acid transporter that is important for the uptake of fatty acids in various tissues (208). Surprisingly, [^{14}C]oleic acid uptake in fasted *Cd36*$^{-/-}$ mouse kidneys was the same as in controls (Figure 12B). TG content in the kidney also tripled after a fast in *Cd36*$^{-/-}$ mice (Figure 12C). TG levels in the fasted *Cd36*$^{-/-}$ mouse kidneys were higher when compared to fasted wild-type mice (Figure 5E). This is likely

due to elevated NEFA in the plasma due to the defect in peripheral NEFA uptake by the heart and skeletal muscle (30). Our data has demonstrated that CD36 is not necessary for fatty acid uptake in kidneys from fasted mice and at first glance appear to contradict the studies of. Kang, *et al.* who showed that overexpression of *Cd36* in the proximal tubule increases TG accumulation in the kidney (152). While forced overexpression of *Cd36* will lead to accumulation of TG in the kidney, we show that it is not necessary for fatty acid transport or TG accumulation in the kidney. It is possible that other fatty acid transporters, such as those from the fatty acid transport protein (FATP) family (209,210), are responsible for uptake in the kidney. However, these FATPs are predominantly intracellular and rather than being transmembrane transporters, are thought to trap intracellular fatty acids by acyl-CoA synthetase actions (193). Another possible route of NEFA uptake into the kidney is *via* uptake of albumin. However, the very rapid turnover of NEFAs compared to that of albumin makes this hypothesis unlikely. Moreover, mRNA levels of purported albumin transporters such as *Lrp2* (megalin) were decreased according to our RNA sequencing (Figure 6). Alternatively, fatty acids may enter the kidney *via* passive diffusion through the membranes, which can occur when fatty acid levels are high (20).

We tested whether fasting-induced renal TGs were derived from circulating lipoproteins and whether kidney TG accumulation requires LpL-mediated hydrolysis of TG to release NEFAs. Blocking or deleting LpL did not decrease TG accumulation in the kidney after a fast. Although LpL is abundant in the kidney during the fasted state there was an increase expression of *Angptl4* may inhibit LpL actions (Figure 6C). *Angptl4* is thought to dissociate the LpL dimer, thus inhibiting its enzymatic action (211). Our data are consistent with those of Ruge *et al*. who reported that kidney LpL activity is highest in the fed state and lowest in the fasted state of mice

(159); we now show that this is likely due to Angptl4. Since LpL loss did not play a role in lipid accumulation in the kidney in either the fed or fasted state, the role of LpL in the kidney is unclear.

In support of our finding that LpL does not play a major role in lipid accumulation, we found that circulating TG levels did not correlate with intracellular lipid content of the kidney. We lowered circulating TGs two ways: pharmacologically with an MTTPi (Figure 14A) and genetically by specifically knocking out *Mttp* in the liver (Figure 14C). The kidney, like the liver, is able to form and release lipoproteins (139). This is highlighted by our data showing that the kidney retains TGs when treated with MTTPi, with a trend to increased kidney TG content after a fast (Figure 10B). When we lowered circulating lipoprotein levels by deleting *Mttp* in the liver, plasma TG levels were markedly reduced, but TG content in the kidney remained mostly unchanged although some of the fasted L-*Mttp*$^{-/-}$ mice had reduced TGs (Figure 14D). Because some NEFAs associate with lipoproteins, this reduction in kidney TG may be due to fewer circulating lipoproteins carrying NEFAs. These MTTP inhibition studies showed that the kidney does not largely rely on exogenous lipoproteins for TGs.

In conclusion, we have found that the kidney primarily takes up NEFAs rather than lipoproteins, and high serum levels of NEFAs cause greater lipid accumulation in the kidney. Figure 15 summarizes the findings from our study. The kidney, despite having high levels of expression of *Cd36* and *Lpl*, does not require either of these proteins for fatty acid uptake during fasting. During fasting, LpL actions in the kidney are likely inhibited by increased Angptl4. Taken together, our data shows that the kidney behaves similarly to the liver with respect to certain aspects of lipid metabolism (e.g. lipid uptake does not involve LpL or CD36). Both the liver and the kidney receive abundant cardiac output of blood, are intensely metabolically active,

and might not depend on a high affinity localized fatty acid uptake pathway. Rather, a lower affinity but higher capacity fatty acid uptake process may be sufficient to extract fatty acids from the circulation. This high volume of blood supply to the kidney may also be why NEFAs on albumin are sufficient for lipid accumulation in the kidney. Comparably less perfused tissues, such as skeletal muscle and adipose tissue, would require the large amounts of fatty acids, in the form of TG, and also the actions of a high affinity NEFA transporter such as CD36. It should be noted that the molecular events required for NEFA uptake by the liver are incompletely characterized and might require a number of known or unique transporters (212). The fatty acids are either shuttled to the mitochondria for oxidation or to LDs for storage in the form of TG. These stored TGs can also be hydrolyzed by HSL and ATGL to release fatty acids for oxidation. Little in the way of kidney lipid metabolism has been studied despite lipid accumulation being present in nearly all forms of kidney injury. Our data add to our understanding of lipid metabolism in the non-diseased kidney.

Acknowledgements

We would like to acknowledge NYULMC Office of Collaborative Science for their technical services, supported in part by the Cancer Center Support Grant P30CA016087, at the Laura and Isaac Perlmutter Cancer Center. We also acknowledge the editing assistance of Stephanie Chiang.

This work was supported by the following grants from the National Institutes of Health: HL45095 and HL73029 (IJG); DK094292, DK089503, DK082841, DK081943 and DK097153 (SP); 2UL1TR000433 (KMS); R56DK046900 (MMH); DK090166 (EEK); DK087635, DK105821, DK108220 (KS); DK33301 (NAA)

Disclosure: All the authors declared no competing interests

Table 4 (Supplemental) Genes Associated with ceramide biosynthesis

Gene Name	Ensembl Gene ID	ΔLog2	padj	Fed				Fasted			
Acer2	ENSMUSG00000038007	0.392	0.121	500.898	776.04	1010.29	507.89	706.85	1097.76	1195.03	784.25
Acer3	ENSMUSG00000030760	0.170	0.238	882.712	797.21	643.27	792.44	850.08	925.51	891.00	819.82
Arsa	ENSMUSG00000022620	-0.161	0.347	361.718	323.12	399.91	386.56	323.66	325.21	267.59	353.00
Asah1	ENSMUSG00000031591	-0.158	0.208	2952.544	2619.00	2353.39	2551.27	2185.65	2407.62	2338.28	2201.60
Asah2	ENSMUSG00000024887	0.058	0.675	3059.720	3469.61	2958.51	3524.10	3295.21	3199.44	3648.40	3366.42
B4galt6	ENSMUSG00000056124	-0.409	0.016	770.326	812.86	891.89	547.62	526.42	470.47	609.03	541.51
Cerk	ENSMUSG00000035891	0.249	0.143	745.021	897.55	782.71	595.94	878.91	1018.06	999.38	904.29
Cers2	ENSMUSG00000015714	0.071	0.721	5180.163	5217.76	3800.42	5054.22	4844.70	5929.70	4968.12	4794.44
Cers3	ENSMUSG00000030510	0.143	NA	2.233	4.60	3.95	6.44	7.44	5.14	1.92	6.22
Cers4	ENSMUSG00000008206	0.165	0.262	250.077	263.28	231.52	260.93	273.44	281.51	269.51	319.21
Cers5	ENSMUSG00000023021	0.039	0.833	1193.819	1204.10	1014.23	1195.10	1157.93	1102.90	1257.38	1080.35
Cers6	ENSMUSG00000027035	-0.082	0.526	2834.204	2737.76	2755.93	2728.44	2511.17	2601.72	2991.42	2596.40
Degs1	ENSMUSG00000038633	-0.383	0.001	5157.835	4875.31	4302.93	4924.29	3543.54	3977.13	3199.54	3344.19
Degs2	ENSMUSG00000021263	0.022	0.945	1215.403	1130.45	776.13	1407.71	1023.07	1416.55	1135.57	981.65
Gal3st1	ENSMUSG00000049721	-0.263	0.067	711.528	624.14	516.98	528.29	503.16	502.60	464.20	521.06
Galc	ENSMUSG00000021003	-0.234	0.127	2872.162	2816.01	3835.94	2738.10	2565.11	2929.50	2553.11	2355.43
Gba	ENSMUSG00000028048	-0.111	0.356	980.956	1013.54	823.49	945.99	875.19	862.53	846.88	874.95
Gba2	ENSMUSG00000028467	-0.146	0.409	366.184	374.67	415.69	414.47	386.91	362.49	373.09	376.12
Gla	ENSMUSG00000031266	0.117	0.559	193.512	208.05	161.80	219.05	198.10	210.81	218.67	201.84
Glb1	ENSMUSG00000045594	-0.256	0.109	4601.861	4898.32	4287.14	4772.89	3529.59	3952.71	3830.63	3155.69
Kdsr	ENSMUSG00000009905	0.011	0.945	1079.945	1096.39	1123.42	1100.61	1140.26	1225.02	1063.64	1012.77
Neu1	ENSMUSG00000007038	-0.454	0.000	13653.005	17105.00	14179.54	16458.69	11170.98	12448.13	10569.24	10650.56
Neu2	ENSMUSG00000079434	-0.200	0.417	183.836	243.95	148.65	241.60	192.52	140.11	211.00	173.39
Neu3	ENSMUSG00000035239	0.116	0.674	113.130	167.54	122.34	100.93	139.51	129.83	117.97	165.39
Phlpp1	ENSMUSG00000044340	0.044	0.767	1213.915	1462.78	1385.20	1342.21	1408.11	1334.28	1447.28	1478.70
Phlpp2	ENSMUSG00000031732	-0.086	0.559	813.494	842.32	966.88	1017.93	854.73	813.68	889.08	876.73
Ppap2b	ENSMUSG00000028517	0.065	0.609	1722.255	1812.59	1724.59	1808.22	2057.30	1754.62	1927.78	1810.36
Sgms1	ENSMUSG00000040451	0.299	0.000	2400.291	2515.90	2427.06	2582.41	3043.16	3208.44	2951.14	2832.92
Sgms2	ENSMUSG00000050931	0.061	0.619	6211.730	6336.24	6345.87	6598.29	6458.35	5916.85	6741.49	7052.95
Sgpl1	ENSMUSG00000020097	0.081	0.432	2632.505	2723.03	2399.43	2612.47	2626.50	2762.39	2690.26	2946.73
Sgpp1	ENSMUSG00000021054	0.283	0.029	5652.779	5315.34	5002.77	6073.22	5915.20	7324.39	6910.29	6061.52
Sgpp2	ENSMUSG00000032908	0.011	0.957	730.135	660.04	801.13	672.18	778.46	628.58	775.91	710.45
Smpd1	ENSMUSG00000037049	-0.265	0.022	2962.220	2874.92	2537.56	2932.46	2207.04	2379.34	2293.20	2120.69
Smpd2	ENSMUSG00000019822	0.079	0.697	1924.699	2077.71	2019.26	1949.96	1765.26	2173.67	2226.06	1855.71
Smpd3	ENSMUSG00000031906	-0.169	0.677	22.328	11.05	17.10	11.81	16.74	16.71	17.26	13.34
Smpd4	ENSMUSG00000005899	-0.038	0.751	788.933	793.53	786.66	823.58	763.58	782.83	789.34	794.92
Sphk1	ENSMUSG00000061878	0.627	0.000	117.596	150.05	169.70	118.11	196.24	221.09	246.49	225.85
Sphk2	ENSMUSG00000057342	0.037	0.883	1064.315	1197.65	1512.80	1438.85	1096.54	1410.12	1293.82	1512.49
Sptlc1	ENSMUSG00000021468	-0.060	0.748	2166.588	2002.23	1677.24	2034.79	1789.44	2006.56	1868.32	1660.09
Sptlc2	ENSMUSG00000021036	-0.149	0.204	3510.751	3695.14	3479.44	3779.66	3143.61	3799.74	3137.20	3041.87
Sptlc3	ENSMUSG00000039092	0.485	0.031	66.241	65.36	59.20	92.34	91.15	129.83	77.69	114.70
Ugcg	ENSMUSG00000028381	-0.183	0.139	718.971	733.69	772.19	671.10	611.05	650.43	658.90	560.18
Ugt8a	ENSMUSG00000032854	-0.461	0.033	5641.615	4114.00	3955.64	3431.76	2433.97	2488.60	3885.30	2255.84

Genes were identified using sphingolipid metabolism KEGG database (Pathway map mmu00600). Differentially expressed genes were identified with Bioconductor package DEseq2 (3.2) and Benjamini and Hochberg's method was used to control for false discovery rate (FDR).

Chapter 4: Krüppel-Like Factors and S100 proteins

4.1 Introduction to Krüppel-like factors

Krüppel-like factors (KLFs) are Zn^{2+} finger transcription factors that control a variety of biological functions such as development, differentiation, proliferation, and metabolism. Humans express 18 isoforms of KLF between various cells types which are highly conserved amongst all mammals (213). However, it is not clear at the moment if KLF18 is a gene or pseudogene. Human KLFs are broadly divided into three groups of structural and functional homology. Group 1 (KLFs 3, 8, and 12) are transcriptional repressors when they interact with C-terminal binding protein (CtBP) (213). Group 2 (KLFs 1, 2, 4, 5, 6, and 7) are transcriptional activators (213). Finally, Group 3 (KLFs 9, 10, 11, 13, 14, and 16) are repressors when they interact with the co-repressor Sin3A (213). KLFs 15, 17, and 18 remain unclassified. However, some KLFs like KLF4 and KLF5 can act as both repressors and activators (214). All isoforms have a conserved C-terminus domain and variable N-terminal domain. This allows for post-translational modifications that influences both their translocation to the nucleus and activation or repressive roles (214). Table 5 summarizes the various KLF isoforms and their major functions in biology.

Table 5. A summary of the notable roles of KLF1-18

KLF	Notable Roles	Ref
KLF1	Erythrocyte and megakaryocyte differentiation.	(215) (216)
KLF2	T-cell quiescence; response to shear stress in endothelial cells; lipid uptake in macrophages.	(217) (218) (219)
KLF3	Inhibits adipogenesis.	(220)
KLF4	Inhibits cell cycle progression; monocyte differentiation to macrophages; Stem cell pluripotency.	(221) (222) (223) (224)
KLF5	Promotes cell cycle progression; cardiac remodeling; adipose tissue differentiation.	(221)
KLF6	Tumor suppressor gene.	(225)
KLF7	Inhibits adipogenesis; SNPs associated with T2DM.	(226) (227) (228)
KLF8	Epithelial–mesenchymal transition in cancers.	(229)
KLF9	Negative regulator of estrogen receptor signaling in endometrial cancer.	(230)
KLF10	Regulatory T-cell development; osteoblast differentiation.	(231) (232)
KLF11	Pancreatic organogenesis; insulin production	(233) (234)
KLF12	Gastric tumor growth	(235)
KLF13	Cardiac development; T-cell activation	(236) (237)
KLF14	SNPs associated with cardiovascular disease; increase in macrophage efflux by regulation of ApoA-1	(238) (239)
KLF15	Hypertrophy in heart; expression of *Glut4* in adipose tissue and skeletal muscle; gluconeogenesis in liver; *de novo* lipogenesis in the liver.	(240) (241) (242)
KLF16	Regulates dopamine receptor in the brain; out-growth of retinal ganglion cells	(243) (244)
KLF17	Tumor suppressor gene which mediates epithelial-mesenchymal transition	(245)
KLF18	No information as of yet on its biological role	(246)

4.2 KLF5 in Health and Disease

Translational research interest surrounding KLF5 stems from its pro-proliferative and anti-apoptotic activity. Its actions and downstream targets have been well characterized in the cells of the intestinal crypts, where it is most highly expressed (247). However, KLF5 controls many cellular pathways in a variety of tissues. KLF5 itself is regulated transcriptionally by Sp1, a transcription factor in a family of structural similarity to KLFs (248). KLF5 uniquely acts to repress or activate gene expression depending on its interaction with transcriptional co-regulators or post-translational modification (249). For example, acetylated KLF5 creates a complex with other co-repressors to repress p21 transcription (250). However, acetylated KLF5 can create another complex with co-activators to transactivate expression of p15 (251). KLF5 has promiscuous and flexible interactions that allow it to play a role in many biological processes and disease progression.

4.2.1 Proliferation and Cancers. KLF5 is a well-characterized regulator of cellular proliferation and apoptosis. In many cell types KLF5 works in opposition to KLF4, which acts to inhibit cellular proliferation(221) (252) (253) (254). Cell cycle progression proteins such as cyclins and cyclin-dependent kinases are transactivated by KLF5, while repressing transcription of cell cycle inhibitors p27 and p15 (255,256) (257) (258). KLF5 is upregulated by mitogens *via* MAPK/EGR-1 signaling pathway and repressed by activation of retinoic acid receptor (RAR) signaling (259) (260) (261) (262). KLF is most active in rapidly dividing cells such as epithelial cells in the crypts of the intestines (263). Total body deletion of *Klf5* is embryonic lethal, however $Klf5^{+/-}$ are born with abnormal villi and intestinal fibrosis (264). $Klf5^{+/-}$ mice are sensitive to bacterial and inflammatory insults to the intestines as they are not able to reconstitute a healthy epithelium (265).

Taking into account its role in regulating the cell cycle, research interest in KLF5 and cancer progression has increased over the years. Much of this research has been done in solid tumors of the intestines. In colorectal cancer cells, KLF5 regulates proto-oncogene serine/threonine-protein kinase, a negative regulator of bcl-2-associated death promoter (266) (267). Therefore, knockdown of *KLF5* in these cells made them susceptible to DNA-damaging agents (266). Induction of KLF5 by lysophosphatidic acid causes proliferation of several colon cancer cell lines (268). Immunohistochemistry analysis of human and mouse intestinal tumor samples with an oncogenic KRAS mutation contain increased levels of KLF5 (269) (270). KLF5 research in the intestine provided information regarding its role in proliferation as well as progression in many intestinal tumors.

4.2.2 Cardiac Remodeling and smooth muscle cell vasculature. Like KLF15 (Table 5), KLF5 plays a role in cardiac hypertrophy. While KLF15 inhibits cardiac hypertrophy (240), KLF5 promotes it. This is primarily due to the pro-fibrotic actions of KLF5. Following administration of AngII, *Klf5*$^{+/-}$ mice have less cardiac hypertrophy and fibrosis than wild-type controls (264). Cultured cardiac fibroblasts treated with AngII have increased expression of the tissue remodeling protein platelet-derived growth factor-A (PDGF-A) and *KLF5* (264). When treated with Am80, a synthetic retinoid receptor agonist, mice have reduced cardiac hypertrophy after being given AngII (264), however this phenotype was due to fibroblasts, not cardiomyocyte, KLF5.

Smooth muscle cells (SMCs) line the walls of hallow organs and are sensitive to contraction and pressure. KLF5 has high expression in fetal SMCs and after vascular injury (271). KLF5 positive human coronary artery specimens were highly associated with restenosis compared with KLF5 negative arteries (271). KLF5 is induced during cardiac allograft

atherosclerosis, vein graft hyperplasia, and AngII hypertension (272) (273) (264). These studies suggest a role for KLF5 after vascular injury. Indeed, KLF5 activates inflammatory growth factors such as inducible nitric oxide synthase, plasminogen activator inhibitor-1, PDGF-A and vascular endothelial growth factor receptor to stimulate proliferation of SMCs (213). The mechanism by which KLF5 regulates SMC proliferation has been identified. AngII stimulates mitogen-activated protein kinase/extracellular signaling-regulated kinase-1 (MAPK/ERK)-1, which then phosphorylates KLF5 by allowing it to bind with other transcriptional regulators such as c-Jun and RARα (274).

4.2.3 Adipose Tissue Development Metabolism. Pre-adipocytes in the perivascular niche become adult adipocytes with a unilocular lipid droplet. This transition is thought to be due, in part, to activity of PPARγ (275). KLF5 has also been shown to control adipogenesis as well by regulating PPARγ via CEBP signaling (276). *Klf5*$^{+/-}$ mice are lipodystrophic due to KLF5 regulating genes that promote adipogenesis, such as CCAAT/enhancer-binding protein alpha (*Cebpa)* and *Pparg2* (276). Overexpression of *Klf5* in 3T3-L1 pre-adipocytes induces differentiation of these cells (276).

Klf5$^{+/-}$ mice are resistant to diet induced obesity even though they consume more food. (277). However, *Klf5*$^{+/-}$ mice have increased energy expenditure in their skeletal muscle as well. Sumoylated KLF5 forms a complex with unliganded PPARδ and co-repressors to suppress lipid oxidation and uncoupling genes in the skeletal muscle (277). Upon exposure to a PPARδ agonist, KLF5 is desumoylated and becomes associated with a transcriptionally active complex (277). Thus, metabolic regulation by KLF5 is dependent on its posttranslational state. KLF5 also regulates lipid and energy metabolism *via* regulation of PPARα. Cardiomyocyte-specific deletion of *Klf5* results in reduced expression of *Ppara* and PPARα target genes, such as *Lpl* and *Cd36*

(278). The hearts of these mice had reduced FAO, increased glucose oxidation and develop cardiac dysfunction with age (278). During sepsis, c-Jun out competes KLF5 for the *Ppara* promoter, leading to reduce cellular ATP, FAO, and heart failure (278).

4.2.4 Inflammation and Immunology. Circulating white blood cells (WBCs) originate from stem cell progenitors in the bone marrow (BM). Cells of the adaptive immune system are descended from a common lymphoid progenitor while cells of the innate immune system are descended from a common myeloid progenitor (CMP). KLF5 has been shown to play a role in differentiation of granulocytes. *Klf5* deleted specifically in the hematopoietic stem cell precursor causes a decrease in neutrophils in peripheral blood and an increase in eosinophils (279). *KLF5*, along with *KLF6*, has lower expression in acute myeloid leukemia (AML) blasts compared to normal granulocytes from healthy donors (280). Often, treatment with all-*trans* retinoic acid (ATRA) reduces *KLF5* expression. However, in the case of NB4 cells (a promyeloblastic leukemia cell line), treatment of ATRA caused an induction of KLF5 (280). Knockdown of *KLF5* in these cells attenuates differentiation into neutrophils (280). Elevated *KLF5* expression in AML may be due to hypermethylation of the *KLF5* promoter (281). These studies suggest that KLF5 is required for formation of granulocytes from stem cell precursors.

Regulation of inflammation and inflammatory cytokines by KLF5 is not well understood. Intestinal epithelial cells treated with LPS induce KLF5, which was associated with a concurrent increase in NF-κB (282). Conversely, when KLF5 is overexpressed in the myocardium, levels of inflammatory cytokines are lowered after oxygen-glucose deprivation/reperfusion (283). KLF5 has been shown to be directly associated with the transcriptional regulation of inflammatory calcium binding proteins S100A8 and S100A9. In a model of kidney injury, KLF5 acts in concert with C/EBPα to drive transcription of *S100a8* and *S100a9* in renal collecting duct

epithelial cells (284). During hyperglycemia in mice, neutrophils have increased expression of *S100a8/a9*, which is associated with an increase in *Klf5* expression (285). Thus, KLF5 may be an important mediator of inflammation in cells *via* control of S100A8 and S100A9.

4.3 S100 Proteins

The immune system can be triggered and mobilized by a variety of different molecules. Broadly, these molecules are either of host origin or foreign. Foreign molecules are referred to as pathogen-associated molecular patterns (PAMPs). Examples of PAMPs are lipopolysaccharide (LPS) from gram-negative bacteria, lipoteichoic acid from gram-positive bacteria, or viral nucleic acids (dsRNA or unmethylated CpG motifs) (286). These PAMPs are recognized by the innate immune system *via* toll-like receptors (TLRs) (286). Damage-associated molecular patterns (DAMPs) are nucleic or cytosolic proteins or nucleic acids released from host cells (286). When a cell is damaged, dying or injured it will release proteins or nucleic acid molecules that will signal the innate immune system. Of particular interest to our studies is the family of S100 proteins.

S100s are a 24-member family of relatively small (21kD), helix-loop-helix, calcium-binding proteins (287). S100 proteins are present in all vertebrates and expressed in epithelial, adipocytes, keratinocytes, and innate immune cells (287). These proteins have both intracellular and extracellular functions. Intracellular S100s have been shown to regulate enzyme activity, cytoskeletal dynamics and structure, cell growth, apoptosis and differentiation, and Ca^{2+} homeostasis (287). Some S100s are excreted and act as alarmins or DAMPs (288). As DAMPs, these molecules can bind to inflammatory receptors on immune cells such as the receptor for advanced glycation end products (RAGE) or TLRs (289).

4.3.1 Intracellular Roles of S100A8 and S100A9. S100A8 and S100A9 are often co-expressed and can function independently or together as a heterodimer complex (290) (291). S100A8 and S100A9 expression is induced by inflammatory molecules such as LPS, IL-1, TNF-α and interferon-gamma (IFN-γ) in a cell-type specific manner (292) (293). S100A8 and S100A9 play a role in managing reactive oxygen species (ROS) in innate immune cells for oxidative bursts. Phagocytic cells, like neutrophils and macrophages use oxidative bursts to neutralize bacteria or fungi. S100A8 and S100A9 make up approximately 40% of the cytosolic protein content of neutrophils and 1% of monocytes (294). In macrophages S100A8, but not S100A9, is induced by oxidative stress (295). S100A8 reduces ROS in cells by scavenging nitrous oxide (NO) and becoming S-nitrosylated S100A8 (296). S100A9 promotes ROS by activating NADPH oxidase (297).

Cells have a dynamic cytoskeletal system that allows for rapid changes of the plasma membrane. As a heterodimer, S100A8/A9 is involved in microtubule assembly, which is crucial for migration and degranulation of monocytes and neutrophils (298). Phosphorylation of S100A9 by MAPK inhibits S100A8/A9 microtubule assembly (298). Granulocytes of *S100a9*$^{-/-}$ mice contain less polymerized tubulin and less recruitment of granulocytes to during wound healing *in vivo* (298). Microtubule assembly and disassembly is regulated by intracellular Ca^{2+} levels (299). S100A8 and S100A9 indirectly regulate intracellular flux of Ca^{2+} by interacting with RAGE (300) or directly by binding and sequestering calcium. S100A8/A9 regulates Fc-receptor mediated phagocytosis by mediating Ca^{2+} depletion in cells (301).

4.3.2 Extracellular Roles of S100A8 and S100A9. S100A8 and S100A9 are secreted from cells as individual proteins or as components of a heterodimer complex called calprotectin. Calprotectin is released from cells after apoptosis/necrosis as molecular DAMPs and bind TLRs

and RAGE (302). S100A8 and S100A9 act as chemoattractant molecules for leukocytes (303) (304). In neutrophils, calprotectin promotes adhesion to fibronectin as well as degranulation (304) (305). Both S100A8 and S100A9 can act as anti-inflammatory molecules as well. As mentioned earlier, S100A8 and S100A9 manage intracellular ROS in cells. S100A8 acts as an anti-oxidant and suppresses mast cell activation by reducing intracellular ROS (306). S-glutathionylation of S100A9 suppresses adhesion rather than promoting it (307). As a heterodimer, high affinity Zn^{2+}-binding sites are exposed on the molecule, which give its antimicrobial properties, particularly against *S. aureus* (308) (309). Like its constituents, calprotectin is a chemoattractant for neutrophils. The release of calprotectin from granules in neutrophils requires intact microtubules and PKC activation (298). Calprotectin is a ligand for RAGE, where it potentiates an inflammatory signal mediated by myeloid differentiation primary response gene 88 (MyD88) (302) (285).

4.4 S100A8 and S100A9 in Health and Disease

4.4.1 Cancer. Tumors create a micro-environment that includes other somatic cell types including innate and adaptive immune cells (310). Tumors recruit myeloid-derived suppressor cells (MDSCs) resulting in T-cell tolerance and suppression of the anti-tumor immune response (291). Changes in expression and/or function of S100 proteins have been associated with cancer development clinically and experimentally. S100A8 and S100A9 are upregulated in skin, breast, lung, gastric colorectal, pancreatic and prostate cancer (291).

Calprotectin-positive myeloid cells are found within several epithelial cancers—suggesting a role for inflammation in cancer progression, mediated by these proteins. RAGE expression has been implicated in the progression of tumors and establishment of the tumor microenvironment (311). Tumors secrete inflammatory cytokines that attract MDSCs, amongst

other immune cell types. These MDSCs release calprotectin, activating RAGE on the tumor itself— promoting proliferation and survival. Calprotectin binds to RAGE on the surface of endothelial cells to facilitate migration of MDSCs. Calprotectin binding to RAGE on myeloid cells potentiates a downstream positive-feedback loop that activates transcription of S100A8 and S100A9, thus increasing further production of calprotectin in these cells (312). Therefore, calprotectin acts in concert with RAGE to create a tumor microenvironment that allows growth and proliferation while avoiding destruction by T-cells. Small molecule inhibitors that block the interaction of S100A9 with their receptors have been developed. Tasquinimod, which blocks the interaction of S100A9 with TLR4, improves progression-free survival of patients with metastatic prostate cancer (313) (314).

4.4.2 Obesity. There is conflicting data on whether calprotectin correlates with obesity. Some publications have reported a positive correlation between obesity and circulating calprotectin levels in the blood (315,316), others have not (317). BMI is a determinant of calprotectin plasma concentrations independent of diabetes status (318). Weight loss from Roux-en-Y gastric bypass leads to a decrease in circulating lipids as well as plasma calprotectin in human subjects (318). In adipose tissue from these subjects, calprotectin was increased mainly in the stromal vascular fraction and was positively associated with monocyte and macrophage markers (318). In *db/db* mice, circulating calprotectin levels were not significantly increased compared to lean animals (317). Neutrophil expression of *S100a8/a9* was also unaffected by obesity (317). This discrepancy in the data may be due to difference of the WBC population in mice and humans. Neutrophils, the chief producers of calprotectin, are the largest population of WBCs in humans, while in mice lymphocytes are the largest population.

Obesity leads to systemic inflammation (319), as well as local inflammation of the adipose tissue. Inflammation of the adipose tissue is characterized, in part, by influx of immune cells and increased release inflammatory cytokines (320). *Ob/ob* mice have increased *S100a8* and *S100a9* mRNA expression in the mature adipocyte and stromal vascular cell fraction, respectively, compared to lean controls (321). Adipose tissue macrophages promote myelopoiesis during obesity when calprotectin binds TLR4 on their cell membranes (317). This leads to interleukin-1beta (IL-1β) production from adipose tissue macrophages (317). IL-1β stimulates myelopoiesis in the BM, causing an increase circulating WBCs (317). Higher leukocyte numbers in the circulation leads to increased flux of monocytes into the adipose tissue, thus exacerbating adipose tissue inflammation (317).

4.4.3 Cardiovascular Disease and Diabetes. The role of inflammation in metabolic diseases is becoming increasingly apparent. Research continues to show calprotectin is associated with cardiovascular risk (322). Monocytes infiltrate atherosclerotic lesions and become fat-laden foam cells (323). Rupture-prone lesions are associated with calprotectin expression in macrophages and in the plasma (324) (325). S100A8 and S100A9 are present in atherosclerotic plaques. Patients with T2D have increased circulating levels of calprotectin, which is correlated with coronary artery disease severity in these patients (326) (327). S100A8 and S100A9 were among the top differentially expressed genes in a study of over 900 type 1 diabetic (T1D) and control subjects' peripheral blood mononuclear cells (328). Research using ultrasound analysis of plaques in T2D patients found a positive correlation between plaque vulnerability and plasma levels of calprotectin (329).

Mouse studies have afforded a glimpse into the direct role S100A8 and S100A9 play in atherogenic risk and progression. *S100a9*$^{-/-}$/ApoE$^{-/-}$ mice have an approximate one-third

reduction in lesion area when given a HFD compared to ApoE$^{-/-}$ mice (330). The lesion area of the double knockout mice had less recruitment of monocytes and neutrophils as well (330). To determine whether WBCs were the source of calprotectin-mediated inflammation, BM *S100a9*$^{-/-}$ was transplanted into *Ldlr*$^{-/-}$ (331). The transplantation of deficient marrow into HFD-fed mice had no effect on lesion area (331). This may be due to non-myeloid cells production of S100A8 and S100A9, such as SMCs (331). An atherosclerotic lesion is a heterogeneous mix of immune cells and vascular SMCs. There is evidence to suggest that calprotectin instigates an inflammatory phenotype in a cell-type specific manner (322). For example, calprotectin induces neutrophil and monocyte chemotaxis, adhesion, and NADPH oxidase activity (332) (333). Calprotectin activates endothelial cells and increases the expression of adhesion molecules on the surface and the permeability of these cells (334). This ultimately leads to invasion of more immune cells into the lesion area. The exogenous role of S100A8, S100A9 and calprotectin in atherogenic progressions appears to be mediated by TLR4 and RAGE signaling (335). Indeed, TLR4 or MyD88 deficient mice have reduced plaque size (336). Glucose induced ROS leads to increased neutrophil secretion of calprotectin (285). Calprotectin binds to RAGE in BM progenitors, stimulating proliferation and differentiation of CMPs (285). Increased circulating neutrophils and Ly6c^{hi} monocytes exacerbate lesions in diabetic *Ldlr*$^{-/-}$ mice (285). Lowering glucose pharmacologically with an SGLT2 inhibitor lowers circulating calprotectin and BM derived leukocytosis (285). These data suggest hyperglycemia is a key mediator between S100A8 and S100A9 and leukocytosis.

Chapter 5: KLF5 does not regulate neutrophil maturation, S100A8, and S100A9.

5.1 Introduction

Hyperglycemia causes the dysregulation of the innate immune system which leads to complications such as cardiovascular disease, kidney disease, and periodontal disease, to name a few (337). Patients with DM often have more circulating innate immune cells such as monocytes and neutrophils (338) (339). These cells can move into tissues and blood vessels and release inflammatory cytokines, which damage the tissues over time. Glucose *per se* may not necessarily be inflammatory, however during hyperglycemia, proteins and lipids can become glycated to create advanced glycation end products (AGEs). These AGEs bind the RAGE, causing a downstream inflammatory cascade (340).

RAGE is expressed constitutively embryonically, but is relatively low in differentiated cells (341). RAGE has multiple ligands in addition to AGEs including S100 proteins (discussed in chapter 4) (340). In the BM, calprotectin binds to RAGE on common myeloid-progenitor cells (CMPs)—stimulating myelopoiesis and differentiation into monocytes and neutrophils (285). Calprotectin is released from neutrophils during hyperglycemia, thus indirectly causing a systemic immune response (285). It is not yet fully understood how glucose stimulates the up-regulation and release of calprotectin from neutrophils or how S100A8 and S100A9 are transcriptionally regulated in neutrophils exposed to high levels of glucose.

A potential transcriptional regulator of S100A8 and S100A9 is KLF5. Fujiu K. *et al.* demonstrated that, in the absence of KLF5 in the renal collecting duct, the production of calprotectin after renal injury was suppressed. Suppression of *Klf5*, and thus calprotectin production, mitigated the influx of monocytes into the damaged cells (284). KLF5 is also adequately expressed in hematopoietic stem cells (HPSC), and deficiency of KLF5 in the

pluripotent stem cell results in decreased circulating neutrophils (279). This suggests KLF5 is necessary for granulocyte lineage determination.

In the current study, we generated a myeloid-specific *Klf5* KO (MKK) mouse to determine whether KLF5 regulates S100A8 and S100A9 production in streptozotocin (STZ)-induced diabetes. We hypothesized that absence of KLF5 will reduce gene expression of S100A8/S100A9 in neutrophils, which contain the most S100A8 and S100A9. This will, in turn, reduce hyperglycemia-induced leukocytosis. We found that absence of KLF5 had no effect on neutrophil gene expression of S100A8 or S100A9 *in vivo* or *in vitro*. Absence of KLF5 also did not have an effect on peripheral white cells or BM progenitors. However, these studies were complicated as the MKK and $Klf5^{fl/fl}$ mouse colonies presented with a defect in breeding and weight gain not found by others. These defects may be due to a constant shifting of these colonies to various vivaria and attempts to rederive the line.

5.2 Materials and Methods

5.2.1 Animal Studies. Mice used for this experiment were raised in multiple vivaria including Columbia University, Charles River Laboratory, Memorial Sloan Kettering, New York University Langone satellite animal facility and Alexandria West Central Animal Facility (AWCAF). Mice were bred and re-derived at Charles River before being temporarily sent to Memorial Sloan Kettering Animal Facility. Mice from Memorial Sloan Kettering bred there and were shipped to NYUMLC satellite facilities for experiments. Finally, these mice were permanently transferred to AWCAF barrier facility where they are bred and used for further experiments.

Littermates were used as controls for all studies. The NYULMC, Institutional Animal Care and Use Committees approved all procedures. Mice with exons 2 and 3 of the mouse *Klf5*

gene flanked with loxP sites (*Klf5*$^{fl/fl}$) (342) were crossed with mice overexpressing Cre recombinase driven by the *LysM* promoter (*LysM*-Cre), generating mice with myeloid-specific *Klf5* gene knockout (MKK). The control group was *Klf5*$^{fl/fl}$ mice. All mice used were male mice 3-4 months of age. Mice were made diabetic by STZ treatment using the protocol adopted by the Diabetic Complications Consortium. Mice were divided into two groups; one group was treated with STZ (Milipore Sigma), the other group was treated with vehicle, or no treatment was given to examine baseline phenotype. STZ was dissolved in sterile citrate buffer and injected IP into mice (50 mg/kg) for five consecutive days. Ten days after the last STZ injection, glucose levels were measured using a One Touch Ultra 2™ glucometer.

STZ-injected mice with glucose levels 250mg/dL were considered to be diabetic.
These mice are being bred at Temple University with *Klf5*$^{fl/fl}$ mice kindly provided by Konstantinos Drosatos and a *LysM*-Cre purchased from Jackson Laboratories.

5.2.2 Measurement of Plasma Lipids and Glucose. 100 μL of blood were drawn from each animal and then centrifuged at 10,000 rpm on a tabletop centrifuge for 10 minutes to obtain plasma. Plasma was used to measure TGs and NEFA using Thermo Scientific Infinity assay (Thermo Scientific) and Wako NEFA kit, respectively. Glucose was measured from whole blood using a One Touch Ultra 2™ glucometer.

5.2.3 Flow Cytometry. Leukocyte subsets were identified from whole blood as previously described (285). EDTA anticoagulated blood was subjected to red blood cell (RBC) lysis. WBCs were resuspended in flow buffer (PBS + 0.5% BSA w/v, 5 mM EDTA) and stained with a cocktail of antibodies (Table 6) for 30 minutes in the dark. Monocytes were identified as CD45^{hi}CD115^{hi} and subsets as Ly6C^{hi} and Ly6C^{lo}; neutrophils were identified as CD45^{hi}CD115^{lo}Ly6C/G^{hi}. WBC differentials were obtained with a Genesis™ hematology system

(Oxford Science)**.** Hematopoietic stem and progenitor cells were analyzed by flow cytometry as previously described (285). BM was harvested from femurs and tibias, and the RBCs were lysed. The cell suspension incubation with a cocktail of antibodies against lineage-committed cells was performed. This was accompanied by markers to identify the stem and progenitor cells that were identified as hematopoietic stem/progenitor cells [(HSPC) lineage^{-}, Sac1^{+}, and ckit^{+})], common myeloid progenitors [(CMPs) (lineage^{-}, Sca1^{-}, ckit^{+}, CD34^{int}, and FcγRII^{int}/FcγRIII^{int})], and granulocyte myeloid progenitors [(GMPs) (lineage^{-}, Sca1^{-}, ckit^{+}, CD34^{int}, and FcγRII^{hi}/FcγRIII^{hi})]. Flow cytometry was performed using and FACSAria^{TM} I (for analysis) or Beckman Coulter MoFLo™ XDP or BD FACSAria™IIu SORP (for sorting); both machines ran FACSDiva software. All flow cytometry data were analyzed using FlowJo software (Tree Star).

5.2.4 RNA extraction and Quantitative Real-Time PCR. RNA was extracted from neutrophils using RNeasy Micro Kit (Qiagen) and amplified using Ovation® Pico WTA System V2 (NuGEN) following manufacturers protocol. Quantitative real-time PCR was performed with Power SYBR Green PCR Master Mix (Life Technologies) using a Quant Studio 7 Flex analyzer (Life Technologies). Mouse quantitative primer sequences are listed in Table 7.

5.2.5 Cell Culture. HL-60 cells were purchased from the American Type Culture Collection (ATCC) and cultured in RPMI 1640 media (ThermoFisher) supplemented with L-glutamine and 25 mM HEPES (Fisher Scientific), 1% penicillin/streptomycin (Invitrogen) and 10% heat-inactivated fetal bovine serum (FBS) (Invitrogen). Cells were maintained in 37^{o}C and 5% CO_2. HL-60 cells were passaged when the cells reached a density between 1 and 2 million cells/mL. High and low glucose or KLF5 inhibitor (KLF5i) CID 5951923 (Milipore Sigma) experiments were conducted as follows. HL-60 cells were stimulated to differentiate by incubating with 1μM all-*trans*-retinoic acid (ATRA) in base medium for 72 hours. Non-attached

cells were aspirated out with the media. Cells were incubated with base media with 1% FBS containing high glucose (25mM) or low glucose (5mM) and 20mM of mannitol to maintain iso-osmotic balance. Cells were also incubated with or without KLF5i at a concentration of 10 μM. Cells were harvested for RNA 24 and 72 hours afterward. RNA was isolated with RNA mini kit (Life Technologies); cDNA was synthesized using Verso cDNA Kit (Thermo Scientific), and quantitative real-time PCR were performed with Power SYBR Green PCR Master Mix (Life Technologies) using a Quant Studio 7 Flex analyzer (Life Technologies). Human quantitative primers are listed on Table 8.

Table 6. List of Flow Cytometry Antibodies

Antibody	**Reactivity**	**Color**	**Clone**	**Marker for:**	**Company**
CD115	Mouse	PE	AFS98	Monocyte	eBioscience
CD45	Mouse	Pe/Cy7	30-F11	Leukocyte	eBioscience
Ly-6C/Ly-6G	Mouse	APC	RB6-8CS	Granulocyte	BioLegend
CD45R	Mouse	FITC	RA3-6B2	Lineage	eBioscience
CD4	Mouse	FITC	GK1.5	Lineage	eBioscience
CD8a	Mouse	FITC	53-6.7	Lineage	eBioscience
Terr119	Mouse	FITC	Terr119	Lineage	eBioscience
Ly6G	Mouse	FITC	RB6-8CS	Lineage	eBioscience
CD11B	Mouse	FITC	M1/70	Lineage	eBioscience
CD19	Mouse	FITC	Ebio1D3	Lineage	eBioscience
CD3e	Mouse	FITC	145-2C1	Lineage	eBioscience
CD2	Mouse	FITC	RM2-5	Lineage	eBioscience
Sca-1	Mouse	Pe/Cy7	D7	HSPC	BioLegend
c-Kit	Mouse	APC/Cy7	2B8	HSPC, CMP, GMP	BioLegend
FcγRII/FcγRIII	Mouse	PE	93	CMP, GMP	BioLegend
CD34	Mouse	PerCP/Cy5.5	HM34	CMP, GMP	BioLegend
CD11B	Human	APC	ICRF44	Granulocyte	Biolegend

Table 7. Mouse primer sequences for quantitative PCR analysis

Gene	Orientation	Sequence
36b4	forward	A A T C T C C A G A G G C A C C A T T G
	reverse	C C G A T C T G C A G A C A C A C A C T
Klf1	forward	A C A C T G G A C A T C G T C C C T T C
	reverse	C C C T G A G G A C A T G T G A G G T T
Klf2	forward	G C C T G T G G G T T C G C T A T A A A
	reverse	A A G G A A T G G T C A G C C A C A T C
Klf3	reverse	C C A T G T G C T C C C A T A G T G T G
	forward	C T C T C G G T A T C C A G C T T T G C
Klf4	forward	C T G A A C A G C A G G G A C T G T C A
	reverse	G T G T G G G T G G C T G T T C T T T T
Klf5	forward	A C C A G A C G G C A G T A A T G G A C
	reverse	G A C T T G G C A T G G T G T A C G T G
Klf6	forward	T G C T A G T C A C G A T T G G C A A G
	reverse	A A A C A A T C C C T G T G G T C A G C
Klf7	forward	T T G C T C T C T C G G G A C A A G T T
	reverse	G A G C T G A G G G A A G C C T T C T T
Klf8	forward	C T A T C C T G G C C T C G T C T C A G
	reverse	C C T C C A A T G A G T G G G A C A G T
Klf9	forward	T G C C C A C T G T G T G A G A A G A G
	reverse	G C C A A A G A A G C A G T G A C C T C
Klf10	forward	G G T G T C A A G T G C T T C T G C A A
	reverse	G A A C T G A G C C C T G T C C T C T G
Klf11	forward	C A G C T G C A C C T G A T C T A C C A
	reverse	G A C C A T G C A T C C T T T G G A G T
Klf12	forward	T C C C T G T G G T G G T A C A G T C A
	reverse	C T G C T C T G G C T A T G G A A A G G
Klf13	forward	G T G C C T G A G T G A A G G G A G A G
	reverse	A T C T G G G G G A A C A G A C A G T G
Klf14	forward	C T G A T G C C C C A C C C T A A G T A
	reverse	C T C T C A C C C C A A A T C C A A G A
Klf15	forward	G A A G C A G G A G G C A G G T A C A G
	reverse	G A A G T T C T G C T G C T G G G T T C
Klf16	forward	A A G C C T A C C C C A C T C C T T G T
	reverse	G A G G G C A G A A C C T A T G G A C A
Klf17	forward	C T C C T G T C A A C C C C A A G T G T
	reverse	G G A C A G T G A A G G C C A G A G A G
S100a8	forward	C C T T T G T C A G C T C C G T C T T C
	reverse	A T C A C C A T C G C A A G G G A A C T C
S100a9	forward	C A G C A T A A C C A C C A T C A T C G
	reverse	G T C C T G G T T T G T G T C C A G G T

Table 8. Human primer sequences for quantitative analysis

Gene	Orientation	Sequence
CD11B	forward	G C T T C T T C A A G C G G C A A T A C
	reverse	G T G C A C A C A C T T G C A C A C A G
CD14	reverse	A G C C T A G A C C T C A G C C A C A A
	forward	C T T G G C T G G C A G T C C T T T A G
CD66B	forward	T A C A T C C G G A G A C T C C C A A G
	reverse	A G G A C A T T C A G G G T G A C T G G
GLUT1	forward	T C A C T G T G C T C C T G G T T C T G
	reverse	C C T G T G C T C C T G A G A G A T C C
KLF5	forward	C C C T T G C A C A C A T A C A C A A T G C
	reverse	A G T T A A C T G G C A G G G G T G G T G
RPL19	forward	A C C T G A A G G T G A A G G G G G A A T
	reverse	G C G T G C T T C C T T G G T C T T A G
S100A9	forward	A T T T C C A T G C C G T C T A C A G G
	reverse	A C G C C C A T C T T T A T C A C C A G
S100A9	forward	C A G C T G A G C T T C G A G G A G T T
	reverse	C C A C A G C C A A G A C A G T T T G A

5.3 Results

5.3.1 Mouse breeding. Floxed *Klf5 (Klf5$^{fl/fl}$)* (343) mice were bred with a *LysM*-cre mice to generate myeloid-specific KLF5 KO mice (MKK). Initially these mice were bred and raised in Columbia University's barrier facility, but were transferred to Charles River Laboratory. This line of mice was rederived at Charles River Laboratory, brought to Memorial Sloan Kettering, followed by New York University Langone satellite animal facility, and Alexandria West Central Animal Facility (AWCAF). Mice were bred and rederived at Charles River before being temporarily sent to Memorial Sloan Kettering Animal Facility. Mice from Memorial Sloan Kettering were bred there and shipped to NYUMLC satellite facilities for experiments. Finally, these mice were permanently transferred to AWCAF barrier facility where they were bred and used for further experiments.

5.3.2. Baseline assessment of MKK glucose, lipid, and peripheral and bone marrow blood cells. We first confirmed our MKK had the expected knockout by testing gene expression *Klf5* by quantitative PCR (qPCR) and saw that it was decreased or not expressed at all in MKK mice (Figure 16). Neutrophils express the highest amount of *Klf5* amongst cells in the myeloid lineage; thus, we focused our studies on neutrophils (http://ds.biogps.org/?dataset=GSE10246&gene=12224). We asked whether deletion of *Klf5* would affect gene expression of other KLFs in neutrophils. We found an almost 100-fold increase in *Klf4*, and a 3-fold increase in *Klf15*. *Klf11* was not detected in the control mice, but was detectable in the MKK group (Figure 16). KLF4 and KLF5 work antagonistically to one another, and compete for the same cis-elements on promoters (221)

Next, we assessed the weight, glucose, and plasma lipids of MKK and *Klf5$^{fl/fl}$* mice. Both genotypes had normal glucose and plasma lipids and mice averaged 23 grams at 3-4 months of

age. There was no significant difference between weight, glucose, plasma NEFA, total cholesterol or TG, between genotypes (Figure 17). To assess the baseline immune phenotype of MKK, 300μL of blood was drawn from each mouse for flow cytometry to assess circulating leukocytes. We assessed two populations of monocytes, Ly6C/G^{hi} and Ly6C/G^{lo} as it has been shown that Ly6C/G positive monocytes are considered more inflammatory and infiltrative (344), There was no difference between the number of circulating neutrophils and monocytes (both Ly6C/G^{hi} and Ly6C/G^{lo}) (Figure 18A-C). Similarly, there was no change in the BM progenitor cells; hematopoietic stem/progenitor cells (HSPCs), CMPs, and granulocyte-macrophage progenitors (GMPs) between genotypes (Figure 18D-F). Thus, we conclude that, at baseline, there is no metabolic or immunologic phenotype in MKK mice.

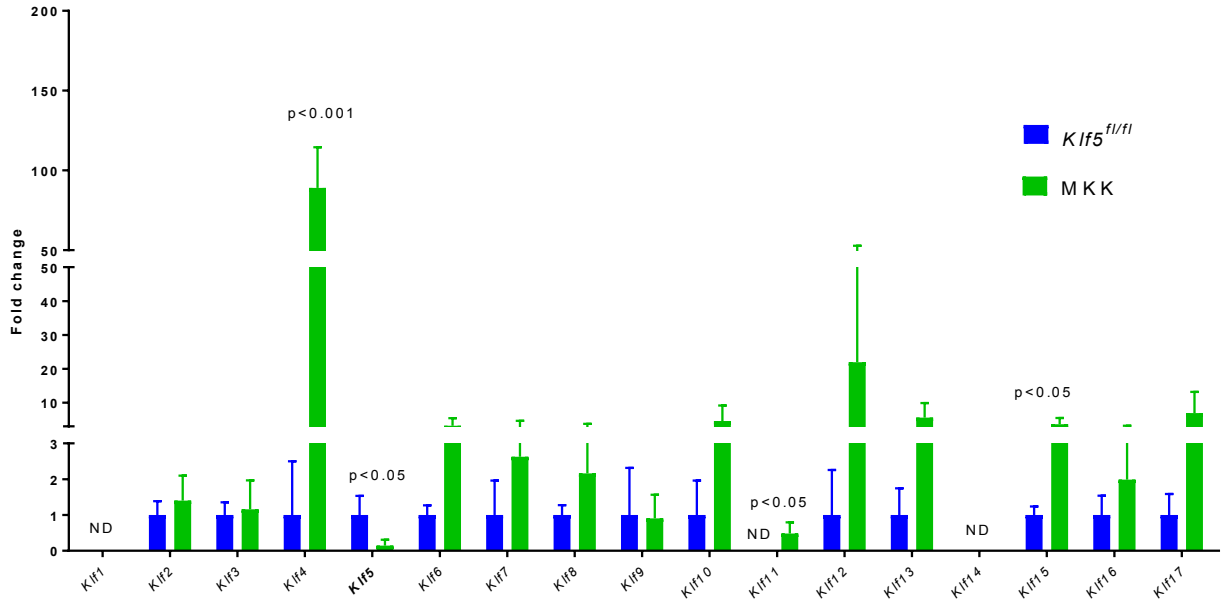

Figure 16. Neutrophils of MKK mice have increased expression of *Klfs 4, 11*, and *15*

Neutrophils were isolated from whole blood of MKK mice and *Klf5*$^{fl/fl}$ controls by flow cytometry and analyzed for gene expression. Expression of the gene of interest was normalized to expression of *36b4*. *Klf5*$^{fl/fl}$ N=4, MKK N= 5. Results are presented as means ± SD. Statistics were performed using unpaired Student's t-test.

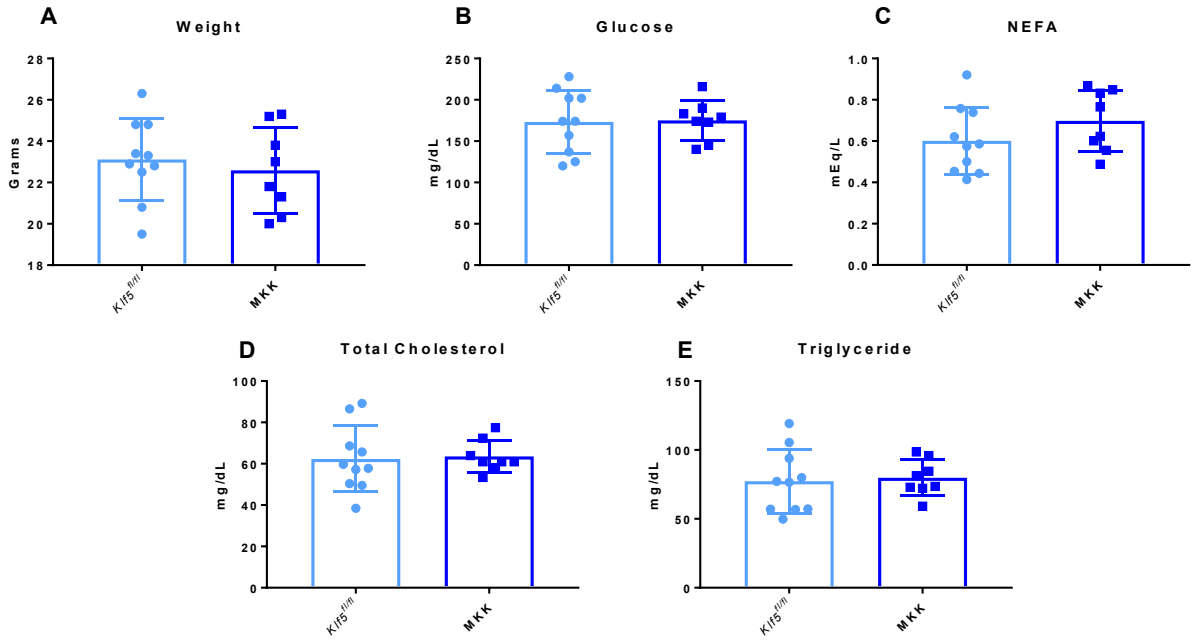

Figure 17. Weight, glucose, and plasma lipids of MKK mice are comparable to *Klf5*$^{fl/fl}$ littermates

Male mice aged 8-12 weeks were used for measurements of A) weight B) glucose. Blood was drawn and centrifuged in order to collect plasma to measure C) total cholesterol D) non-esterified fatty acids (NEFA) and E) TGs. Mice were postprandial for measurements. *Klf5*$^{fl/fl}$ N=9, MKK N= 8. Results are presented as means ± SD. Statistics were performed using unpaired Student's t-test.

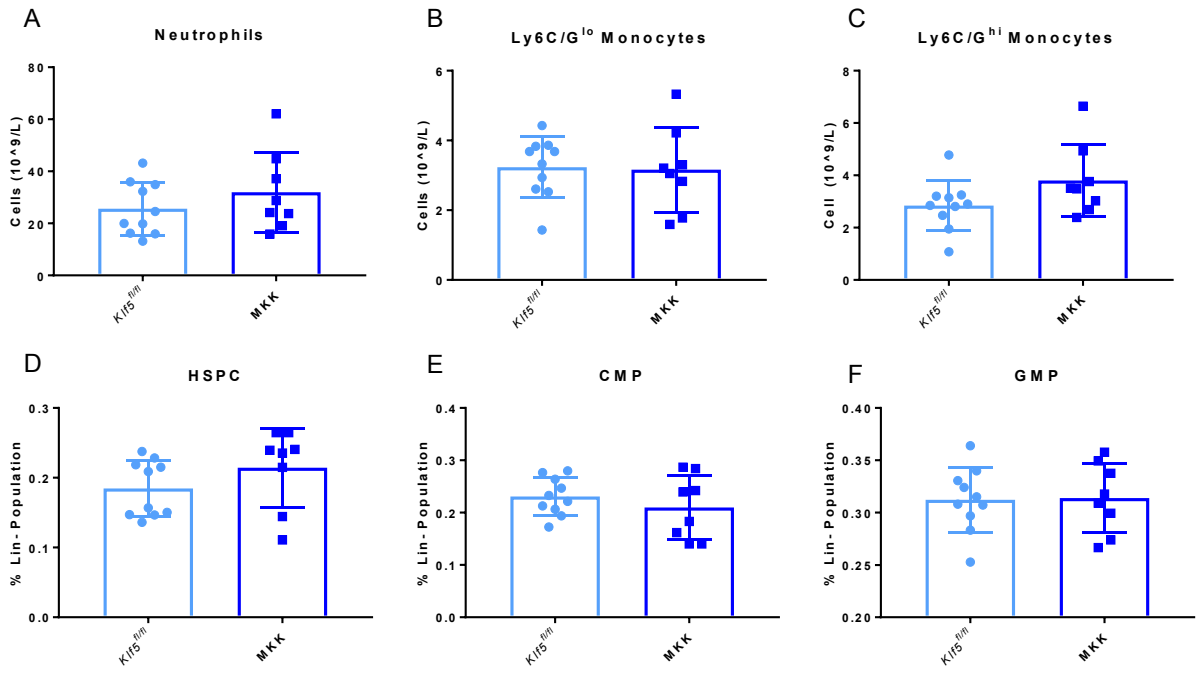

Figure 18. MKK mice do not have any differences in peripheral white blood cells or bone marrow progenitors at baseline

Whole blood was sorted with flow cytometry for neutrophils and Ly6C/G^{lo} and Ly6C/G^{hi} populations of monocytes. A) Neutrophils, B) Ly6C/G^{lo} monocytes, and C) Ly6C/G^{hi} monocytes. Bone marrow was taken from mouse femurs and stem cell progenitors were sorted out of lineage^{+} cell populations to obtain E) hematopoietic stem/progenitor cells (HSPCs), common myeloid progenitors (CMP), and granulocyte-macrophage progenitors (GMPs). *Klf5$^{fl/fl}$* N=9, MKK N= 8. Results are presented as means ± SD. Statistics were performed using unpaired Student's t-test.

5.3.3 Neutrophils from MKK mice do not express less *S100A8* and *S100A9*. Next, we isolated neutrophils from the circulation to analyze gene expression. Contrary to our hypothesis, we found that despite the absence of *Klf5*, MKK mice had a higher trend of mRNA levels of *S100a8* and *S100a9* (Figure 19A-C) Thus it appears KLF5 does not directly regulate *S100a8* and *S100a9* in neutrophils at baseline.

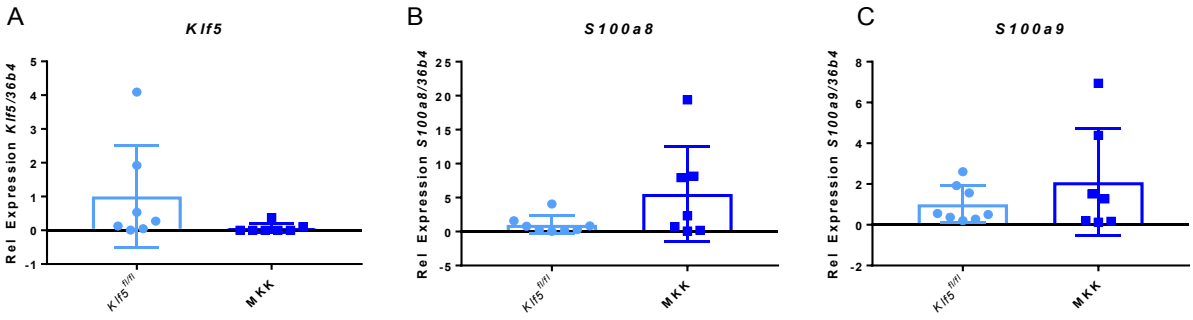

Figure 19. Neutrophils of MKK mice do not have lower expression of S100a8 and S100a9 at baseline

Neutrophils were isolated from whole blood of either MKK mice or *Klf5*$^{fl/fl}$ controls by flow cytometry and analyzed for gene expression. Expressions of the genes of interest were normalized to expression of *36b4*. A) *Klf5*. B) *S100a8*. C) *S100a9*. *Klf5*$^{fl/fl}$ N=9, MKK N= 8. Results are presented as means ± SD. Statistics were performed using unpaired Student's t-test.

5.3.4 Diabetic *Klf5*$^{fl/fl}$ and MKK mice peripheral and bone marrow blood cells are comparable. We then asked whether hyperglycemia would play a role in S100A8/S100A9 gene expression in MKK mice. To assess whether hyperglycemia plays a role in *Klf5* regulation of neutrophil and *S100a8* and *S100a9*, we made MKK mice diabetic with STZ. After two weeks of hyperglycemia, both MKK and *Klf5*$^{fl/fl}$ mice had glucose levels above 400 mg/dL (Figure 20A). The low number of *Klf5*$^{fl/fl}$ mice was caused by death after STZ injections, likely due to low body weights before injections. Complete blood counts also showed that there were higher circulating total WBCs, neutrophils, and monocytes compared to baseline in both *Klf5*$^{fl/fl}$ and MKK mice (Figure 20B-D). When circulating cells were assessed by flow cytometry, we again saw no difference between genotypes in the number of neutrophils and monocytes (Figure 21A-C). This corresponded to no change in BM stem cells between genotypes (Figure 21E-F). When neutrophil gene expression was assessed, MKK mice expressed less *Klf5*. However there was no change in gene expression in *S100a8* and *S100a9* between MKK and *Klf5*$^{fl/fl}$ mice (Figure 22A-C).

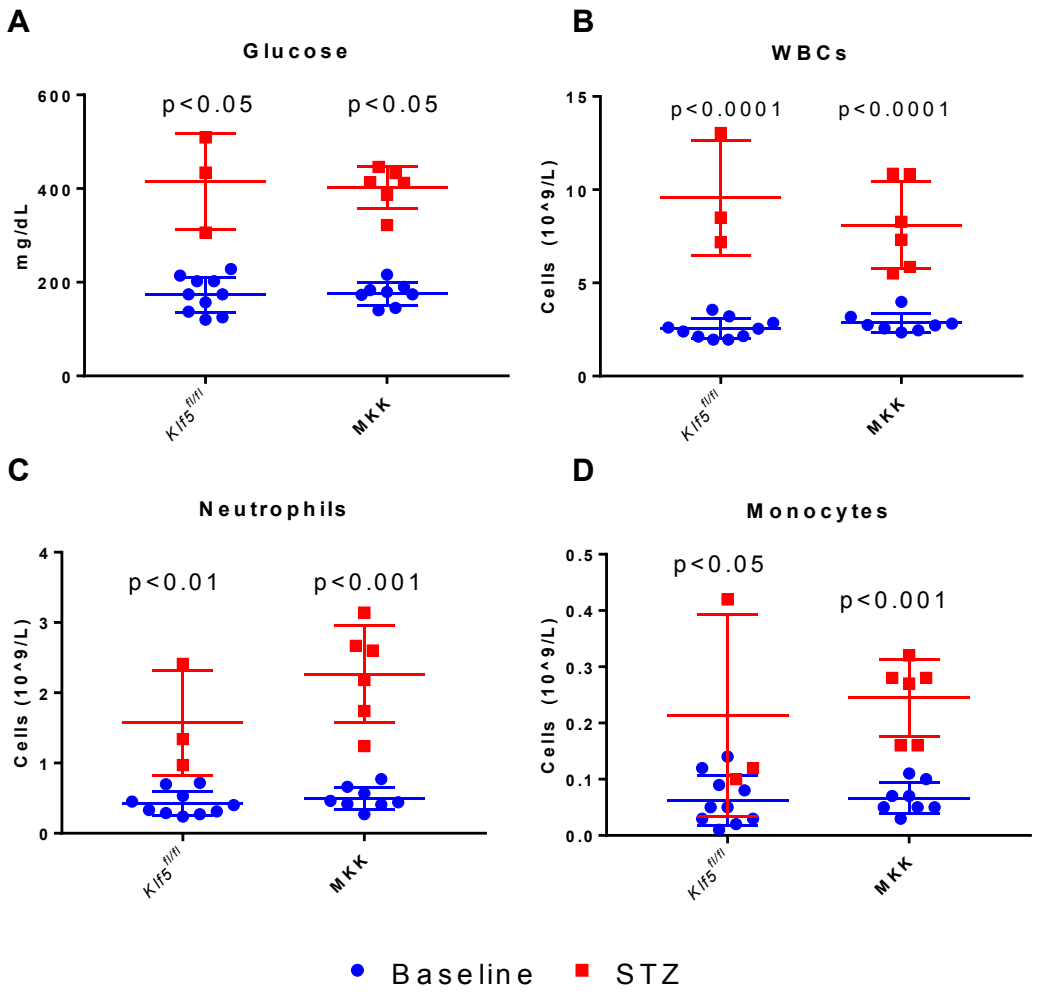

Figure 20. MMK and *Klf5*$^{fl/fl}$ mice both present with leukocytosis during diabetes

Male mice were made diabetic with five low-dose injections of streptozotocin. After two weeks, glucose was measured as well as complete peripheral blood count. These results were compared to that of similar, normoglycemic (baseline) mice. A) Glucose, B) total white bloods cells (WBCs), C) neutrophils and D) monocytes. Baseline *Klf5*$^{fl/fl}$ N=9, Baseline MKK N= 8 Diabetic *Klf5*$^{fl/fl}$ N=3, Diabetic MKK N=6. Results are presented as means ± SD. P values represent significant values when diabetic groups are compared to baseline. Statistics were performed using the two-way ANOVA Tukey's multiple comparison test.

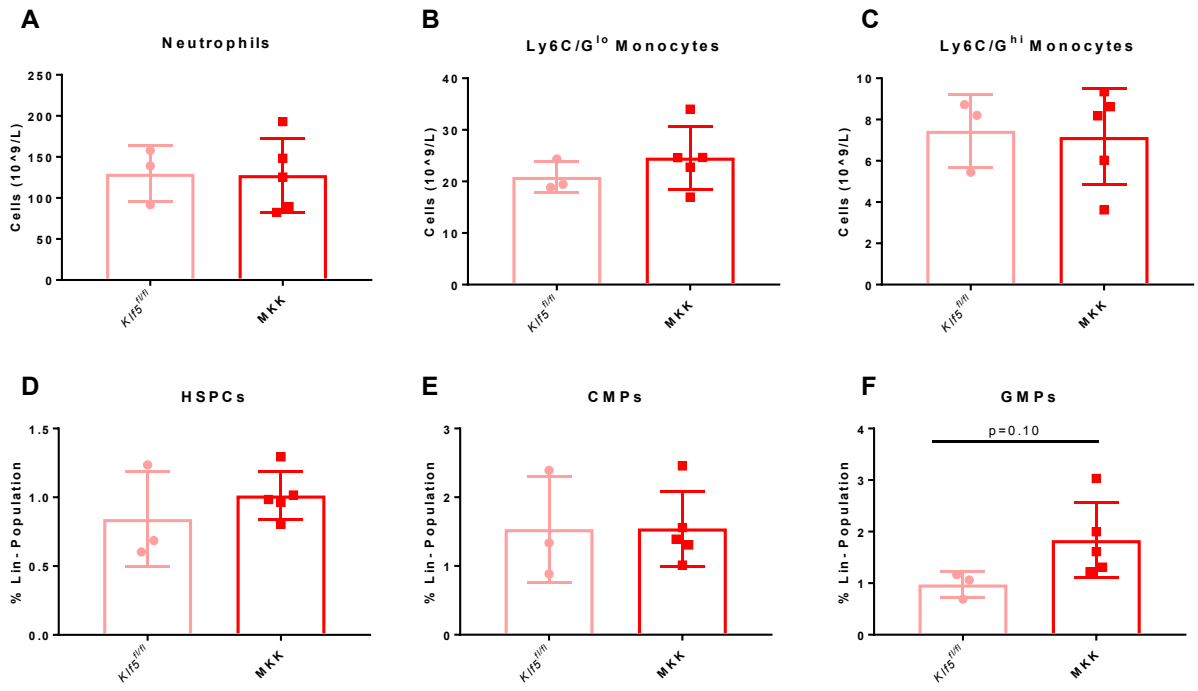

Figure 21. MKK mice do not have any differences in peripheral white blood cells or bone marrow progenitors during diabetes

Whole blood was sorted with flow cytometry for neutrophils and Ly6C/G^{lo} and Ly6C/G^{hi} populations of monocytes. A) Neutrophils, B) Ly6C/G^{lo} monocytes, and C) Ly6C/G^{hi} monocytes. Bone marrow was taken from mouse femurs and stem cell progenitors were sorted out of lineage^{+} cell populations to obtain E) hematopoietic stem/progenitor cells (HSPCs), common myeloid progenitors (CMP), and granulocyte-macrophage progenitors (GMPs). *Klf5$^{fl/fl}$* N=3, MKK N= 5. Results are presented as means ± SD. Statistics were performed using unpaired Student's t-test.

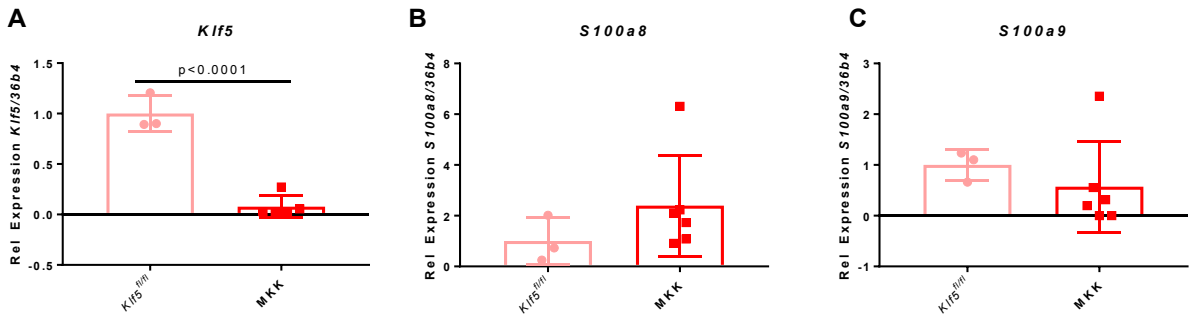

Figure 22. Neutrophils of MKK mice do not have lower expression of S100a8 and S100a9 during diabetes

Neutrophils were isolated from whole blood of either MKK mice or *Klf5*$^{fl/fl}$ controls by flow cytometry and analyzed for gene expression. Expressions of the genes of interest were normalized to expression of *36b4*. A) *Klf5*. B) *S100a8*. C) *S100a9*. *Klf5*$^{fl/fl}$ N=3, MKK N= 5. Results are presented as means ± SD. Statistics were performed using unpaired Student's t-test.

5.3.5 Differentiating promyeloblasts lose KLF5 and gain S100A8 and S100A9. Next, we differentiated a human promyeloblastic cell line (HL-60) to neutrophils in order to assess the role of hyperglycemia on KLF5 in these cells. We determined 1μM of ATRA incubated for 3 days was sufficient to differentiate cells. At day 3, these cells highly expressed CD66B (Figure 23A), CD11B (Figure 23B), S100A8 and S100A9 (Figure 23E and F, respectively) — markers of neutrophil maturity. However, longer time periods further increased CD11B and CD14, a monocyte cell surface marker (Figure 23C), and decreased S100A8 and S100A9. KLF5 decreased with neutrophil differentiation (Figure 23D). Next, we assessed the role of a KLF5 small molecule inhibitor (KLF5i) on the role of differentiating neutrophils. This particular inhibitor mechanism is not yet known, however, it is shown to downregulate the EGFR/MEK/ERK pathway (345). This pathway is known to stimulate *Klf5* expression and *vice versa* creating a positive feedback loop (346). At a concentration of 10μM, we found that there was no effect of the KLF5i on neutrophil differentiation based on CD11B expression or detection on the cell surface by flow cytometry (Figure 24A-B). 10μM, of KLF5i did not change expression of *KLF5*, *S100A8,* and *S100A9* (Figure 24C-E).

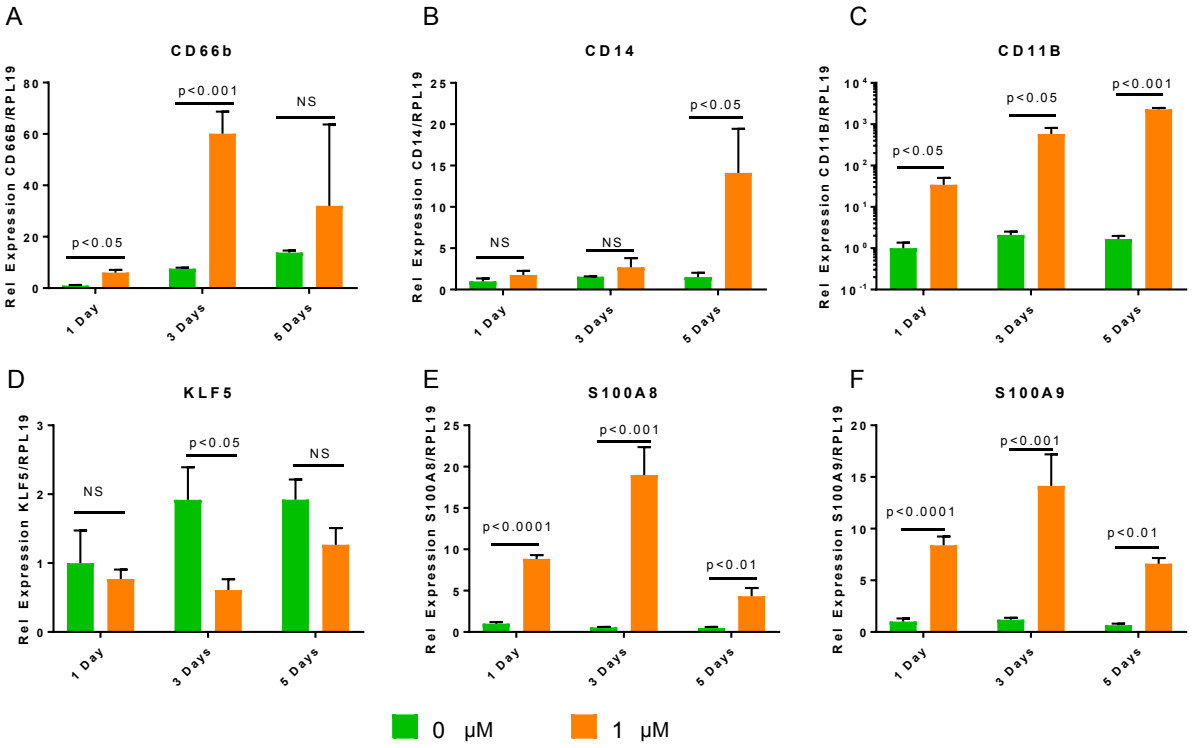

Figure 23. HL-60 cells express lower KLF5 and more S100A8 and S100A9 as they differentiate into neutrophils

HL-60 cells were differentiated to neutrophils using 1µM all-trans retinoic acid (ATRA) for either 1, 3 or 5 days. Cells were collected and gene expression was measure for A) CD66B, a cell surface marker for neutrophils, B) CD14, a cell surface marker for monocytes, and CD11B a cell surface marker phagocytic cells. We also analyzed expression of D) *KLF5*, E) *S100A8*, and F) *S100A9*. Each group represents experiments run in triplicate. Results are presented as means ± SD. Statistics were performed using unpaired Student's t-test and compare treatment of 0µM or 1µM.

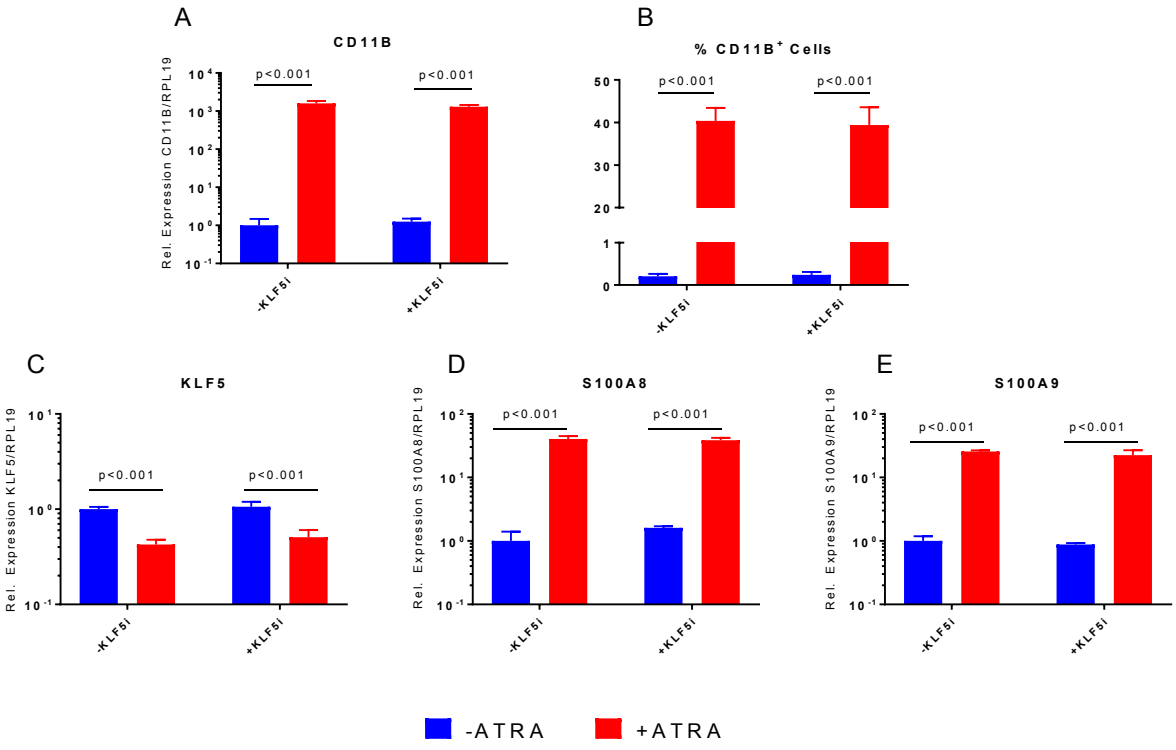

Figure 24. Inhibition of KLF5 does increase HL-60 cells differentiation to neutrophils

HL-60 cells were differentiated to neutrophils using 1µM all-trans retinoic acid (ATRA) for 3 days ± a KLF5i at a concentration of 10µM. After which cells were collected and analyzed for expression of A) CD11B or with B) flow cytometry for CD11B surface marker. Cells were collected and gene expression was measure for C) *KLF5*, B) *S100A8*, and C) *S100A9*. Each group represents experiments run in triplicate. Results are presented as means ± SD. Statistics were performed using the two-way ANOVA Tukey's multiple comparison tests.

5.3.6 Hyperglycemia does not increase gene expression of KLF5, S100A8 or S100A9 in neutrophils. We assessed the role hyperglycemia plays on neutrophils with or without KLF5. HL-60 cells were differentiated to neutrophils and incubated in control low glucose media (5mM) or high glucose media (25mM) for 24 (Figure 25) of 72 hours (Figure 26). We found that high glucose concentration did not affect gene expression of *CD11B*, *GLUT1*, *KLF5*, or *S100A8* (Figure 25 and Figure 26 A-D). However, the presence of the KLF5i created a trend towards increase of *S100A9* after 24 hours (Figure 26E) and significantly increased *S100A9* expression after 72 hours (Figure 26E). Hyperglycemia does not change KLF5 or S100A8/A9 in cultured neutrophils; but inhibition of KLF5 causes an increase in S100A9. Morris *et al.* demonstrates lentiviral overexpression of KLF4 in THP-1 cells (an acute monocytic leukemia cell line) induces expression of *S100A8* and *S100A9* (347). Thus, KLF5 might be inhibitory to *S100A9* or its absence induces expression of KLF4 in these cells.

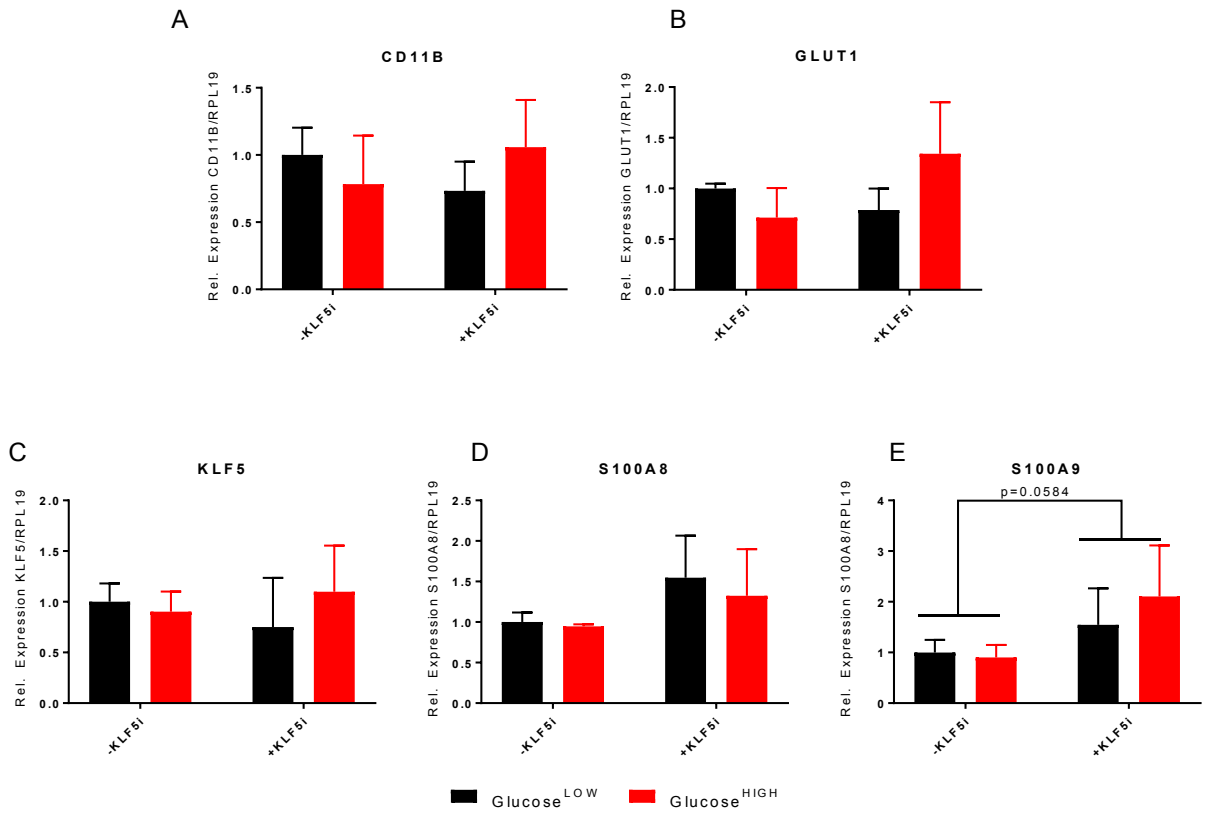

Figure 25. Hyperglycemia does not increase gene expression KLF5, S100A8 or S100A9 in neutrophils after 24 hours

HL-60 cells were differentiated to neutrophils using 1µM all-*trans* retinoic acid (ATRA) for 3 days ± a KLF5i at a concentration of 10µM. Unattached cells were aspirated out and remaining cells were incubated for 24 hours in media containing low glucose (black bars, 5mM) or high glucose (red bars, 25mM). Afterwards, cells were collected and analyzed for expression of A) *CD11B,* B) *GLUT1*, C) *KLF5*, B) *S100A8*, and C) *S100A9*. Each group represents experiments run in triplicates. Results are presented as means ± SD. Statistics were performed using the two-way ANOVA Tukey's multiple comparison test.

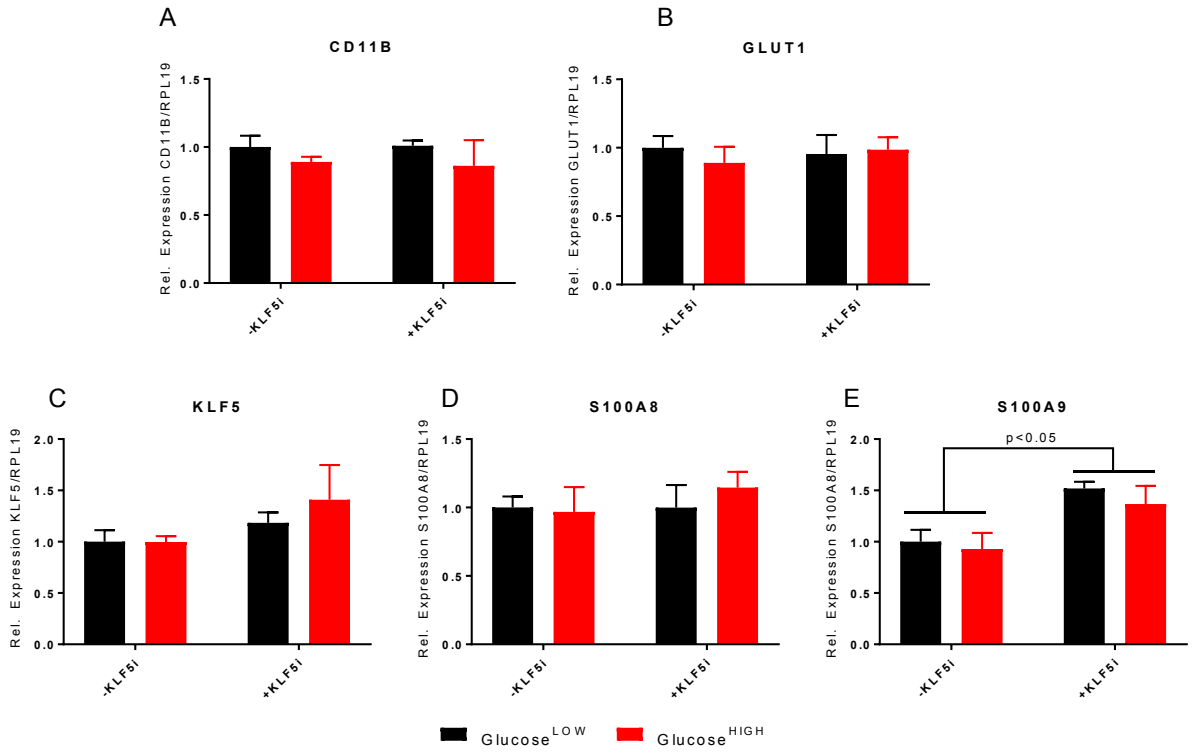

Figure 26. Hyperglycemia does not increase gene expression KLF5, S100A8 or S100A9 in neutrophils after 72 hours

HL-60 cells were differentiated to neutrophils using 1µM all-*trans* retinoic acid (ATRA) for 3 days ± a KLF5i at a concentration of 10µM. Unattached cells were aspirated out and remaining cells were incubated for 72 hours in media containing low glucose (black bars, 5mM) or high glucose (red bars, 25mM). Afterwards, cells were collected and analyzed for expression of A) *CD11B* B) *GLUT1*, C) *KLF5*, B) *S100A8*, and C) S100A9. Each group represents experiments run in triplicates. Results are presented as means ± SD Statistics were performed using the two-way ANOVA Tukey's multiple comparison test.

5.4 Discussion

Calprotectin is a crucial component during the inflammatory response in diabetic hyperglycemia. Relative to other cell types, neutrophils have a higher proportion of their cellular protein content. Naggareddy and Murphy *et al.* demonstrate that hyperglycemia triggers the release of calprotectin and that these molecules are associated with uncontrolled glucose (285). KLF5 has been shown to regulate *S100a8* and *S100a9* in collecting duct cells during acute kidney injury (284). Therefore, we predicted KLF5 would regulate S100A8 and S100A9 in neutrophils. We generated a myeloid-Cre specific knock out of *Klf5* that we refer to as MKK. By knocking out *Klf5*, we observed a 100-fold increase of *Klf4* in neutrophils (Figure 16). KLF4 and KLF5 compete for binding on DNA binding sites as well opposing roles in regulating cellular proliferation (221). Feinberg *et al*. demonstrate that KLF4 is an essential regulator in monocyte differentiation in CMPs. Knockdown of *Klf4* blocked phorbol ester-induced monocyte differentiation in HL-60 cells and increased differentiation to granulocytes (223). Thus, we predicted MKK mice would have lower circulating neutrophils and higher circulating monocytes compared the $Klf5^{-/-}$ littermates. However, at baseline, we found that MKK mice and $Klf5^{fl/fl}$ littermates had similar circulating neutrophils, Ly6C/G^{lo}, and Ly6C/G^{hi} (Figure 18A-C). Conversely, BM progenitors HSPC, CMP, and GMP, were unchanged (Figure 18D-F). Shahrin *et al*. demonstrates a *Klf5* deficiency in HPSC leads to decreased peripheral neutrophils—suggesting KLF5 is a determinant for neutrophil lineage. This discrepancy between our data and what is previously published may be due to selection of Cre (279). Shahrin *et al*. used a *Vav*-Cre, which abolishes KLF5 at the HSPC stage, rather than the CMP stage of *LysM*-cre.

We show that *KLF5* is decreased when promyeloblastic cells differentiate into neutrophils with ATRA (Figure 23D). ATRA has been used as a treatment for certain AMLs and

causes a decrease in circulating promyeloblastic cells (348). ATRA has also been shown to decrease *KLF5* expression in intestinal epithelial cells—inhibiting their proliferation (349). However, in NB-4 cells (a promyeloblastic cell line), Humbult *et al.* shows ATRA transactivated *KLF5* expression (280). These data run contrary to what is in the literature and our own data, possibly because of differences in cell line origin or dosage protocol. HL-60 cells treated with 1μM of ATRA had a >50% decrease in *KLF5* (Figure 23D) expression after 3 days and a 50-fold increase in *CD66B*, a neutrophil surface marker (Figure 23A). When we treated HL-60 cells with KLF5i and examined CD11B by flow cytometry, we found there was no effect of the KLF5 inhibitor (Figure 24B).

We observed no difference in peripheral WBCs (Figure 21A-C) or in BM progenitor cells (Figure 21E-F) when MKK and *Klf5*$^{fl/fl}$ mice were made hyperglycemic. When neutrophils were isolated from mice at baseline, we found that MKK mice expressed *S100a8* and *S100a9* similarly to *Klf5*$^{fl/fl}$ (Figure 19B-C). This is contrary to our hypothesis and what was shown in kidney collect ducts. When we isolated neutrophils from diabetic MKK mice and *Klf5*$^{fl/fl}$ mice, we found no change in *S100a8* and *S100a9 (*Figure 22B-C*)*. We differentiated promyeloblastic cells to neutrophils and found *S100A8* and *S100A9* increased by two orders of magnitude after 3 days (Figure 22E and F, respectively). When we challenged these differentiated with 25mM glucose, we observed no change in *S100A8* and *S100A9* expression. (Figure 25D-E; Figure 26D-E). Ultimately, these data suggest KLF5 in neutrophils, does not have a direct effect on *S100A8* and *S100A9* expression, and KLF5 may inversely affect *S100A9* in neutrophils differentiated from HL-60 cells.

5.5 Conclusions

Our data cannot conclusively confirm a role of KLF5 in regulating S100A8 and S100A9 in neutrophils. As S100A8/A9 is a major protein in neutrophils, it may be that there are multiple redundant layers of regulation. Deletion of KLF5 is not sufficient to block S100A8/S100A9. Another aspect that may confound our conclusions is the multiple displacements of the mice. Compared to other wild-type mice, both *Klf5*$^{fl/fl}$ and MKK mice were underweight for their age, which made performing STZ studies difficult. It was also difficult to reproduce immunophenotypes shown in previous data with these mice as well. We believe the constant shifting of vivaria and rederiving this line has changed their underlying phenotype in a yet undetermined way. Therefore, we will repeat these studies in another set of mice to definitively answer the question of whether KLF5 plays a role during diabetic inflammation in neutrophils by controlling the transcription of S100A8 and S100A9.

Chapter 6: Conclusions and future directions

This thesis has contributed to the pool of knowledge of lipid metabolism in the kidney, which is slowly growing. I demonstrate that serum NEFA is important in TG accumulation in the kidney— a significant finding because many metabolic diseases have elevated circulating NEFAs. Our data also indicates that the kidney can handle a 3-4 fold increase in TG content while still not accumulating lipotoxic species such as ceramides and sphingolipids (Figure 9C-D). More importantly, I demonstrate a role, or lack thereof, of LpL and CD36. In the context of fasting, LpL activity is lower (159). There is also an increase in kidney expression of *Angplt4* (Figure 7B), an inhibitor of LpL (350). The kidney, like the heart, has a high demand for fatty acids and energy. However, unlike the heart, LpL does not seem to be necessary for TG accumulation (173). Even in the fed state, an absence of LpL does not affect overall TG content in the kidney (Figure 13I). There is high LpL activity in the kidneys of mice (159) and, as of yet, LpL has not been knocked out in any kidney cell type. Thus, it remains to be determined whether absence of LpL in the kidney is detrimental.

Interestingly, I show that CD36 is disposable for lipid accumulation in the kidney. CD36 has been widely shown to play a role in lipid accumulation and renal damage progression (Discussed in Chapter 2). While, not discounting a role for CD36 in taking up fatty acids, I show in the fasted state (Figure 12A-C) that it is not necessary for lipid uptake or lipid accumulation. Fatty acids can enter the cell through non-receptor mediated ways as well. During fasting and certain metabolic diseases (such as DM), plasma NEFAs are at least double. Thus, the higher substrate availability favors movement of NEFA into the cells at a rate that will lead to lipid accumulation. This is especially true in an organ, such as the kidney, that receives 20% of cardiac output. The kidney does have other fatty acid transport proteins such as FATP2. In our

future research, I will explore the possible FATP2 (gene name *Slc27a2*) has on fatty acid uptake in the kidney.

In this research, I have established a better understanding of fatty acid uptake in the kidney during a healthy state. While it seems CD36 is not a major fatty acid transporter in the kidney, I will test whether FATP2 is important for fatty acid transport. In the liver, deletion of the liver-specific isoform, FATP5, resulted in lower hepatic TG content despite increased expression of *Fasn* (351). Therefore, it is plausible that a kidney tubule specific KO of *Slc27a2* may produce similar results to that of the liver. To achieve this, I will knockdown *Slc27a2* with an anti-sense oligonucleotide, an adenoviral vector, or proximal tubule specific gene KO. To test uptake and lipid accumulation in the presence or absence of *Slc27a2*, I will repeat the experiments outlined in this thesis using the fasted and fed model. Should FATP2 be required for fatty acid transport in the kidney, I expect to find fasting induced TG accumulation will be blunted when FATP2 is knocked down. FATP2 uptake of [^{14}C]oleic acid would also be decreased in these mice. Conversely, by overexpressing *Slc27a2*, I would see an increase in TG accumulation in the kidney and [^{14}C]oleic acid uptake.

I will next transition to how fatty acid uptake is altered in the diseased state. LpL is understudied in renal disease pathology and a continuation of this research would determine the contribution LpL plays in acute renal injury. Renal nephropathy and lipid accumulation can be induced with a high dose injection of niacin. Using this method in *iLpL*$^{-/-}$ mice, I will gain insight into the role this protein plays in lipid accumulation and fatty acid uptake with kidney disease. I will also determine whether absence of LpL affects the progression of tubulointerstitial fibrosis. This is largely done through histology to stain for collagen (trichrome or Sirius red) in the tubules and clinical metrics associated with nephropathy such as blood urea nitrogen, GRF, and

proteinuria. Finally, I will perform lipodomic analysis in the kidney to determine if lipotoxic species are present during nephropathy and whether *iLpL*$^{-/-}$ mice contain less of these species. Of particular interest, I will want to probe for ceramides, sphingolipids, DAGs, and NEFAs. If I find FATP2 has a role in fatty acid uptake in the kidney, I will repeat these experiments in a FATP2 deficient model as well. I predict in these models that fatty acid uptake will be reduced during kidney injury and intracellular TG and toxic lipid species would be decreased in the absence of LpL or FATP2. Fenofibrate treatment in mice demonstrates oxidation of lipids, not access to fatty acid, leads to energy insufficiency in the kidney (152) (151). Thus, by blocking excess uptake of fatty acids, lipotoxicity will be allayed. A possible limitation with this study would be if the diseased state has lower LpL activity overall. Renal injury is associated with increased Angplt4 in the circulation and lower LpL activity in peripheral tissues (122) (352). Furthermore, LpL activity will already be decreased following renal injury and the absence of LpL will only provide null results.

In my study of diabetic inflammation, I concluded there is no perceivable effect of the transcription factor KLF5 on expression of S100A8 and S100A9 or circulating leukocytes. Calprotectin is elevated in cells during injury and inflammation (discussed in Chapter 4) and is particularly highly expressed in neutrophils. I found it important to explore how S100A8 and S100A9 are regulated in these cells. From my data, it appears there is no direct regulation of S100A8 and S100A9 by KLF5 on neutrophils. I observed no change in peripheral leukocytes or BM progenitors in MKK mice compared to *Klf5*$^{fl/fl}$ mice at baseline (Figure 18) or with hyperglycemia (Figure 21). There was no relationship between the expression of *Klf5* and *S100a8* and *S100a9* in neutrophils at baseline (Figure 19) or during hyperglycemia (Figure 22). However, my *in vivo* data needs to be redone on a different set of MKK mice. The constant

shifting of our colony to multiple vivaria as well as being rederived at Charles River may have affected the phenotype of these mice (explained in methods of Chapter 5). For my future studies, I am breeding MKK mice at Temple University with the help of Konstantinos Drosatos, using mice that have not been rederived or shuffled in vivaria (explained in methods of Chapter 5). In this, I hope to achieve reliable results concerning the effect of KLF5 *in vivo*. In my *in vitro* studies, I determined *KLF5* and *S100A8/89* are inversely regulated in promyeloblasts differentiated into neutrophils (Figure 23D-F). High glucose media has no effect on neutrophil *KLF5* or *S100A8/A9* (Figure 25 C-E; Figure 26 C-E). Use of a KLF5 inhibitor did not affect promyeloblastic differentiation (Figure 24B) or *S100A8* and *S100A9* expression (Figure 24 D-E) in neutrophils. In future studies, I will do western blots for KLF5 and post-translational modifications of KLF5 in these cells to determine the efficacy of the KLF5i. As well as redoing these experiments on a new cohort of mice, I will explore future applications of this cell line in studying atherosclerosis as well as an alternative approach to uncover the transcriptional regulation of S100A8 and S100A9 in neutrophils.

After I establish a role for KLF5 (if one exists) in the production of S100A8/S100A9, I will explore whether absence of KLF5 in myeloid cells has an impact on atherosclerosis. Naggareddy and Murphy *et al.* have demonstrated the importance of S100A8 and S100A9 produced by neutrophils in atherosclerosis progression (285). My experiments would demonstrate that KLF5 is the transcriptional mediator in neutrophils that drives atherosclerotic progression. To do this I will cross MKK mice in an $Ldlr^{-/-}$ background and put the MKK/$Ldlr^{-/-}$ mice on a western diet to induce atherosclerosis. I will also make these mice diabetic, as it has been shown that glucose primarily drives production and release of S100A8/S100A9 from neutrophils. I predict that MKK/$Ldlr^{-/-}$ mice will have less circulating S100A8/S100A9,

monocytes, and neutrophils and less macrophage infiltration into aortic lesions (as determined by CD68 staining of *en face* aortas). I will also explore the mechanism behind glucose activation of KLF5. Sp1, a regulator of *Klf5* transcription, is phosphorylated by ERK1/2 (353). When AGEs bind to RAGE, ERK1/2 is phosphorylated (354). Thus, RAGE may activate KLF5 transcription *via* an ERK/Sp1 pathway. To test this I will differentiate HL-60 cells to neutrophils and incubate these cells with AGEs. I will next probe these cells by western blot for phospho-ERK, phospho-Sp1, and Klf5. If this pathway determines KLF5 transcription, I would expect to see an increase in all three of these proteins after incubating with AGEs in a dose-dependent manner.

I will next explore in future *in vitro* studies whether KLF5 has a role in neutrophil migration. The role of neutrophils in atherosclerotic lesions is understudied compared to the role of macrophages. Neutrophils are the most abundant WBC in circulation and neutrophil count positively correlates with coronary artery stenosis (355). Neutrophils are also a major cellular component in atherosclerotic lesions in $ApoE^{-/-}$ mice (356). I discuss in Section 4.3 how S100A8 and S100A9 regulate microtubule assembly *via* affecting intracellular Ca^{2+}. Thus by regulating these two proteins, I will determine whether KLF5 plays a role in neutrophil migration. To assess if KLF5 plays a role in microtubule assembly, I will knockdown KLF5 in neutrophils (differentiated from HL-60 cells) with an siRNA. Next, I will determine whether knockdown of *Klf5* affects microtubule polymerization by measuring fluorescent intensity of diamindino-phenylindole (357). To determine if KLF5 affects cell migration I will place these cells on a transwell plate and measure their chemotaxis towards a stimulus such as IL-8 (358). If KLF5 plays a role in microtubule assembly and neutrophil migration, I predict that by knocking down KLF5 there will be less microtubule assembly and fewer cells migrating through the transwell.

A large limitation to these studies is that KLF5 may play no role in neutrophil S100A8/A9 production or cellular functions like microtubule assembly. If this is the case, I will continue to find a transcriptional regulator of S100A8 and S100A9 in the neutrophils by taking an unbiased approach. A technique that has been recently developed allows one to understand the regulation of expression at a molecular level. Hybridization Capture of Chromatin Associated Proteins for Proteomics (HyCCAPP) uses the principles of Chip-Seq, but in reverse (359). Single-stranded DNA oligonucleotides hybridize to genomic sequences of interest (in our case S100A8 and S100A9) of cross-linked chromatin fragments. Proteins associated with this region are identified with mass spectrometry. I identified that differentiation of HL-60 cells to neutrophils dramatically increases *S100A8* and *S100A9*. Using this method, I can pinpoint the proteins involved in the transcription of S100A8 and S100A9 of HL-60 cells treated or not treated with ATRA. By finding the factors involved in S100A8 and S100A9 transcription, we will be able to elucidate the regulation of these DAMPs.

In conclusion, this thesis describes lipid metabolism in the kidney during the fasted state as well as sets a direction for future *in vivo* nephropathy studies. The thesis explored preliminary *in vitro* and *in vivo* data about KLF5 in neutrophils. Future studies will better elucidate how KLF5 affects neutrophil inflammation and function.

References

1. Quinlan, G. J., Martin, G. S., and Evans, T. W. (2005) Albumin: biochemical properties and therapeutic potential. *Hepatology* **41**, 1211-1219

2. Wang, Y., Tran, K., and Yao, Z. (1999) The activity of microsomal triglyceride transfer protein is essential for accumulation of triglyceride within microsomes in McA-RH7777 cells. A unified model for the assembly of very low density lipoproteins. *The Journal of biological chemistry* **274**, 27793-27800

3. Goldberg, I. J., Scheraldi, C. A., Yacoub, L. K., Saxena, U., and Bisgaier, C. L. (1990) Lipoprotein ApoC-II activation of lipoprotein lipase. Modulation by apolipoprotein A-IV. *Journal of Biological Chemistry* **265**, 4266-4272

4. Davies, B. S., Goulbourne, C. N., Barnes, R. H., 2nd, Turlo, K. A., Gin, P., Vaughan, S., Vaux, D. J., Bensadoun, A., Beigneux, A. P., Fong, L. G., and Young, S. G. (2012) Assessing mechanisms of GPIHBP1 and lipoprotein lipase movement across endothelial cells. *Journal of lipid research* **53**, 2690-2697

5. Goldberg, I. J., and Merkel, M. (2001) Lipoprotein lipase: physiology, biochemistry, and molecular biology. *Front Biosci* **6**, D388-405

6. Goulbourne, Chris N., Gin, P., Tatar, A., Nobumori, C., Hoenger, A., Jiang, H., Grovenor, Chris R. M., Adeyo, O., Esko, Jeffrey D., Goldberg, Ira J., Reue, K., Tontonoz, P., Bensadoun, A., Beigneux, Anne P., Young, Stephen G., and Fong, Loren G. (2014) The GPIHBP1–LPL Complex Is Responsible for the Margination of Triglyceride-Rich Lipoproteins in Capillaries. *Cell metabolism* **19**, 849-860

7. Burnett, J. R., Hooper, A. J., and Hegele, R. A. (1993) Familial Lipoprotein Lipase Deficiency. in *GeneReviews(R)* (Pagon, R. A., Adam, M. P., Ardinger, H. H., Wallace, S. E., Amemiya, A., Bean, L. J. H., Bird, T. D., Ledbetter, N., Mefford, H. C., Smith, R. J. H., and Stephens, K. eds.), Seattle (WA). pp

8. Brown, W. V. (1972) Some functional aspects of the plasma apolipoproteins. *Verh Dtsch Ges Inn Med* **78**, 1292

9. Brown, W. V., Levy, R. I., and Fredrickson, D. S. (1969) Studies of the proteins in human plasma very low density lipoproteins. *The Journal of biological chemistry* **244**, 5687-5694

10. Gordts, P. L., Nock, R., Son, N. H., Ramms, B., Lew, I., Gonzales, J. C., Thacker, B. E., Basu, D., Lee, R. G., Mullick, A. E., Graham, M. J., Goldberg, I. J., Crooke, R. M., Witztum, J. L., and Esko, J. D. (2016) ApoC-III inhibits clearance of triglyceride-rich lipoproteins through LDL family receptors. *The Journal of clinical investigation* **126**, 2855-2866

11. Fujimoto, E., Kobayashi, T., Fujimoto, N., Akiyama, M., Tajima, S., and Nagai, R. (2010) AGE-modified collagens I and III induce keratinocyte terminal differentiation through AGE receptor CD36: epidermal-dermal interaction in acquired perforating dermatosis. *The Journal of investigative dermatology* **130**, 405-414

12. Dijk, W., and Kersten, S. (2014) Regulation of lipoprotein lipase by Angptl4. *Trends in Endocrinology & Metabolism* **25**, 146-155

13. Dijk, W., Beigneux, A. P., Larsson, M., Bensadoun, A., Young, S. G., and Kersten, S. (2016) Angiopoietin-like 4 promotes intracellular degradation of lipoprotein lipase in adipocytes. *Journal of lipid research* **57**, 1670-1683

14. Lestavel, S., and Fruchart, J. C. (1994) Lipoprotein receptors. *Cell Mol Biol (Noisy-le-grand)* **40**, 461-481

15. Sudhof, T. C., Van der Westhuyzen, D. R., Goldstein, J. L., Brown, M. S., and Russell, D. W. (1987) Three direct repeats and a TATA-like sequence are required for regulated expression of the human low density lipoprotein receptor gene. *The Journal of biological chemistry* **262**, 10773-10779

16. Smith, J. R., Osborne, T. F., Goldstein, J. L., and Brown, M. S. (1990) Identification of nucleotides responsible for enhancer activity of sterol regulatory element in low density lipoprotein receptor gene. *The Journal of biological chemistry* **265**, 2306-2310

17. Lagace, T. A. (2014) PCSK9 and LDLR degradation: regulatory mechanisms in circulation and in cells. *Current opinion in lipidology* **25**, 387-393

18. Alique, M., Luna, C., Carracedo, J., and Ramírez, R. (2015) LDL biochemical modifications: a link between atherosclerosis and aging. *Food & Nutrition Research* **59**

19. Parthasarathy, S., Raghavamenon, A., Garelnabi, M. O., and Santanam, N. (2010) Oxidized low-density lipoprotein. *Methods Mol Biol* **610**, 403-417

20. Hamilton, J. A. (1999) Transport of fatty acids across membranes by the diffusion mechanism. *Prostaglandins Leukot Essent Fatty Acids* **60**, 291-297

21. Abumrad, N., Coburn, C., and Ibrahimi, A. (1999) Membrane proteins implicated in long-chain fatty acid uptake by mammalian cells: CD36, FATP and FABPm. *Biochimica et biophysica acta* **1441**, 4-13

22. Baldwin, J., Snow, R. J., Carey, M. F., and Febbraio, M. A. (1999) Muscle IMP accumulation during fatiguing submaximal exercise in endurance trained and untrained men. *The American journal of physiology* **277**, R295-300

23. Weisiger, R. A. (2002) Cytosolic fatty acid binding proteins catalyze two distinct steps in intracellular transport of their ligands. *Molecular and Cellular Biochemistry* **239**, 35-43

24. Stahl, A. (2004) A current review of fatty acid transport proteins (SLC27). *Pflugers Archiv : European journal of physiology* **447**, 722-727

25. Nicholson, A. C., Frieda, S., Pearce, A., and Silverstein, R. L. (1995) Oxidized LDL Binds to CD36 on Human Monocyte-Derived Macrophages and Transfected Cell Lines. *Evidence Implicating the Lipid Moiety of the Lipoprotein as the Binding Site* **15**, 269-275

26. Silverstein, R. L., Baird, M., Lo, S. K., and Yesner, L. M. (1992) Sense and antisense cDNA transfection of CD36 (glycoprotein IV) in melanoma cells. Role of CD36 as a thrombospondin receptor. *The Journal of biological chemistry* **267**, 16607-16612

27. Ockenhouse, C. F., Tandon, N. N., Magowan, C., Jamieson, G. A., and Chulay, J. D. (1989) Identification of a platelet membrane glycoprotein as a falciparum malaria sequestration receptor. *Science* **243**, 1469-1471

28. Baillie, A. G., Coburn, C. T., and Abumrad, N. A. (1996) Reversible binding of long-chain fatty acids to purified FAT, the adipose CD36 homolog. *J Membr Biol* **153**, 75-81

29. Febbraio, M., Abumrad, N. A., Hajjar, D. P., Sharma, K., Cheng, W., Pearce, S. F., and Silverstein, R. L. (1999) A null mutation in murine CD36 reveals an important role in fatty acid and lipoprotein metabolism. *The Journal of biological chemistry* **274**, 19055-19062

30. Coburn, C. T., Knapp, F. F., Jr., Febbraio, M., Beets, A. L., Silverstein, R. L., and Abumrad, N. A. (2000) Defective uptake and utilization of long chain fatty acids in muscle and adipose tissues of CD36 knockout mice. *J Biol Chem* **275**, 32523-32529

31. Ibrahimi, A., Bonen, A., Blinn, W. D., Hajri, T., Li, X., Zhong, K., Cameron, R., and Abumrad, N. A. (1999) Muscle-specific overexpression of FAT/CD36 enhances fatty acid oxidation by contracting muscle, reduces plasma triglycerides and fatty acids, and increases plasma glucose and insulin. *The Journal of biological chemistry* **274**, 26761-26766

32. Kazantzis, M., and Stahl, A. (2012) Fatty Acid transport Proteins, implications in physiology and disease. *Biochimica et biophysica acta* **1821**, 852-857

33. Hall, A. M., Smith, A. J., and Bernlohr, D. A. (2003) Characterization of the Acyl-CoA synthetase activity of purified murine fatty acid transport protein 1. *The Journal of biological chemistry* **278**, 43008-43013

34. Hall, A. M., Wiczer, B. M., Herrmann, T., Stremmel, W., and Bernlohr, D. A. (2005) Enzymatic properties of purified murine fatty acid transport protein 4 and analysis of acyl-CoA synthetase activities in tissues from FATP4 null mice. *The Journal of biological chemistry* **280**, 11948-11954

35. Storey, S. M., McIntosh, A. L., Huang, H., Martin, G. G., Landrock, K. K., Landrock, D., Payne, H. R., Kier, A. B., and Schroeder, F. (2012) Loss of intracellular lipid binding proteins differentially impacts saturated fatty acid uptake and nuclear targeting in mouse hepatocytes. *Am J Physiol Gastrointest Liver Physiol* **303**, G837-850

36. Tan, N. S., Shaw, N. S., Vinckenbosch, N., Liu, P., Yasmin, R., Desvergne, B., Wahli, W., and Noy, N. (2002) Selective cooperation between fatty acid binding proteins and peroxisome proliferator-activated receptors in regulating transcription. *Molecular and cellular biology* **22**, 5114-5127

37. Bonnefont, J. P., Djouadi, F., Prip-Buus, C., Gobin, S., Munnich, A., and Bastin, J. (2004) Carnitine palmitoyltransferases 1 and 2: biochemical, molecular and medical aspects. *Molecular aspects of medicine* **25**, 495-520

38. Dekker, M. J., Su, Q., Baker, C., Rutledge, A. C., and Adeli, K. (2010) Fructose: a highly lipogenic nutrient implicated in insulin resistance, hepatic steatosis, and the metabolic syndrome. *American journal of physiology. Endocrinology and metabolism* **299**, E685-694

39. Donaldson, W. E. (1979) Regulation of fatty acid synthesis. *Federation proceedings* **38**, 2617-2621

40. Wakil, S. J. (1989) Fatty acid synthase, a proficient multifunctional enzyme. *Biochemistry* **28**, 4523-4530

41. Fon Tacer, K., and Rozman, D. (2011) Nonalcoholic Fatty liver disease: focus on lipoprotein and lipid deregulation. *J Lipids* **2011**, 783976

42. Sanders, F. W. B., and Griffin, J. L. (2016). *Biological Reviews of the Cambridge Philosophical Society* **91**, 452-468

43. da Silva Xavier, G., Rutter, G. A., Diraison, F., Andreolas, C., and Leclerc, I. (2006) ChREBP binding to fatty acid synthase and L-type pyruvate kinase genes is stimulated by glucose in pancreatic beta-cells. *Journal of lipid research* **47**, 2482-2491

44. O'Callaghan, B. L., Koo, S. H., Wu, Y., Freake, H. C., and Towle, H. C. (2001) Glucose regulation of the acetyl-CoA carboxylase promoter PI in rat hepatocytes. *The Journal of biological chemistry* **276**, 16033-16039

45. Lin, M. E., Herr, D. R., and Chun, J. (2010) Lysophosphatidic acid (LPA) receptors: signaling properties and disease relevance. *Prostaglandins & other lipid mediators* **91**, 130-138

46. Lipp, P., and Reither, G. (2011) Protein Kinase C: The "Masters" of Calcium and Lipid. *Cold Spring Harbor Perspectives in Biology* **3**

47. Shi, Y., and Cheng, D. (2009) Beyond triglyceride synthesis: the dynamic functional roles of MGAT and DGAT enzymes in energy metabolism. *American journal of physiology. Endocrinology and metabolism* **297**, E10-18

48. Itabe, H., Yamaguchi, T., Nimura, S., and Sasabe, N. (2017) Perilipins: a diversity of intracellular lipid droplet proteins. *Lipids in Health and Disease* **16**

49. Kraemer, F. B., and Shen, W. J. (2002) Hormone-sensitive lipase: control of intracellular tri-(di-)acylglycerol and cholesteryl ester hydrolysis. *Journal of lipid research* **43**, 1585-1594

50. Kim, J. Y., Tillison, K., Lee, J. H., Rearick, D. A., and Smas, C. M. (2006) The adipose tissue triglyceride lipase ATGL/PNPLA2 is downregulated by insulin and TNF-alpha in 3T3-L1 adipocytes and is a target for transactivation by PPARgamma. *American journal of physiology. Endocrinology and metabolism* **291**, E115-127

51. Birn, H., Nexo, E., Christensen, E. I., and Nielsen, R. (2003) Diversity in rat tissue accumulation of vitamin B12 supports a distinct role for the kidney in vitamin B12 homeostasis. *Nephrology, dialysis, transplantation : official publication of the European Dialysis and Transplant Association - European Renal Association* **18**, 1095-1100

52. Monsalve, F. A., Pyarasani, R. D., Delgado-Lopez, F., and Moore-Carrasco, R. (2013) Peroxisome Proliferator-Activated Receptor Targets for the Treatment of Metabolic Diseases. *Mediators of inflammation* **2013**, 18

53. Tyagi, S., Gupta, P., Saini, A., Kaushal, C., and Sharma, S. (2011) The peroxisome proliferator-activated receptor: A family of nuclear receptors role in various diseases. *Journal of Advanced Pharmaceutical Technology & Research* **2**, 236-240

54. Bonen, A., Campbell, S. E., Benton, C. R., Chabowski, A., Coort, S. L., Han, X. X., Koonen, D. P., Glatz, J. F., and Luiken, J. J. (2004) Regulation of fatty acid transport by fatty acid translocase/CD36. *The Proceedings of the Nutrition Society* **63**, 245-249

55. Sato, O., Kuriki, C., Fukui, Y., and Motojima, K. (2002) Dual promoter structure of mouse and human fatty acid translocase/CD36 genes and unique transcriptional activation by peroxisome proliferator-activated receptor alpha and gamma ligands. *The Journal of biological chemistry* **277**, 15703-15711

56. Lee, W. S., and Kim, J. (2015) Peroxisome Proliferator-Activated Receptors and the Heart: Lessons from the Past and Future Directions. *PPAR Res* **2015**, 271983

57. Plutzky, J. (2000) Peroxisome proliferator-activated receptors in vascular biology and atherosclerosis: emerging insights for evolving paradigms. *Current atherosclerosis reports* **2**

58. Grygiel-Górniak, B. (2014) Peroxisome proliferator-activated receptors and their ligands: nutritional and clinical implications - a review. *Nutrition Journal* **13**, 17

59. Wang, Y. X., Zhang, C. L., Yu, R. T., Cho, H. K., Nelson, M. C., Bayuga-Ocampo, C. R., Ham, J., Kang, H., and Evans, R. M. (2004) Regulation of muscle fiber type and running endurance by PPARdelta. *PLoS Biol* **2**, e294

60. Wang, P., Liu, J., Li, Y., Wu, S., Luo, J., Yang, H., Subbiah, R., Chatham, J., Zhelyabovska, O., and Yang, Q. (2010) Peroxisome Proliferator-Activated Receptor δ Is an Essential Transcriptional Regulator for Mitochondrial Protection and Biogenesis in Adult Heart. *Circulation research* **106**, 911-919

61. Roy, D., Farabaugh, K. T., Wu, J., Charrier, A., Smas, C., Hatzoglou, M., Thirumurugan, K., and Buchner, D. A. (2017) Coordinated transcriptional control of adipocyte triglyceride lipase (Atgl) by transcription factors Sp1 and peroxisome proliferator-activated receptor gamma (PPARgamma) during adipocyte differentiation. *The Journal of biological chemistry* **292**, 14827-14835

62. Siersbaek, R., Nielsen, R., and Mandrup, S. (2010) PPARgamma in adipocyte differentiation and metabolism--novel insights from genome-wide studies. *FEBS letters* **584**, 3242-3249

63. Jones, J. R., Barrick, C., Kim, K.-A., Lindner, J., Blondeau, B., Fujimoto, Y., Shiota, M., Kesterson, R. A., Kahn, B. B., and Magnuson, M. A. (2005) Deletion of PPARγ in adipose tissues of mice protects against high fat diet-induced obesity and insulin resistance. *Proceedings of the National Academy of Sciences of the United States of America* **102**, 6207-6212

64. Dalen, K. T., Schoonjans, K., Ulven, S. M., Weedon-Fekjaer, M. S., Bentzen, T. G., Koutnikova, H., Auwerx, J., and Nebb, H. I. (2004) Adipose tissue expression of the lipid droplet-associating proteins S3-12 and perilipin is controlled by peroxisome proliferator-activated receptor-gamma. *Diabetes* **53**, 1243-1252

65. Guan, H.-P., Li, Y., Jensen, M. V., Newgard, C. B., Steppan, C. M., and Lazar, M. A. (2002) A futile metabolic cycle activated in adipocytes by antidiabetic agents. *Nature medicine* **8**, 1122-1128

66. Dumasia, R., Eagle, K. A., Kline-Rogers, E., May, N., Cho, L., and Mukherjee, D. (2005) Role of PPAR- gamma agonist thiazolidinediones in treatment of pre-diabetic and diabetic individuals: a cardiovascular perspective. *Current drug targets. Cardiovascular & haematological disorders* **5**, 377-386

67. Hauner, H. (2002) The mode of action of thiazolidinediones. *Diabetes/metabolism research and reviews* **18 Suppl 2**, S10-15

68. Huang, Y., Powers, C., Moore, V., Schafer, C., Ren, M., Phoon, C. K., James, J. F., Glukhov, A. V., Javadov, S., Vaz, F. M., Jefferies, J. L., Strauss, A. W., and Khuchua, Z.

(2017) The PPAR pan-agonist bezafibrate ameliorates cardiomyopathy in a mouse model of Barth syndrome. *Orphanet J Rare Dis* **12**, 49

69. Feng, L., Luo, H., Xu, Z., Yang, Z., Du, G., Zhang, Y., Yu, L., Hu, K., Zhu, W., Tong, Q., Chen, K., Guo, F., Huang, C., and Li, Y. (2016) Bavachinin, as a novel natural pan-PPAR agonist, exhibits unique synergistic effects with synthetic PPAR-gamma and PPAR-alpha agonists on carbohydrate and lipid metabolism in db/db and diet-induced obese mice. *Diabetologia* **59**, 1276-1286

70. Lee, Y., Hirose, H., Ohneda, M., Johnson, J. H., McGarry, J. D., and Unger, R. H. (1994) Beta-cell lipotoxicity in the pathogenesis of non-insulin-dependent diabetes mellitus of obese rats: impairment in adipocyte-beta-cell relationships. *Proceedings of the National Academy of Sciences of the United States of America* **91**, 10878-10882

71. Alkhouri, N., Dixon, L. J., and Feldstein, A. E. (2009) Lipotoxicity in nonalcoholic fatty liver disease: not all lipids are created equal. *Expert Rev Gastroenterol Hepatol* **3**, 445-451

72. Bosma, M., Kersten, S., Hesselink, M. K., and Schrauwen, P. (2012) Re-evaluating lipotoxic triggers in skeletal muscle: relating intramyocellular lipid metabolism to insulin sensitivity. *Prog Lipid Res* **51**, 36-49

73. Izquierdo-Lahuerta, A., Martinez-Garcia, C., and Medina-Gomez, G. (2016) Lipotoxicity as a trigger factor of renal disease. *Journal of nephrology* **29**, 603-610

74. Wende, A. R., and Abel, E. D. (2010) Lipotoxicity in the heart. *Biochimica et biophysica acta* **1801**, 311-319

75. Gordon, G. B. (1977) Saturated free fatty acid toxicity. II. Lipid accumulation, ultrastructural alterations, and toxicity in mammalian cells in culture. *Exp Mol Pathol* **27**, 262-276

76. Listenberger, L. L., Han, X., Lewis, S. E., Cases, S., Farese, R. V., Jr., Ory, D. S., and Schaffer, J. E. (2003) Triglyceride accumulation protects against fatty acid-induced lipotoxicity. *Proceedings of the National Academy of Sciences of the United States of America* **100**, 3077-3082

77. Li, Z. Z., Berk, M., McIntyre, T. M., and Feldstein, A. E. (2009) Hepatic lipid partitioning and liver damage in nonalcoholic fatty liver disease: role of stearoyl-CoA desaturase. *The Journal of biological chemistry* **284**, 5637-5644

78. Kharroubi, I., Ladriere, L., Cardozo, A. K., Dogusan, Z., Cnop, M., and Eizirik, D. L. (2004) Free fatty acids and cytokines induce pancreatic beta-cell apoptosis by different mechanisms: role of nuclear factor-kappaB and endoplasmic reticulum stress. *Endocrinology* **145**, 5087-5096

79. Bosma, M., Dapito, D. H., Drosatos-Tampakaki, Z., Huiping-Son, N., Huang, L. S., Kersten, S., Drosatos, K., and Goldberg, I. J. (2014) Sequestration of fatty acids in triglycerides prevents endoplasmic reticulum stress in an in vitro model of cardiomyocyte lipotoxicity. *Biochimica et biophysica acta* **1841**, 1648-1655

80. Feldstein, A. E., Canbay, A., Guicciardi, M. E., Higuchi, H., Bronk, S. F., and Gores, G. J. (2003) Diet associated hepatic steatosis sensitizes to Fas mediated liver injury in mice. *J Hepatol* **39**, 978-983

81. Pusl, T., Wild, N., Vennegeerts, T., Wimmer, R., Goke, B., Brand, S., and Rust, C. (2008) Free fatty acids sensitize hepatocytes to bile acid-induced apoptosis. *Biochemical and biophysical research communications* **371**, 441-445

82. Yant, L. J., Ran, Q., Rao, L., Van Remmen, H., Shibatani, T., Belter, J. G., Motta, L., Richardson, A., and Prolla, T. A. (2003) The selenoprotein GPX4 is essential for mouse development and protects from radiation and oxidative damage insults. *Free Radic Biol Med* **34**, 496-502

83. Summers, S. A. (2006) Ceramides in insulin resistance and lipotoxicity. *Prog Lipid Res* **45**, 42-72

84. Szendroedi, J., Yoshimura, T., Phielix, E., Koliaki, C., Marcucci, M., Zhang, D., Jelenik, T., Muller, J., Herder, C., Nowotny, P., Shulman, G. I., and Roden, M. (2014) Role of diacylglycerol activation of PKCtheta in lipid-induced muscle insulin resistance in humans. *Proceedings of the National Academy of Sciences of the United States of America* **111**, 9597-9602

85. Drosatos, K., Bharadwaj, K. G., Lymperopoulos, A., Ikeda, S., Khan, R., Hu, Y., Agarwal, R., Yu, S., Jiang, H., Steinberg, S. F., Blaner, W. S., Koch, W. J., and Goldberg, I. J. (2011) Cardiomyocyte lipids impair beta-adrenergic receptor function via PKC activation. *American journal of physiology. Endocrinology and metabolism* **300**, E489-499

86. Ishibashi, Y., Kohyama-Koganeya, A., and Hirabayashi, Y. (2013) New insights on glucosylated lipids: metabolism and functions. *Biochimica et biophysica acta* **1831**, 1475-1485

87. Kitatani, K., Idkowiak-Baldys, J., and Hannun, Y. A. (2008) The sphingolipid salvage pathway in ceramide metabolism and signaling. *Cellular signalling* **20**, 1010-1018

88. Park, T.-S., Hu, Y., Noh, H.-L., Drosatos, K., Okajima, K., Buchanan, J., Tuinei, J., Homma, S., Jiang, X.-C., Abel, E. D., and Goldberg, I. J. (2008) Ceramide is a cardiotoxin in lipotoxic cardiomyopathy. *Journal of lipid research* **49**, 2101-2112

89. Dyntar, D., Eppenberger-Eberhardt, M., Maedler, K., Pruschy, M., Eppenberger, H. M., Spinas, G. A., and Donath, M. Y. (2001) Glucose and palmitic acid induce degeneration of myofibrils and modulate apoptosis in rat adult cardiomyocytes. *Diabetes* **50**, 2105-2113

90. Yang, G., Badeanlou, L., Bielawski, J., Roberts, A. J., Hannun, Y. A., and Samad, F. (2009) Central role of ceramide biosynthesis in body weight regulation, energy metabolism, and the metabolic syndrome. *American journal of physiology. Endocrinology and metabolism* **297**, E211-224

91. Febbraio, M. A. (2014) Role of interleukins in obesity: implications for metabolic disease. *Trends in endocrinology and metabolism: TEM* **25**, 312-319

92. Boucher, J., Kleinridders, A., and Kahn, C. R. (2014) Insulin Receptor Signaling in Normal and Insulin-Resistant States. *Cold Spring Harbor Perspectives in Biology* **6**

93. Huang, S., and Czech, M. P. (2007) The GLUT4 glucose transporter. *Cell metabolism* **5**, 237-252

94. Liu, L., Trent, C. M., Fang, X., Son, N. H., Jiang, H., Blaner, W. S., Hu, Y., Yin, Y. X., Farese, R. V., Jr., Homma, S., Turnbull, A. V., Eriksson, J. W., Hu, S. L., Ginsberg, H. N., Huang, L. S., and Goldberg, I. J. (2014) Cardiomyocyte-specific loss of diacylglycerol acyltransferase 1 (DGAT1) reproduces the abnormalities in lipids found in severe heart failure. *The Journal of biological chemistry* **289**, 29881-29891

95. van Hees, A. M., Jans, A., Hul, G. B., Roche, H. M., Saris, W. H., and Blaak, E. E. (2011) Skeletal muscle fatty acid handling in insulin resistant men. *Obesity (Silver Spring, Md.)* **19**, 1350-1359

96. Wakelam, M. J. (1998) Diacylglycerol--when is it an intracellular messenger? *Biochimica et biophysica acta* **1436**, 117-126

97. Eichmann, T. O., Kumari, M., Haas, J. T., Farese, R. V., Jr., Zimmermann, R., Lass, A., and Zechner, R. (2012) Studies on the substrate and stereo/regioselectivity of adipose triglyceride lipase, hormone-sensitive lipase, and diacylglycerol-O-acyltransferases. *The Journal of biological chemistry* **287**, 41446-41457

98. Preuss, H. G. (1993) Basics of renal anatomy and physiology. *Clin Lab Med* **13**, 1-11

99. Sahay, M., Kalra, S., and Bandgar, T. (2012) Renal endocrinology: The new frontier. *Indian Journal of Endocrinology and Metabolism* **16**, 154-155

100. Jaikumkao, K., Pongchaidecha, A., Chatsudthipong, V., Chattipakorn, S. C., Chattipakorn, N., and Lungkaphin, A. (2017) The roles of sodium-glucose cotransporter 2 inhibitors in preventing kidney injury in diabetes. *Biomedicine & Pharmacotherapy* **94**, 176-187

101. Webster, A. C., Nagler, E. V., Morton, R. L., and Masson, P. (2017) Chronic Kidney Disease. *Lancet* **389**, 1238-1252

102. Scheen, A. J. (2017) Pharmacological management of type 2 diabetes: what's new in 2017? *Expert Rev Clin Pharmacol*

103. Pearce, D., Soundararajan, R., Trimpert, C., Kashlan, O. B., Deen, P. M. T., and Kohan, D. E. (2015) Collecting Duct Principal Cell Transport Processes and Their Regulation. *Clinical Journal of the American Society of Nephrology : CJASN* **10**, 135-146

104. Kurts, C., Panzer, U., Anders, H. J., and Rees, A. J. (2013) The immune system and kidney disease: basic concepts and clinical implications. *Nat Rev Immunol* **13**, 738-753

105. Liu, J., and Wang, W. (2017) Genetic basis of adult-onset nephrotic syndrome and focal segmental glomerulosclerosis. *Frontiers of medicine* **11**, 333-339

106. Pal, A., and Kaskel, F. (2016) History of Nephrotic Syndrome and Evolution of its Treatment. *Frontiers in pediatrics* **4**

107. Williams, M. E. (2010) Diabetic CKD/ESRD 2010: a progress report? *Semin Dial* **23**, 129-133

108. Shahbazian, H. (2013) Diabetic kidney disease; review of the current knowledge. **2**, 73-80

109. Perico, N., Ruggenenti, P., and Remuzzi, G. (2017) ACE and SGLT2 inhibitors: the future for non-diabetic and diabetic proteinuric renal disease. *Current opinion in pharmacology* **33**, 34-40

110. Ruggenenti, P., Fassi, A., Ilieva, A. P., Bruno, S., Iliev, I. P., Brusegan, V., Rubis, N., Gherardi, G., Arnoldi, F., Ganeva, M., Ene-Iordache, B., Gaspari, F., Perna, A., Bossi, A., Trevisan, R., Dodesini, A. R., Remuzzi, G., and Bergamo Nephrologic Diabetes Complications Trial, I. (2004) Preventing microalbuminuria in type 2 diabetes. *The New England journal of medicine* **351**, 1941-1951

111. Satirapoj, B. (2017) Sodium-Glucose Cotransporter 2 Inhibitors with Renoprotective Effects. *Kidney Dis (Basel)* **3**, 24-32

112. Park, T. S. (2012) How much glycemic control is needed to prevent progression of diabetic nephropathy? *Journal of Diabetes Investigation* **3**, 411-412

113. Andrassy, K. M. (2013) Comments on 'KDIGO 2012 Clinical Practice Guideline for the Evaluation and Management of Chronic Kidney Disease'. *Kidney international* **84**, 622-623

114. Zanoli, L., Granata, A., Lentini, P., Rastelli, S., Fatuzzo, P., Rapisarda, F., and Castellino, P. (2015) Sodium-glucose linked transporter-2 inhibitors in chronic kidney disease. *TheScientificWorldJournal* **2015**, 317507

115. Kojima, N., Williams, J. M., Slaughter, T. N., Kato, S., Takahashi, T., Miyata, N., and Roman, R. J. (2015) Renoprotective effects of combined SGLT2 and ACE inhibitor therapy in diabetic Dahl S rats. *Physiol Rep* **3**

116. Chen, S., and Tseng, C. H. (2013) Dyslipidemia, Kidney Disease, and Cardiovascular Disease in Diabetic Patients. *The Review of Diabetic Studies : RDS* **10**, 88-100

117. Manjunath, C. N., Rawal, J. R., Irani, P. M., and Madhu, K. (2013) Atherogenic dyslipidemia. *Indian Journal of Endocrinology and Metabolism* **17**, 969-976

118. Su, X., Zhang, L., Lv, J., Wang, J., Hou, W., Xie, X., and Zhang, H. (2016) Effect of Statins on Kidney Disease Outcomes: A Systematic Review and Meta-analysis. *American*

journal of kidney diseases : the official journal of the National Kidney Foundation **67**, 881-892

119. Strippoli, G. F. M., Navaneethan, S. D., Johnson, D. W., Perkovic, V., Pellegrini, F., Nicolucci, A., and Craig, J. C. (2008) Effects of statins in patients with chronic kidney disease: meta-analysis and meta-regression of randomised controlled trials. *Bmj* **336**, 645-651

120. Ruan, X. Z., Varghese, Z., and Moorhead, J. F. (2009) An update on the lipid nephrotoxicity hypothesis. *Nature reviews. Nephrology* **5**, 713-721

121. Vaziri, N. D., Yuan, J., Ni, Z., Nicholas, S. B., and Norris, K. C. (2012) Lipoprotein lipase deficiency in chronic kidney disease is accompanied by down-regulation of endothelial GPIHBP1 expression. *Clinical and experimental nephrology* **16**, 238-243

122. Clement, L. C., Mace, C., Avila-Casado, C., Joles, J. A., Kersten, S., and Chugh, S. S. (2014) Circulating angiopoietin-like 4 links proteinuria with hypertriglyceridemia in nephrotic syndrome. *Nature medicine* **20**, 37-46

123. Han, S., Vaziri, N. D., Gollapudi, P., Kwok, V., and Moradi, H. (2013) Hepatic fatty acid and cholesterol metabolism in nephrotic syndrome. *Am J Transl Res* **5**, 246-253

124. Vaziri, N. D., and Liang, K. (1997) Down-regulation of VLDL receptor expression in chronic experimental renal failure. *Kidney international* **51**, 913-919

125. Bonomini, F., Rodella, L. F., Moghadasian, M., Lonati, C., Coleman, R., and Rezzani, R. (2011) Role of apolipoprotein E in renal damage protection. *Histochemistry and cell biology* **135**, 571-579

126. Kasiske, B. L., O'Donnell, M. P., Schmitz, P. G., Kim, Y., and Keane, W. F. (1990) Renal injury of diet-induced hypercholesterolemia in rats. *Kidney international* **37**, 880-891

127. Taneja, D., Thompson, J., Wilson, P., Brandewie, K., Schaefer, L., Mitchell, B., and Tannock, L. R. (2010) Reversibility of renal injury with cholesterol lowering in hyperlipidemic diabetic mice. *Journal of lipid research* **51**, 1464-1470

128. Grone, H. J., Walli, A., Grone, E., Niedmann, P., Thiery, J., Seidel, D., and Helmchen, U. (1989) Induction of glomerulosclerosis by dietary lipids. A functional and morphologic study in the rat. *Lab Invest* **60**, 433-446

129. Hirashio, S., Ueno, T., Naito, T., and Masaki, T. (2014) Characteristic kidney pathology, gene abnormality and treatments in LCAT deficiency. *Clinical and experimental nephrology* **18**, 189-193

130. Liu, S., and Vaziri, N. D. (2014) Role of PCSK9 and IDOL in the pathogenesis of acquired LDL receptor deficiency and hypercholesterolemia in nephrotic syndrome. *Nephrology, dialysis, transplantation : official publication of the European Dialysis and Transplant Association - European Renal Association* **29**, 538-543

131. Vaziri, N. D., and Liang, K. H. (1996) Down-regulation of hepatic LDL receptor expression in experimental nephrosis. *Kidney international* **50**, 887-893

132. Zewinger, S., Speer, T., Kleber, M. E., Scharnagl, H., Woitas, R., Lepper, P. M., Pfahler, K., Seiler, S., Heine, G. H., Marz, W., Silbernagel, G., and Fliser, D. (2014) HDL cholesterol is not associated with lower mortality in patients with kidney dysfunction. *Journal of the American Society of Nephrology : JASN* **25**, 1073-1082

133. Parsa, A., Kao, W. H., Xie, D., Astor, B. C., Li, M., Hsu, C. Y., Feldman, H. I., Parekh, R. S., Kusek, J. W., Greene, T. H., Fink, J. C., Anderson, A. H., Choi, M. J., Wright, J. T., Jr., Lash, J. P., Freedman, B. I., Ojo, A., Winkler, C. A., Raj, D. S., Kopp, J. B., He, J., Jensvold, N. G., Tao, K., Lipkowitz, M. S., Appel, L. J., Investigators, A. S., and Investigators, C. S. (2013) APOL1 risk variants, race, and progression of chronic kidney disease. *The New England journal of medicine* **369**, 2183-2196

134. Liang, K., and Vaziri, N. D. (2002) Upregulation of acyl-CoA: cholesterol acyltransferase in chronic renal failure. *American journal of physiology. Endocrinology and metabolism* **283**, E676-681

135. Vaziri, N. D. (2009) Causes of dysregulation of lipid metabolism in chronic renal failure. *Semin Dial* **22**, 644-651

136. Dummer, P. D., Limou, S., Rosenberg, A. Z., Heymann, J., Nelson, G., Winkler, C. A., and Kopp, J. B. (2015) APOL1 Kidney Disease Risk Variants: An Evolving Landscape. *Seminars in nephrology* **35**, 222-236

137. Kimmelstiel, P., and Wilson, C. (1936) Intercapillary Lesions in the Glomeruli of the Kidney. *The American journal of pathology* **12**, 83-98.87

138. Bobulescu, I. A. (2010) Renal lipid metabolism and lipotoxicity. *Current opinion in nephrology and hypertension* **19**, 393-402

139. Krzystanek, M., Pedersen, T. X., Bartels, E. D., Kjaehr, J., Straarup, E. M., and Nielsen, L. B. (2010) Expression of apolipoprotein B in the kidney attenuates renal lipid accumulation. *The Journal of biological chemistry* **285**, 10583-10590

140. Walzem, R. L., Hansen, R. J., Williams, D. L., and Hamilton, R. L. (1999) Estrogen induction of VLDLy assembly in egg-laying hens. *The Journal of nutrition* **129**, 467s-472s

141. Wang, Z., Jiang, T., Li, J., Proctor, G., McManaman, J. L., Lucia, S., Chua, S., and Levi, M. (2005) Regulation of renal lipid metabolism, lipid accumulation, and glomerulosclerosis in FVBdb/db mice with type 2 diabetes. *Diabetes* **54**, 2328-2335

142. Sun, L., Halaihel, N., Zhang, W., Rogers, T., and Levi, M. (2002) Role of sterol regulatory element-binding protein 1 in regulation of renal lipid metabolism and glomerulosclerosis in diabetes mellitus. *The Journal of biological chemistry* **277**, 18919-18927

143. Jiang, T., Wang, Z., Proctor, G., Moskowitz, S., Liebman, S. E., Rogers, T., Lucia, M. S., Li, J., and Levi, M. (2005) Diet-induced obesity in C57BL/6J mice causes increased renal lipid accumulation and glomerulosclerosis via a sterol regulatory element-binding protein-1c-dependent pathway. *The Journal of biological chemistry* **280**, 32317-32325

144. Stadler, K., Goldberg, I. J., and Susztak, K. (2015) The Evolving Understanding of the Contribution of Lipid Metabolism to Diabetic Kidney Disease. *Current diabetes reports* **15**, 40

145. Herman-Edelstein, M., Scherzer, P., Tobar, A., Levi, M., and Gafter, U. (2014) Altered renal lipid metabolism and renal lipid accumulation in human diabetic nephropathy. *Journal of lipid research* **55**, 561-572

146. Nieth, H., and Schollmeyer, P. (1966) Substrate-utilization of the human kidney. *Nature* **209**, 1244-1245

147. Uchida, S., and Endou, H. (1988) Substrate specificity to maintain cellular ATP along the mouse nephron. *The American journal of physiology* **255**, F977-983

148. Ruan, X., Zheng, F., and Guan, Y. (2008) PPARs and the kidney in metabolic syndrome. *American journal of physiology. Renal physiology* **294**, F1032-1047

149. Portilla, D., Li, S., Nagothu, K. K., Megyesi, J., Kaissling, B., Schnackenberg, L., Safirstein, R. L., and Beger, R. D. (2006) Metabolomic study of cisplatin-induced nephrotoxicity. *Kidney international* **69**, 2194-2204

150. Portilla, D., Dai, G., McClure, T., Bates, L., Kurten, R., Megyesi, J., Price, P., and Li, S. (2002) Alterations of PPARalpha and its coactivator PGC-1 in cisplatin-induced acute renal failure. *Kidney international* **62**, 1208-1218

151. Li, S., Basnakian, A., Bhatt, R., Megyesi, J., Gokden, N., Shah, S. V., and Portilla, D. (2004) PPAR-alpha ligand ameliorates acute renal failure by reducing cisplatin-induced increased expression of renal endonuclease G. *American journal of physiology. Renal physiology* **287**, F990-998

152. Kang, H. M., Ahn, S. H., Choi, P., Ko, Y. A., Han, S. H., Chinga, F., Park, A. S., Tao, J., Sharma, K., Pullman, J., Bottinger, E. P., Goldberg, I. J., and Susztak, K. (2015) Defective fatty acid oxidation in renal tubular epithelial cells has a key role in kidney fibrosis development. *Nat Med* **21**, 37-46

153. Cheng, R., Ding, L., He, X., Takahashi, Y., and Ma, J. X. (2016) Interaction of PPARalpha With the Canonic Wnt Pathway in the Regulation of Renal Fibrosis. *Diabetes* **65**, 3730-3743

154. Li, L., Emmett, N., Mann, D., and Zhao, X. (2010) Fenofibrate attenuates tubulointerstitial fibrosis and inflammation through suppression of nuclear factor-kappaB and transforming growth factor-beta1/Smad3 in diabetic nephropathy. *Experimental biology and medicine* **235**, 383-391

155. Kostapanos, M. S., Florentin, M., and Elisaf, M. S. (2013) Fenofibrate and the kidney: an overview. *European journal of clinical investigation* **43**, 522-531

156. Harada, M., Kamijo, Y., Nakajima, T., Hashimoto, K., Yamada, Y., Shimojo, H., Gonzalez, F. J., and Aoyama, T. (2016) Peroxisome proliferator-activated receptor alpha-dependent renoprotection of murine kidney by irbesartan. *Clin Sci (Lond)* **130**, 1969-1981

157. Cui, S., Verroust, P. J., Moestrup, S. K., and Christensen, E. I. (1996) Megalin/gp330 mediates uptake of albumin in renal proximal tubule. *The American journal of physiology* **271**, F900-907

158. Moorhead, J. F., Chan, M. K., El-Nahas, M., and Varghese, Z. (1982) Lipid nephrotoxicity in chronic progressive glomerular and tubulo-interstitial disease. *Lancet* **2**, 1309-1311

159. Ruge, T., Neuger, L., Sukonina, V., Wu, G., Barath, S., Gupta, J., Frankel, B., Christophersen, B., Nordstoga, K., Olivecrona, T., and Olivecrona, G. (2004) Lipoprotein lipase in the kidney: activity varies widely among animal species. *American journal of physiology. Renal physiology* **287**, F1131-1139

160. Yang, Y. L., Lin, S. H., Chuang, L. Y., Guh, J. Y., Liao, T. N., Lee, T. C., Chang, W. T., Chang, F. R., Hung, M. Y., Chiang, T. A., and Hung, C. Y. (2007) CD36 is a novel and potential anti-fibrogenic target in albumin-induced renal proximal tubule fibrosis. *Journal of cellular biochemistry* **101**, 735-744

161. Baines, R. J., Chana, R. S., Hall, M., Febbraio, M., Kennedy, D., and Brunskill, N. J. (2012) CD36 mediates proximal tubular binding and uptake of albumin and is upregulated in proteinuric nephropathies. *American journal of physiology. Renal physiology* **303**, F1006-1014

162. Feng, L., Gu, C., Li, Y., and Huang, J. (2017) High Glucose Promotes CD36 Expression by Upregulating Peroxisome Proliferator-Activated Receptor gamma Levels to Exacerbate Lipid Deposition in Renal Tubular Cells. *Biomed Res Int* **2017**, 1414070

163. Spencer, M. W., Muhlfeld, A. S., Segerer, S., Hudkins, K. L., Kirk, E., LeBoeuf, R. C., and Alpers, C. E. (2004) Hyperglycemia and hyperlipidemia act synergistically to induce renal disease in LDL receptor-deficient BALB mice. *American journal of nephrology* **24**, 20-31

164. Williams, M. E., and Garg, R. (2014) Glycemic management in ESRD and earlier stages of CKD. *American journal of kidney diseases : the official journal of the National Kidney Foundation* **63**, S22-38

165. Filippatos, T. D., and Elisaf, M. S. (2013) Effects of glucagon-like peptide-1 receptor agonists on renal function. *World J Diabetes* **4**, 190-201

166. Silverstein, R. L., Li, W., Park, Y. M., and Rahaman, S. O. (2010) Mechanisms of Cell Signaling by the Scavenger Receptor CD36: Implications in Atherosclerosis and Thrombosis. *Transactions of the American Clinical and Climatological Association* **121**, 206-220

167. Kennedy, D. J., Chen, Y., Huang, W., Viterna, J., Liu, J., Westfall, K., Tian, J., Bartlett, D. J., Tang, W. H., Xie, Z., Shapiro, J. I., and Silverstein, R. L. (2013) CD36 and Na/K-ATPase-alpha1 form a proinflammatory signaling loop in kidney. *Hypertension* **61**, 216-224

168. Souza, A. C., Bocharov, A. V., Baranova, I. N., Vishnyakova, T. G., Huang, Y. G., Wilkins, K. J., Hu, X., Street, J. M., Alvarez-Prats, A., Mullick, A. E., Patterson, A. P., Remaley, A. T., Eggerman, T. L., Yuen, P. S., and Star, R. A. (2016) Antagonism of scavenger receptor CD36 by 5A peptide prevents chronic kidney disease progression in mice independent of blood pressure regulation. *Kidney international* **89**, 809-822

169. Yang, P., Xiao, Y., Luo, X., Zhao, Y., Zhao, L., Wang, Y., Wu, T., Wei, L., and Chen, Y. (2017) Inflammatory stress promotes the development of obesity-related chronic kidney disease via CD36 in mice. *Journal of lipid research* **58**, 1417-1427

170. Scerbo, D., Son, N. H., Sirwi, A., Zeng, L., Sas, K. M., Cifarelli, V., Schoiswohl, G., Huggins, L. A., Gumaste, N., Hu, Y., Pennathur, S., Abumrad, N. A., Kershaw, E. E., Hussain, M. M., Susztak, K., and Goldberg, I. J. (2017) Kidney triglyceride accumulation in the fasted mouse is dependent upon serum free fatty acids. *Journal of lipid research* **58**, 1132-1142

171. Jiang, T., Liebman, S. E., Lucia, M. S., Li, J., and Levi, M. (2005) Role of altered renal lipid metabolism and the sterol regulatory element binding proteins in the pathogenesis of age-related renal disease. *Kidney international* **68**, 2608-2620

172. Simon, N., and Hertig, A. (2015) Alteration of Fatty Acid Oxidation in Tubular Epithelial Cells: From Acute Kidney Injury to Renal Fibrogenesis. *Frontiers in medicine* **2**, 52

173. Trent, C. M., Yu, S., Hu, Y., Skoller, N., Huggins, L. A., Homma, S., and Goldberg, I. J. (2014) Lipoprotein lipase activity is required for cardiac lipid droplet production. *Journal of lipid research* **55**, 645-658

174. Goldberg, I. J., Trent, C. M., and Schulze, P. C. (2012) Lipid metabolism and toxicity in the heart. *Cell metabolism* **15**, 805-812

175. Hamilton, J. A. (1998) Fatty acid transport: difficult or easy? *Journal of lipid research* **39**, 467-481

176. Schwenk, R. W., Holloway, G. P., Luiken, J. J., Bonen, A., and Glatz, J. F. (2010) Fatty acid transport across the cell membrane: regulation by fatty acid transporters. *Prostaglandins Leukot Essent Fatty Acids* **82**, 149-154

177. Harmon, C. M., and Abumrad, N. A. (1993) Binding of sulfosuccinimidyl fatty acids to adipocyte membrane proteins: isolation and amino-terminal sequence of an 88-kD protein implicated in transport of long-chain fatty acids. *J Membr Biol* **133**, 43-49

178. Goldberg, I. J., Soprano, D. R., Wyatt, M. L., Vanni, T. M., Kirchgessner, T. G., and Schotz, M. C. (1989) Localization of lipoprotein lipase mRNA in selected rat tissues. *Journal of lipid research* **30**, 1569-1577

179. Susztak, K., Ciccone, E., McCue, P., Sharma, K., and Bottinger, E. P. (2005) Multiple metabolic hits converge on CD36 as novel mediator of tubular epithelial apoptosis in diabetic nephropathy. *PLoS medicine* **2**, e45

180. Susztak, K., Bottinger, E., Novetsky, A., Liang, D., Zhu, Y., Ciccone, E., Wu, D., Dunn, S., McCue, P., and Sharma, K. (2004) Molecular profiling of diabetic mouse kidney reveals novel genes linked to glomerular disease. *Diabetes* **53**, 784-794

181. Sitnick, M. T., Basantani, M. K., Cai, L., Schoiswohl, G., Yazbeck, C. F., Distefano, G., Ritov, V., DeLany, J. P., Schreiber, R., Stolz, D. B., Gardner, N. P., Kienesberger, P. C., Pulinilkunnil, T., Zechner, R., Goodpaster, B. H., Coen, P., and Kershaw, E. E. (2013) Skeletal muscle triacylglycerol hydrolysis does not influence metabolic complications of obesity. *Diabetes* **62**, 3350-3361

182. Schoiswohl, G., Stefanovic-Racic, M., Menke, M. N., Wills, R. C., Surlow, B. A., Basantani, M. K., Sitnick, M. T., Cai, L., Yazbeck, C. F., Stolz, D. B., Pulinilkunnil, T., O'Doherty, R. M., and Kershaw, E. E. (2015) Impact of Reduced ATGL-Mediated Adipocyte Lipolysis on Obesity-Associated Insulin Resistance and Inflammation in Male Mice. *Endocrinology* **156**, 3610-3624

183. Millar, J. S., Cromley, D. A., McCoy, M. G., Rader, D. J., and Billheimer, J. T. (2005) Determining hepatic triglyceride production in mice: comparison of poloxamer 407 with Triton WR-1339. *Journal of lipid research* **46**, 2023-2028

184. Noh, H. L., Okajima, K., Molkentin, J. D., Homma, S., and Goldberg, I. J. (2006) Acute lipoprotein lipase deletion in adult mice leads to dyslipidemia and cardiac dysfunction. *American journal of physiology. Endocrinology and metabolism* **291**, E755-760

185. Kosteli, A., Sugaru, E., Haemmerle, G., Martin, J. F., Lei, J., Zechner, R., and Ferrante, A. W., Jr. (2010) Weight loss and lipolysis promote a dynamic immune response in murine adipose tissue. *The Journal of clinical investigation* **120**, 3466-3479

186. Josekutty, J., Iqbal, J., Iwawaki, T., Kohno, K., and Hussain, M. M. (2013) Microsomal triglyceride transfer protein inhibition induces endoplasmic reticulum stress and increases gene transcription via Ire1alpha/cJun to enhance plasma ALT/AST. *The Journal of biological chemistry* **288**, 14372-14383

187. Kako, Y., Huang, L. S., Yang, J., Katopodis, T., Ramakrishnan, R., and Goldberg, I. J. (1999) Streptozotocin-induced diabetes in human apolipoprotein B transgenic mice. Effects on lipoproteins and atherosclerosis. *Journal of lipid research* **40**, 2185-2194

188. Folch, J., Lees, M., and Sloane Stanley, G. H. (1957) A simple method for the isolation and purification of total lipides from animal tissues. *The Journal of biological chemistry* **226**, 497-509

189. Han, C. Y., Umemoto, T., Omer, M., Den Hartigh, L. J., Chiba, T., LeBoeuf, R., Buller, C. L., Sweet, I. R., Pennathur, S., Abel, E. D., and Chait, A. (2012) NADPH oxidase-derived reactive oxygen species increases expression of monocyte chemotactic factor genes in cultured adipocytes. *The Journal of biological chemistry* **287**, 10379-10393

190. Sas, K. M., Nair, V., Byun, J., Kayampilly, P., Zhang, H., Saha, J., Brosius, F. C., 3rd, Kretzler, M., and Pennathur, S. (2015) Targeted Lipidomic and Transcriptomic Analysis Identifies Dysregulated Renal Ceramide Metabolism in a Mouse Model of Diabetic Kidney Disease. *Journal of proteomics & bioinformatics* **Suppl 14**

191. Sas, K. M., Kayampilly, P., Byun, J., Nair, V., Hinder, L. M., Hur, J., Zhang, H., Lin, C., Qi, N. R., Michailidis, G., Groop, P.-H., Nelson, R. G., Darshi, M., Sharma, K., Schelling, J. R., Sedor, J. R., Pop-Busui, R., Weinberg, J. M., Soleimanpour, S. A., Abcouwer, S. F., Gardner, T. W., Burant, C. F., Feldman, E. L., Kretzler, M., Brosius, F. C., III, and Pennathur, S. Tissue-specific metabolic reprogramming drives nutrient flux in diabetic complications. *JCI Insight* **1**

192. Bligh, E. G., and Dyer, W. J. (1959) A rapid method of total lipid extraction and purification. *Canadian journal of biochemistry and physiology* **37**, 911-917

193. Coe, N. R., Smith, A. J., Frohnert, B. I., Watkins, P. A., and Bernlohr, D. A. (1999) The fatty acid transport protein (FATP1) is a very long chain acyl-CoA synthetase. *The Journal of biological chemistry* **274**, 36300-36304

194. Marvyn, P. M., Bradley, R. M., Button, E. B., Mardian, E. B., and Duncan, R. E. (2015) Fasting upregulates adipose triglyceride lipase and hormone-sensitive lipase levels and phosphorylation in mouse kidney. *Biochem Cell Biol* **93**, 262-267

195. Hohenegger, M., and Schuh, H. (1980) Uptake and fatty acid synthesis by the rat kidney. *Int J Biochem* **12**, 169-172

196. Koves, T. R., Ussher, J. R., Noland, R. C., Slentz, D., Mosedale, M., Ilkayeva, O., Bain, J., Stevens, R., Dyck, J. R., Newgard, C. B., Lopaschuk, G. D., and Muoio, D. M. (2008) Mitochondrial overload and incomplete fatty acid oxidation contribute to skeletal muscle insulin resistance. *Cell metabolism* **7**, 45-56

197. Dbaibo, G. S., El-Assaad, W., Krikorian, A., Liu, B., Diab, K., Idriss, N. Z., El-Sabban, M., Driscoll, T. A., Perry, D. K., and Hannun, Y. A. (2001) Ceramide generation by two distinct pathways in tumor necrosis factor alpha-induced cell death. *FEBS letters* **503**, 7-12

198. Rotolo, J. A., Zhang, J., Donepudi, M., Lee, H., Fuks, Z., and Kolesnick, R. (2005) Caspase-dependent and -independent activation of acid sphingomyelinase signaling. *The Journal of biological chemistry* **280**, 26425-26434

199. Merkel, M., Eckel, R. H., and Goldberg, I. J. (2002) Lipoprotein lipase: genetics, lipid uptake, and regulation. *Journal of lipid research* **43**, 1997-2006

200. Han, S., Akiyama, T. E., Previs, S. F., Herath, K., Roddy, T. P., Jensen, K. K., Guan, H. P., Murphy, B. A., McNamara, L. A., Shen, X., Strapps, W., Hubbard, B. K., Pinto, S., Li, C., and Li, J. (2013) Effects of small interfering RNA-mediated hepatic glucagon receptor inhibition on lipid metabolism in db/db mice. *Journal of lipid research* **54**, 2615-2622

201. Hussain, M. M., Shi, J., and Dreizen, P. (2003) Microsomal triglyceride transfer protein and its role in apoB-lipoprotein assembly. *Journal of lipid research* **44**, 22-32

202. Raabe, M., Veniant, M. M., Sullivan, M. A., Zlot, C. H., Bjorkegren, J., Nielsen, L. B., Wong, J. S., Hamilton, R. L., and Young, S. G. (1999) Analysis of the role of microsomal

triglyceride transfer protein in the liver of tissue-specific knockout mice. *The Journal of clinical investigation* **103**, 1287-1298

203. Elhamri, M., Martin, M., Ferrier, B., and Baverel, G. (1993) Substrate uptake and utilization by the kidney of fed and starved rats in vivo. *Renal physiology and biochemistry* **16**, 311-324

204. Koves, T. R., Li, P., An, J., Akimoto, T., Slentz, D., Ilkayeva, O., Dohm, G. L., Yan, Z., Newgard, C. B., and Muoio, D. M. (2005) Peroxisome proliferator-activated receptor-gamma co-activator 1alpha-mediated metabolic remodeling of skeletal myocytes mimics exercise training and reverses lipid-induced mitochondrial inefficiency. *The Journal of biological chemistry* **280**, 33588-33598

205. Subathra, M., Korrapati, M., Howell, L. A., Arthur, J. M., Shayman, J. A., Schnellmann, R. G., and Siskind, L. J. (2015) Kidney glycosphingolipids are elevated early in diabetic nephropathy and mediate hypertrophy of mesangial cells. *American journal of physiology. Renal physiology* **309**, F204-215

206. Poulsen, L., Siersbaek, M., and Mandrup, S. (2012) PPARs: fatty acid sensors controlling metabolism. *Seminars in cell & developmental biology* **23**, 631-639

207. Egan, B., and Zierath, J. R. (2013) Exercise metabolism and the molecular regulation of skeletal muscle adaptation. *Cell metabolism* **17**, 162-184

208. Goldberg, I. J., Eckel, R. H., and Abumrad, N. A. (2009) Regulation of fatty acid uptake into tissues: lipoprotein lipase- and CD36-mediated pathways. *Journal of lipid research* **50 Suppl**, S86-90

209. Falcon, A., Doege, H., Fluitt, A., Tsang, B., Watson, N., Kay, M. A., and Stahl, A. (2010) FATP2 is a hepatic fatty acid transporter and peroxisomal very long-chain acyl-CoA synthetase. *Am J Physiol Endocrinol Metab* **299**, E384-393

210. Kazantzis, M., and Stahl, A. (2012) Fatty acid transport proteins, implications in physiology and disease. *Biochimica et biophysica acta* **1821**, 852-857

211. Sukonina, V., Lookene, A., Olivecrona, T., and Olivecrona, G. (2006) Angiopoietin-like protein 4 converts lipoprotein lipase to inactive monomers and modulates lipase activity in adipose tissue. *Proceedings of the National Academy of Sciences of the United States of America* **103**, 17450-17455

212. Mashek, D. G. (2013) Hepatic fatty acid trafficking: multiple forks in the road. *Advances in nutrition* **4**, 697-710

213. McConnell, B. B., and Yang, V. W. (2010) Mammalian Kruppel-like factors in health and diseases. *Physiological reviews* **90**, 1337-1381

214. Dang, D. T., Pevsner, J., and Yang, V. W. (2000) The biology of the mammalian Kruppel-like family of transcription factors. *The international journal of biochemistry & cell biology* **32**, 1103-1121

215. Drissen, R., von Lindern, M., Kolbus, A., Driegen, S., Steinlein, P., Beug, H., Grosveld, F., and Philipsen, S. (2005) The erythroid phenotype of EKLF-null mice: defects in hemoglobin metabolism and membrane stability. *Molecular and cellular biology* **25**, 5205-5214

216. Frontelo, P., Manwani, D., Galdass, M., Karsunky, H., Lohmann, F., Gallagher, P. G., and Bieker, J. J. (2007) Novel role for EKLF in megakaryocyte lineage commitment. *Blood* **110**, 3871-3880

217. Endrizzi, B. T., and Jameson, S. C. (2003) Differential role for IL-7 in inducing lung Kruppel-like factor (Kruppel-like factor 2) expression by naive versus activated T cells. *International Immunology* **15**, 1341-1348

218. Lee, J. S., Yu, Q., Shin, J. T., Sebzda, E., Bertozzi, C., Chen, M., Mericko, P., Stadtfeld, M., Zhou, D., Cheng, L., Graf, T., MacRae, C. A., Lepore, J. J., Lo, C. W., and Kahn, M. L. (2006) Klf2 is an essential regulator of vascular hemodynamic forces in vivo. *Developmental cell* **11**, 845-857

219. Atkins, G. B., Wang, Y., Mahabeleshwar, G. H., Shi, H., Gao, H., Kawanami, D., Natesan, V., Lin, Z., Simon, D. I., and Jain, M. K. (2008) Hemizygous deficiency of Krüppel-like factor 2 augments experimental atherosclerosis. *Circulation research* **103**, 690-693

220. Sue, N., Jack, B. H., Eaton, S. A., Pearson, R. C., Funnell, A. P., Turner, J., Czolij, R., Denyer, G., Bao, S., Molero-Navajas, J. C., Perkins, A., Fujiwara, Y., Orkin, S. H., Bell-Anderson, K., and Crossley, M. (2008) Targeted disruption of the basic Kruppel-like factor gene (Klf3) reveals a role in adipogenesis. *Molecular and cellular biology* **28**, 3967-3978

221. Ghaleb, A. M., Nandan, M. O., Chanchevalap, S., Dalton, W. B., Hisamuddin, I. M., and Yang, V. W. (2005) Kruppel-like factors 4 and 5: the yin and yang regulators of cellular proliferation. *Cell Res* **15**, 92-96

222. Alder, J. K., Georgantas, R. W., 3rd, Hildreth, R. L., Kaplan, I. M., Morisot, S., Yu, X., McDevitt, M., and Civin, C. I. (2008) Kruppel-like factor 4 is essential for inflammatory monocyte differentiation in vivo. *Journal of immunology* **180**, 5645-5652

223. Feinberg, M. W., Wara, A. K., Cao, Z., Lebedeva, M. A., Rosenbauer, F., Iwasaki, H., Hirai, H., Katz, J. P., Haspel, R. L., Gray, S., Akashi, K., Segre, J., Kaestner, K. H., Tenen, D. G., and Jain, M. K. (2007) The Kruppel-like factor KLF4 is a critical regulator of monocyte differentiation. *The EMBO journal* **26**, 4138-4148

224. Takahashi, K., and Yamanaka, S. (2006) Induction of pluripotent stem cells from mouse embryonic and adult fibroblast cultures by defined factors. *Cell* **126**, 663-676

225. Narla, G., Heath, K. E., Reeves, H. L., Li, D., Giono, L. E., Kimmelman, A. C., Glucksman, M. J., Narla, J., Eng, F. J., Chan, A. M., Ferrari, A. C., Martignetti, J. A., and Friedman, S. L. (2001) KLF6, a candidate tumor suppressor gene mutated in prostate cancer. *Science* **294**, 2563-2566

226. Kawamura, Y., Tanaka, Y., Kawamori, R., and Maeda, S. (2006) Overexpression of Kruppel-like factor 7 regulates adipocytokine gene expressions in human adipocytes and inhibits glucose-induced insulin secretion in pancreatic beta-cell line. *Molecular endocrinology (Baltimore, Md.)* **20**, 844-856

227. Kanazawa, A., Kawamura, Y., Sekine, A., Iida, A., Tsunoda, T., Kashiwagi, A., Tanaka, Y., Babazono, T., Matsuda, M., Kawai, K., Iiizumi, T., Fujioka, T., Imanishi, M., Kaku, K., Iwamoto, Y., Kawamori, R., Kikkawa, R., Nakamura, Y., and Maeda, S. (2005) Single nucleotide polymorphisms in the gene encoding Kruppel-like factor 7 are associated with type 2 diabetes. *Diabetologia* **48**, 1315-1322

228. Zobel, D. P., Andreasen, C. H., Burgdorf, K. S., Andersson, E. A., Sandbaek, A., Lauritzen, T., Borch-Johnsen, K., Jorgensen, T., Maeda, S., Nakamura, Y., Eiberg, H., Pedersen, O., and Hansen, T. (2009) Variation in the gene encoding Kruppel-like factor 7 influences body fat: studies of 14 818 Danes. *European journal of endocrinology* **160**, 603-609

229. Wang, X., Zheng, M., Liu, G., Xia, W., McKeown-Longo, P. J., Hung, M. C., and Zhao, J. (2007) Kruppel-like factor 8 induces epithelial to mesenchymal transition and epithelial cell invasion. *Cancer research* **67**, 7184-7193

230. Velarde, M. C., Zeng, Z., McQuown, J. R., Simmen, F. A., and Simmen, R. C. (2007) Kruppel-like factor 9 is a negative regulator of ligand-dependent estrogen receptor alpha signaling in Ishikawa endometrial adenocarcinoma cells. *Molecular endocrinology (Baltimore, Md.)* **21**, 2988-3001

231. Venuprasad, K., Huang, H., Harada, Y., Elly, C., Subramaniam, M., Spelsberg, T., Su, J., and Liu, Y. C. (2008) The E3 ubiquitin ligase Itch regulates expression of transcription factor Foxp3 and airway inflammation by enhancing the function of transcription factor TIEG1. *Nature immunology* **9**, 245-253

232. Subramaniam, M., Gorny, G., Johnsen, S. A., Monroe, D. G., Evans, G. L., Fraser, D. G., Rickard, D. J., Rasmussen, K., van Deursen, J. M., Turner, R. T., Oursler, M. J., and Spelsberg, T. C. (2005) TIEG1 null mouse-derived osteoblasts are defective in mineralization and in support of osteoclast differentiation in vitro. *Molecular and cellular biology* **25**, 1191-1199

233. Fernandez-Zapico, M. E., van Velkinburgh, J. C., Gutierrez-Aguilar, R., Neve, B., Froguel, P., Urrutia, R., and Stein, R. (2009) MODY7 gene, KLF11, is a novel p300-dependent regulator of Pdx-1 (MODY4) transcription in pancreatic islet beta cells. *The Journal of biological chemistry* **284**, 36482-36490

234. Neve, B., Fernandez-Zapico, M. E., Ashkenazi-Katalan, V., Dina, C., Hamid, Y. H., Joly, E., Vaillant, E., Benmezroua, Y., Durand, E., Bakaher, N., Delannoy, V., Vaxillaire, M., Cook, T., Dallinga-Thie, G. M., Jansen, H., Charles, M. A., Clement, K., Galan, P., Hercberg, S., Helbecque, N., Charpentier, G., Prentki, M., Hansen, T., Pedersen, O., Urrutia, R., Melloul, D., and Froguel, P. (2005) Role of transcription factor KLF11 and its diabetes-associated gene variants in pancreatic beta cell function. *Proceedings of the National Academy of Sciences of the United States of America* **102**, 4807-4812

235. Nakamura, Y., Migita, T., Hosoda, F., Okada, N., Gotoh, M., Arai, Y., Fukushima, M., Ohki, M., Miyata, S., Takeuchi, K., Imoto, I., Katai, H., Yamaguchi, T., Inazawa, J., Hirohashi, S., Ishikawa, Y., and Shibata, T. (2009) Kruppel-like factor 12 plays a significant role in poorly differentiated gastric cancer progression. *International journal of cancer. Journal international du cancer* **125**, 1859-1867

236. Lavallee, G., Andelfinger, G., Nadeau, M., Lefebvre, C., Nemer, G., Horb, M. E., and Nemer, M. (2006) The Kruppel-like transcription factor KLF13 is a novel regulator of heart development. *The EMBO journal* **25**, 5201-5213

237. Song, A., Chen, Y. F., Thamatrakoln, K., Storm, T. A., and Krensky, A. M. (1999) RFLAT-1: a new zinc finger transcription factor that activates RANTES gene expression in T lymphocytes. *Immunity* **10**, 93-103

238. Gao, K., Wang, J., Li, L., Zhai, Y., Ren, Y., You, H., Wang, B., Wu, X., Li, J., Liu, Z., Li, X., Huang, Y., Luo, X. P., Hu, D., Ohno, K., and Wang, C. (2016) Polymorphisms in Four Genes (KCNQ1 rs151290, KLF14 rs972283, GCKR rs780094 and MTNR1B rs10830963) and Their Correlation with Type 2 Diabetes Mellitus in Han Chinese in Henan Province, China. *Int J Environ Res Public Health* **13**

239. Guo, Y., Fan, Y., Zhang, J., Lomberk, G. A., Zhou, Z., Sun, L., Mathison, A. J., Garcia-Barrio, M. T., Zhang, J., Zeng, L., Li, L., Pennathur, S., Willer, C. J., Rader, D. J., Urrutia, R., and Chen, Y. E. (2015) Perhexiline activates KLF14 and reduces atherosclerosis by modulating ApoA-I production. *The Journal of clinical investigation* **125**, 3819-3830

240. Fisch, S., Gray, S., Heymans, S., Haldar, S. M., Wang, B., Pfister, O., Cui, L., Kumar, A., Lin, Z., Sen-Banerjee, S., Das, H., Petersen, C. A., Mende, U., Burleigh, B. A., Zhu, Y., Pinto, Y. M., Liao, R., and Jain, M. K. (2007) Kruppel-like factor 15 is a regulator of cardiomyocyte hypertrophy. *Proceedings of the National Academy of Sciences of the United States of America* **104**, 7074-7079

241. Gray, S., Feinberg, M. W., Hull, S., Kuo, C. T., Watanabe, M., Sen-Banerjee, S., DePina, A., Haspel, R., and Jain, M. K. (2002) The Kruppel-like factor KLF15 regulates the insulin-sensitive glucose transporter GLUT4. *The Journal of biological chemistry* **277**, 34322-34328

242. Gray, S., Wang, B., Orihuela, Y., Hong, E. G., Fisch, S., Haldar, S., Cline, G. W., Kim, J. K., Peroni, O. D., Kahn, B. B., and Jain, M. K. (2007) Regulation of gluconeogenesis by Kruppel-like factor 15. *Cell metabolism* **5**, 305-312

243. Lee, S. H., Jang, M. K., Lee, O. H., Kim, O. S., Kim, Y. M., Yajima, S., Lee, Y. C., and Mouradian, M. M. (2008) Transcriptional auto-regulation of the dopamine receptor regulating factor (DRRF) gene. *Molecular and cellular endocrinology* **289**, 23-28

244. Wang, J., Galvao, J., Beach, K. M., Luo, W., Urrutia, R. A., Goldberg, J. L., and Otteson, D. C. (2016) Novel Roles and Mechanism for Kruppel-like Factor 16 (KLF16) Regulation of Neurite Outgrowth and Ephrin Receptor A5 (EphA5) Expression in Retinal Ganglion Cells. *The Journal of biological chemistry* **291**, 18084-18095

245. Zhou, S., Tang, X., and Tang, F. (2016) Kruppel-like factor 17, a novel tumor suppressor: its low expression is involved in cancer metastasis. *Tumour biology : the journal of the International Society for Oncodevelopmental Biology and Medicine* **37**, 1505-1513

246. Pei, J., and Grishin, N. V. (2013) A new family of predicted Kruppel-like factor genes and pseudogenes in placental mammals. *PloS one* **8**, e81109

247. Conkright, M. D., Wani, M. A., Anderson, K. P., and Lingrel, J. B. (1999) A gene encoding an intestinal-enriched member of the Kruppel-like factor family expressed in intestinal epithelial cells. *Nucleic acids research* **27**, 1263-1270

248. Chen, C., Zhou, Y., Zhou, Z., Sun, X., Otto, K. B., Uht, R. M., and Dong, J. T. (2004) Regulation of KLF5 involves the Sp1 transcription factor in human epithelial cells. *Gene* **330**, 133-142

249. Diakiw, S. M., D'Andrea, R. J., and Brown, A. L. (2013) The double life of KLF5: Opposing roles in regulation of gene-expression, cellular function, and transformation. *IUBMB Life* **65**, 999-1011

250. Zheng, B., Han, M., Shu, Y. N., Li, Y. J., Miao, S. B., Zhang, X. H., Shi, H. J., Zhang, T., and Wen, J. K. (2011) HDAC2 phosphorylation-dependent Klf5 deacetylation and RARalpha acetylation induced by RAR agonist switch the transcription regulatory programs of p21 in VSMCs. *Cell Res* **21**, 1487-1508

251. Guo, P., Zhao, K. W., Dong, X. Y., Sun, X., and Dong, J. T. (2009) Acetylation of KLF5 alters the assembly of p15 transcription factors in transforming growth factor-beta-mediated induction in epithelial cells. *The Journal of biological chemistry* **284**, 18184-18193

252. Nandan, M. O., Ghaleb, A. M., Bialkowska, A. B., and Yang, V. W. (2015) Krüppel-like factor 5 is essential for proliferation and survival of mouse intestinal epithelial stem cells. *Stem cell research* **14**, 10-19

253. An, J., Golech, S., Klaewsongkram, J., Zhang, Y., Subedi, K., Huston, G. E., Wood, W. H., 3rd, Wersto, R. P., Becker, K. G., Swain, S. L., and Weng, N. (2011) Kruppel-like factor 4 (KLF4) directly regulates proliferation in thymocyte development and IL-17 expression during Th17 differentiation. *FASEB J* **25**, 3634-3645

254. Li, J., Zheng, H., Yu, F., Yu, T., Liu, C., Huang, S., Wang, T. C., and Ai, W. (2012) Deficiency of the Kruppel-like factor KLF4 correlates with increased cell proliferation and enhanced skin tumorigenesis. *Carcinogenesis* **33**, 1239-1246

255. Du, J. X., Bialkowska, A. B., McConnell, B. B., and Yang, V. W. (2008) SUMOylation regulates nuclear localization of Krüppel-like factor 5. *Journal of Biological Chemistry* **283**, 31991-32002

256. Du, J. X., Yun, C. C., Bialkowska, A., and Yang, V. W. (2007) Protein inhibitor of activated STAT1 interacts with and up-regulates activities of the pro-proliferative transcription factor Krüppel-like factor 5. *Journal of Biological Chemistry* **282**, 4782-4793

257. Chen, C., Benjamin, M. S., Sun, X., Otto, K. B., Guo, P., Dong, X. Y., Bao, Y., Zhou, Z., Cheng, X., Simons, J. W., and Dong, J. T. (2006) KLF5 promotes cell proliferation and tumorigenesis through gene regulation and the TSU-Pr1 human bladder cancer cell line. *International journal of cancer. Journal international du cancer* **118**, 1346-1355

258. Nandan, M. O., Chanchevalap, S., Dalton, W. B., and Yang, V. W. (2005) Kruppel-like factor 5 promotes mitosis by activating the cyclin B1/Cdc2 complex during oncogenic Ras-mediated transformation. *FEBS letters* **579**, 4757-4762

259. Kawai-Kowase, K., Kurabayashi, M., Hoshino, Y., Ohyama, Y., and Nagai, R. (1999) Transcriptional activation of the zinc finger transcription factor BTEB2 gene by Egr-1 through mitogen-activated protein kinase pathways in vascular smooth muscle cells. *Circulation research* **85**, 787-795

260. Fujiu, K., Manabe, I., Ishihara, A., Oishi, Y., Iwata, H., Nishimura, G., Shindo, T., Maemura, K., Kagechika, H., Shudo, K., and Nagai, R. (2005) Synthetic retinoid Am80 suppresses smooth muscle phenotypic modulation and in-stent neointima formation by inhibiting KLF5. *Circ Res* **97**, 1132-1141

261. Zhang, X. H., Zheng, B., Han, M., Miao, S. B., and Wen, J. K. (2009) Synthetic retinoid Am80 inhibits interaction of KLF5 with RAR alpha through inducing KLF5 dephosphorylation mediated by the PI3K/Akt signaling in vascular smooth muscle cells. *FEBS letters* **583**, 1231-1236

262. Chanchevalap, S., Nandan, M. O., Merlin, D., and Yang, V. W. (2004) All-trans retinoic acid inhibits proliferation of intestinal epithelial cells by inhibiting expression of the gene encoding Kruppel-like factor 5. *FEBS letters* **578**, 99-105

263. McConnell, B. B., Ghaleb, A. M., Nandan, M. O., and Yang, V. W. (2007) The diverse functions of Kruppel-like factors 4 and 5 in epithelial biology and pathobiology. *BioEssays : news and reviews in molecular, cellular and developmental biology* **29**, 549-557

264. Shindo, T., Manabe, I., Fukushima, Y., Tobe, K., Aizawa, K., Miyamoto, S., Kawai-Kowase, K., Moriyama, N., Imai, Y., Kawakami, H., Nishimatsu, H., Ishikawa, T., Suzuki, T., Morita, H., Maemura, K., Sata, M., Hirata, Y., Komukai, M., Kagechika, H., Kadowaki, T., Kurabayashi, M., and Nagai, R. (2002) Kruppel-like zinc-finger transcription factor KLF5/BTEB2 is a target for angiotensin II signaling and an essential regulator of cardiovascular remodeling. *Nature medicine* **8**, 856-863

265. McConnell, B. B., Klapproth, J. M., Sasaki, M., Nandan, M. O., and Yang, V. W. (2008) Kruppel-like factor 5 mediates transmissible murine colonic hyperplasia caused by Citrobacter rodentium infection. *Gastroenterology* **134**, 1007-1016

266. Zhao, Y., Hamza, M. S., Leong, H. S., Lim, C. B., Pan, Y. F., Cheung, E., Soo, K. C., and Iyer, N. G. (2008) Kruppel-like factor 5 modulates p53-independent apoptosis through Pim1 survival kinase in cancer cells. *Oncogene* **27**, 1-8

267. Xie, Y., and Bayakhmetov, S. (2016) PIM1 kinase as a promise of targeted therapy in prostate cancer stem cells. *Molecular and clinical oncology* **4**, 13-17

268. Zhang, H., Bialkowska, A., Rusovici, R., Chanchevalap, S., Shim, H., Katz, J. P., Yang, V. W., and Yun, C. C. (2007) Lysophosphatidic acid facilitates proliferation of colon cancer cells via induction of Kruppel-like factor 5. *The Journal of biological chemistry* **282**, 15541-15549

269. Nandan, M. O., McConnell, B. B., Ghaleb, A. M., Bialkowska, A. B., Sheng, H., Shao, J., Babbin, B. A., Robine, S., and Yang, V. W. (2008) Kruppel-like factor 5 mediates cellular transformation during oncogenic KRAS-induced intestinal tumorigenesis. *Gastroenterology* **134**, 120-130

270. Nandan, M. O., Yoon, H. S., Zhao, W., Ouko, L. A., Chanchevalap, S., and Yang, V. W. (2004) Kruppel-like factor 5 mediates the transforming activity of oncogenic H-Ras. *Oncogene* **23**, 3404-3413

271. Hoshino, Y., Kurabayashi, M., Kanda, T., Hasegawa, A., Sakamoto, H., Okamoto, E., Kowase, K., Watanabe, N., Manabe, I., Suzuki, T., Nakano, A., Takase, S., Wilcox, J. N., and Nagai, R. (2000) Regulated expression of the BTEB2 transcription factor in vascular

smooth muscle cells: analysis of developmental and pathological expression profiles shows implications as a predictive factor for restenosis. *Circulation* **102**, 2528-2534

272. Ogata, T., Kurabayashi, M., Hoshino, Y., Ishikawa, S., Takeyoshi, I., Morishita, Y., and Nagai, R. (2000) Inducible expression of BTEB2, a member of the zinc-finger family of transcription factors, in cardiac allograft arteriosclerosis. *Transplantation proceedings* **32**, 2032-2033

273. Bafford, R., Sui, X. X., Wang, G., and Conte, M. (2006) Angiotensin II and tumor necrosis factor-alpha upregulate survivin and Kruppel-like factor 5 in smooth muscle cells: Potential relevance to vein graft hyperplasia. *Surgery* **140**, 289-296

274. He, M., Han, M., Zheng, B., Shu, Y. N., and Wen, J. K. (2009) Angiotensin II stimulates KLF5 phosphorylation and its interaction with c-Jun leading to suppression of p21 expression in vascular smooth muscle cells. *Journal of biochemistry* **146**, 683-691

275. Berry, D. C., Stenesen, D., Zeve, D., and Graff, J. M. (2013) The developmental origins of adipose tissue. *Development* **140**, 3939-3949

276. Oishi, Y., Manabe, I., Tobe, K., Tsushima, K., Shindo, T., Fujiu, K., Nishimura, G., Maemura, K., Yamauchi, T., Kubota, N., Suzuki, R., Kitamura, T., Akira, S., Kadowaki, T., and Nagai, R. (2005) Kruppel-like transcription factor KLF5 is a key regulator of adipocyte differentiation. *Cell metabolism* **1**, 27-39

277. Oishi, Y., Manabe, I., Tobe, K., Ohsugi, M., Kubota, T., Fujiu, K., Maemura, K., Kubota, N., Kadowaki, T., and Nagai, R. (2008) SUMOylation of Kruppel-like transcription factor 5 acts as a molecular switch in transcriptional programs of lipid metabolism involving PPAR-delta. *Nature medicine* **14**, 656-666

278. Drosatos, K., Pollak, N. M., Pol, C. J., Ntziachristos, P., Willecke, F., Valenti, M. C., Trent, C. M., Hu, Y., Guo, S., Aifantis, I., and Goldberg, I. J. (2016) Cardiac Myocyte KLF5 Regulates Ppara Expression and Cardiac Function. *Circ Res* **118**, 241-253

279. Shahrin, N. H., Diakiw, S., Dent, L. A., Brown, A. L., and D'Andrea, R. J. (2016) Conditional knockout mice demonstrate function of Klf5 as a myeloid transcription factor. *Blood* **128**, 55-59

280. Humbert, M., Halter, V., Shan, D., Laedrach, J., Leibundgut, E. O., Baerlocher, G. M., Tobler, A., Fey, M. F., and Tschan, M. P. (2011) Deregulated expression of Kruppel-like factors in acute myeloid leukemia. *Leukemia research* **35**, 909-913

281. Diakiw, S. M., Perugini, M., Kok, C. H., Engler, G. A., Cummings, N., To, L. B., Wei, A. H., Lewis, I. D., Brown, A. L., and D'Andrea, R. J. (2013) Methylation of KLF5 contributes to reduced expression in acute myeloid leukaemia and is associated with poor overall survival. *British journal of haematology* **161**, 884-888

282. Chanchevalap, S., Nandan, M. O., McConnell, B. B., Charrier, L., Merlin, D., Katz, J. P., and Yang, V. W. (2006) Kruppel-like factor 5 is an important mediator for lipopolysaccharide-induced proinflammatory response in intestinal epithelial cells. *Nucleic acids research* **34**, 1216-1223

283. Li, Y., Li, J., Hou, Z., Yu, Y., and Yu, B. (2016) KLF5 overexpression attenuates cardiomyocyte inflammation induced by oxygen-glucose deprivation/reperfusion through the PPARgamma/PGC-1alpha/TNF-alpha signaling pathway. *Biomedicine & pharmacotherapy = Biomedecine & pharmacotherapie* **84**, 940-946

284. Fujiu, K., Manabe, I., and Nagai, R. (2011) Renal collecting duct epithelial cells regulate inflammation in tubulointerstitial damage in mice. *The Journal of clinical investigation* **121**, 3425-3441

285. Nagareddy, P. R., Murphy, A. J., Stirzaker, R. A., Hu, Y., Yu, S., Miller, R. G., Ramkhelawon, B., Distel, E., Westerterp, M., Huang, L. S., Schmidt, A. M., Orchard, T. J., Fisher, E. A., Tall, A. R., and Goldberg, I. J. (2013) Hyperglycemia promotes myelopoiesis and impairs the resolution of atherosclerosis. *Cell Metab* **17**, 695-708

286. Jounai, N., Kobiyama, K., Takeshita, F., and Ishii, K. J. (2012) Recognition of damage-associated molecular patterns related to nucleic acids during inflammation and vaccination. *Front Cell Infect Microbiol* **2**, 168

287. Donato, R., Cannon, B. R., Sorci, G., Riuzzi, F., Hsu, K., Weber, D. J., and Geczy, C. L. (2013) Functions of S100 proteins. *Curr Mol Med* **13**, 24-57

288. Schiopu, A., and Cotoi, O. S. (2013) S100A8 and S100A9: DAMPs at the crossroads between innate immunity, traditional risk factors, and cardiovascular disease. *Mediators of inflammation* **2013**, 828354

289. Ibrahim, Z. A., Armour, C. L., Phipps, S., and Sukkar, M. B. (2013) RAGE and TLRs: relatives, friends or neighbours? *Mol Immunol* **56**, 739-744

290. Gebhardt, C., Breitenbach, U., Tuckermann, J. P., Dittrich, B. T., Richter, K. H., and Angel, P. (2002) Calgranulins S100A8 and S100A9 are negatively regulated by

glucocorticoids in a c-Fos-dependent manner and overexpressed throughout skin carcinogenesis. *Oncogene* **21**, 4266-4276

291. Gebhardt, C., Nemeth, J., Angel, P., and Hess, J. (2006) S100A8 and S100A9 in inflammation and cancer. *Biochemical pharmacology* **72**, 1622-1631

292. Yen, T., Harrison, C. A., Devery, J. M., Leong, S., Iismaa, S. E., Yoshimura, T., and Geczy, C. L. (1997) Induction of the S100 chemotactic protein, CP-10, in murine microvascular endothelial cells by proinflammatory stimuli. *Blood* **90**, 4812-4821

293. Xu, K., and Geczy, C. L. (2000) IFN-gamma and TNF regulate macrophage expression of the chemotactic S100 protein S100A8. *Journal of immunology* **164**, 4916-4923

294. Edgeworth, J., Gorman, M., Bennett, R., Freemont, P., and Hogg, N. (1991) Identification of p8,14 as a highly abundant heterodimeric calcium binding protein complex of myeloid cells. *The Journal of biological chemistry* **266**, 7706-7713

295. Grimbaldeston, M. A., Geczy, C. L., Tedla, N., Finlay-Jones, J. J., and Hart, P. H. (2003) S100A8 induction in keratinocytes by ultraviolet A irradiation is dependent on reactive oxygen intermediates. *The Journal of investigative dermatology* **121**, 1168-1174

296. Lim, S. Y., Raftery, M., Cai, H., Hsu, K., Yan, W. X., Hseih, H. L., Watts, R. N., Richardson, D., Thomas, S., Perry, M., and Geczy, C. L. (2008) S-nitrosylated S100A8: novel anti-inflammatory properties. *Journal of immunology* **181**, 5627-5636

297. Simard, J. C., Simon, M. M., Tessier, P. A., and Girard, D. (2011) Damage-associated molecular pattern S100A9 increases bactericidal activity of human neutrophils by enhancing phagocytosis. *Journal of immunology* **186**, 3622-3631

298. Vogl, T., Ludwig, S., Goebeler, M., Strey, A., Thorey, I. S., Reichelt, R., Foell, D., Gerke, V., Manitz, M. P., Nacken, W., Werner, S., Sorg, C., and Roth, J. (2004) MRP8 and MRP14 control microtubule reorganization during transendothelial migration of phagocytes. *Blood* **104**, 4260-4268

299. Weisenberg, R. C. (1972) Microtubule formation in vitro in solutions containing low calcium concentrations. *Science* **177**, 1104-1105

300. Boyd, J. H., Kan, B., Roberts, H., Wang, Y., and Walley, K. R. (2008) S100A8 and S100A9 mediate endotoxin-induced cardiomyocyte dysfunction via the receptor for advanced glycation end products. *Circulation research* **102**, 1239-1246

301. Steinckwich, N., Schenten, V., Melchior, C., Brechard, S., and Tschirhart, E. J. (2011) An essential role of STIM1, Orai1, and S100A8-A9 proteins for Ca2+ signaling and FcgammaR-mediated phagosomal oxidative activity. *Journal of immunology* **186**, 2182-2191

302. Foell, D., Wittkowski, H., Vogl, T., and Roth, J. (2007) S100 proteins expressed in phagocytes: a novel group of damage-associated molecular pattern molecules. *J Leukoc Biol* **81**, 28-37

303. Lim, S. Y., Raftery, M. J., and Geczy, C. L. (2011) Oxidative modifications of DAMPs suppress inflammation: the case for S100A8 and S100A9. *Antioxidants & redox signaling* **15**, 2235-2248

304. Anceriz, N., Vandal, K., and Tessier, P. A. (2007) S100A9 mediates neutrophil adhesion to fibronectin through activation of beta2 integrins. *Biochemical and biophysical research communications* **354**, 84-89

305. Simard, J. C., Girard, D., and Tessier, P. A. (2010) Induction of neutrophil degranulation by S100A9 via a MAPK-dependent mechanism. *J Leukoc Biol* **87**, 905-914

306. Zhao, J., Endoh, I., Hsu, K., Tedla, N., Endoh, Y., and Geczy, C. L. (2011) S100A8 modulates mast cell function and suppresses eosinophil migration in acute asthma. *Antioxidants & redox signaling* **14**, 1589-1600

307. Lim, S. Y., Raftery, M. J., Goyette, J., and Geczy, C. L. (2010) S-glutathionylation regulates inflammatory activities of S100A9. *The Journal of biological chemistry* **285**, 14377-14388

308. Kehl-Fie, T. E., Chitayat, S., Hood, M. I., Damo, S., Restrepo, N., Garcia, C., Munro, K. A., Chazin, W. J., and Skaar, E. P. (2011) Nutrient metal sequestration by calprotectin inhibits bacterial superoxide defense, enhancing neutrophil killing of Staphylococcus aureus. *Cell Host Microbe* **10**, 158-164

309. Korndorfer, I. P., Brueckner, F., and Skerra, A. (2007) The crystal structure of the human (S100A8/S100A9)2 heterotetramer, calprotectin, illustrates how conformational changes

of interacting alpha-helices can determine specific association of two EF-hand proteins. *Journal of molecular biology* **370**, 887-898

310. Balkwill, F. R., Capasso, M., and Hagemann, T. (2012) The tumor microenvironment at a glance. *Journal of cell science* **125**, 5591-5596

311. Ramasamy, R., Shekhtman, A., and Schmidt, A. M. (2016) The multiple faces of RAGE--opportunities for therapeutic intervention in aging and chronic disease. *Expert opinion on therapeutic targets* **20**, 431-446

312. Bresnick, A. R., Weber, D. J., and Zimmer, D. B. (2015) S100 proteins in cancer. *Nat Rev Cancer* **15**, 96-109

313. Bjork, P., Bjork, A., Vogl, T., Stenstrom, M., Liberg, D., Olsson, A., Roth, J., Ivars, F., and Leanderson, T. (2009) Identification of human S100A9 as a novel target for treatment of autoimmune disease via binding to quinoline-3-carboxamides. *PLoS Biol* **7**, e97

314. Pili, R., Haggman, M., Stadler, W. M., Gingrich, J. R., Assikis, V. J., Bjork, A., Nordle, O., Forsberg, G., Carducci, M. A., and Armstrong, A. J. (2011) Phase II randomized, double-blind, placebo-controlled study of tasquinimod in men with minimally symptomatic metastatic castrate-resistant prostate cancer. *Journal of clinical oncology : official journal of the American Society of Clinical Oncology* **29**, 4022-4028

315. Nijhuis, J., Rensen, S. S., Slaats, Y., van Dielen, F. M., Buurman, W. A., and Greve, J. W. (2009) Neutrophil activation in morbid obesity, chronic activation of acute inflammation. *Obesity (Silver Spring, Md.)* **17**, 2014-2018

316. Mortensen, O. H., Nielsen, A. R., Erikstrup, C., Plomgaard, P., Fischer, C. P., Krogh-Madsen, R., Lindegaard, B., Petersen, A. M., Taudorf, S., and Pedersen, B. K. (2009) Calprotectin--a novel marker of obesity. *PloS one* **4**, e7419

317. Nagareddy, P. R., Kraakman, M., Masters, S. L., Stirzaker, R. A., Gorman, D. J., Grant, R. W., Dragoljevic, D., Hong, E. S., Abdel-Latif, A., Smyth, S. S., Choi, S. H., Korner, J., Bornfeldt, K. E., Fisher, E. A., Dixit, V. D., Tall, A. R., Goldberg, I. J., and Murphy, A. J. (2014) Adipose tissue macrophages promote myelopoiesis and monocytosis in obesity. *Cell metabolism* **19**, 821-835

318. Catalan, V., Gomez-Ambrosi, J., Rodriguez, A., Ramirez, B., Rotellar, F., Valenti, V., Silva, C., Gil, M. J., Fernandez-Real, J. M., Salvador, J., and Fruhbeck, G. (2011)

Increased levels of calprotectin in obesity are related to macrophage content: impact on inflammation and effect of weight loss. *Molecular medicine (Cambridge, Mass.)* **17**, 1157-1167

319. Murphy, A. J., and Tall, A. R. (2016) Disordered haematopoiesis and athero-thrombosis. *European heart journal* **37**, 1113-1121

320. Monteiro, R., and Azevedo, I. (2010) Chronic Inflammation in Obesity and the Metabolic Syndrome. *Mediators of inflammation* **2010**

321. Sekimoto, R., Kishida, K., Nakatsuji, H., Nakagawa, T., Funahashi, T., and Shimomura, I. (2012) High circulating levels of S100A8/A9 complex (calprotectin) in male Japanese with abdominal adiposity and dysregulated expression of S100A8 and S100A9 in adipose tissues of obese mice. *Biochemical and biophysical research communications* **419**, 782-789

322. Averill, M. M., Kerkhoff, C., and Bornfeldt, K. E. (2012) S100A8 and S100A9 in cardiovascular biology and disease. *Arteriosclerosis, thrombosis, and vascular biology* **32**, 223-229

323. Cochain, C., and Zernecke, A. (2017) Macrophages in vascular inflammation and atherosclerosis. *Pflugers Archiv : European journal of physiology* **469**, 485-499

324. Ionita, M. G., Vink, A., Dijke, I. E., Laman, J. D., Peeters, W., van der Kraak, P. H., Moll, F. L., de Vries, J. P., Pasterkamp, G., and de Kleijn, D. P. (2009) High levels of myeloid-related protein 14 in human atherosclerotic plaques correlate with the characteristics of rupture-prone lesions. *Arteriosclerosis, thrombosis, and vascular biology* **29**, 1220-1227

325. Langley, S. R., Willeit, K., Didangelos, A., Matic, L. P., Skroblin, P., Barallobre-Barreiro, J., Lengquist, M., Rungger, G., Kapustin, A., Kedenko, L., Molenaar, C., Lu, R., Barwari, T., Suna, G., Yin, X., Iglseder, B., Paulweber, B., Willeit, P., Shalhoub, J., Pasterkamp, G., Davies, A. H., Monaco, C., Hedin, U., Shanahan, C. M., Willeit, J., Kiechl, S., and Mayr, M. (2017) Extracellular matrix proteomics identifies molecular signature of symptomatic carotid plaques. *The Journal of clinical investigation* **127**, 1546-1560

326. Ortega, F. J., Sabater, M., Moreno-Navarrete, J. M., Pueyo, N., Botas, P., Delgado, E., Ricart, W., Fruhbeck, G., and Fernandez-Real, J. M. (2012) Serum and urinary concentrations of calprotectin as markers of insulin resistance and type 2 diabetes. *European journal of endocrinology* **167**, 569-578

327. Peng, W. H., Jian, W. X., Li, H. L., Hou, L., Wei, Y. D., Li, W. M., and Xu, Y. W. (2011) Increased serum myeloid-related protein 8/14 level is associated with atherosclerosis in type 2 diabetic patients. *Cardiovascular diabetology* **10**, 41

328. Jin, Y., Sharma, A., Carey, C., Hopkins, D., Wang, X., Robertson, D. G., Bode, B., Anderson, S. W., Reed, J. C., Steed, R. D., Steed, L., and She, J. X. (2013) The expression of inflammatory genes is upregulated in peripheral blood of patients with type 1 diabetes. *Diabetes care* **36**, 2794-2802

329. Hirata, A., Kishida, K., Nakatsuji, H., Hiuge-Shimizu, A., Funahashi, T., and Shimomura, I. (2012) High serum S100A8/A9 levels and high cardiovascular complication rate in type 2 diabetics with ultrasonographic low carotid plaque density. *Diabetes research and clinical practice* **97**, 82-90

330. Croce, K., Gao, H., Wang, Y., Mooroka, T., Sakuma, M., Shi, C., Sukhova, G. K., Packard, R. R., Hogg, N., Libby, P., and Simon, D. I. (2009) Myeloid-related protein-8/14 is critical for the biological response to vascular injury. *Circulation* **120**, 427-436

331. Averill, M. M., Barnhart, S., Becker, L., Li, X., Heinecke, J. W., Leboeuf, R. C., Hamerman, J. A., Sorg, C., Kerkhoff, C., and Bornfeldt, K. E. (2011) S100A9 differentially modifies phenotypic states of neutrophils, macrophages, and dendritic cells: implications for atherosclerosis and adipose tissue inflammation. *Circulation* **123**, 1216-1226

332. Ryckman, C., Vandal, K., Rouleau, P., Talbot, M., and Tessier, P. A. (2003) Proinflammatory activities of S100: proteins S100A8, S100A9, and S100A8/A9 induce neutrophil chemotaxis and adhesion. *Journal of immunology* **170**, 3233-3242

333. Kerkhoff, C., Nacken, W., Benedyk, M., Dagher, M. C., Sopalla, C., and Doussiere, J. (2005) The arachidonic acid-binding protein S100A8/A9 promotes NADPH oxidase activation by interaction with p67phox and Rac-2. *FASEB J* **19**, 467-469

334. Viemann, D., Strey, A., Janning, A., Jurk, K., Klimmek, K., Vogl, T., Hirono, K., Ichida, F., Foell, D., Kehrel, B., Gerke, V., Sorg, C., and Roth, J. (2005) Myeloid-related proteins 8 and 14 induce a specific inflammatory response in human microvascular endothelial cells. *Blood* **105**, 2955-2962

335. Schiopu, A., and Cotoi, O. S. (2013) S100A8 and S100A9: DAMPs at the Crossroads between Innate Immunity, Traditional Risk Factors, and Cardiovascular Disease. *Mediators of inflammation* **2013**

336. Naiki, Y., Sorrentino, R., Wong, M. H., Michelsen, K. S., Shimada, K., Chen, S., Yilmaz, A., Slepenkin, A., Schröder, N. W. J., Crother, T. R., Bulut, Y., Doherty, T. M., Bradley, M., Shaposhnik, Z., Peterson, E. M., Tontonoz, P., Shah, P. K., and Arditi, M. (2008) TLR/MyD88 and LXRα Signaling Pathways Reciprocally Control Chlamydia Pneumoniae-Induced Acceleration of Atherosclerosis. *Journal of immunology* **181**, 7176-7185

337. Graves, D. T., and Kayal, R. A. Diabetic complications and dysregulated innate immunity. *Front Biosci* **13**, 1227-1239

338. Ohshita, K., Yamane, K., Hanafusa, M., Mori, H., Mito, K., Okubo, M., Hara, H., and Kohno, N. (2004) Elevated white blood cell count in subjects with impaired glucose tolerance. *Diabetes care* **27**, 491-496

339. Vozarova, B., Weyer, C., Lindsay, R. S., Pratley, R. E., Bogardus, C., and Tataranni, P. A. (2002) High white blood cell count is associated with a worsening of insulin sensitivity and predicts the development of type 2 diabetes. *Diabetes* **51**, 455-461

340. Chuah, Y. K., Basir, R., Talib, H., Tie, T. H., and Nordin, N. (2013) Receptor for Advanced Glycation End Products and Its Involvement in Inflammatory Diseases. *International Journal of Inflammation* **2013**

341. Brett, J., Schmidt, A. M., Yan, S. D., Zou, Y. S., Weidman, E., Pinsky, D., Nowygrod, R., Neeper, M., Przysiecki, C., Shaw, A., and et al. (1993) Survey of the distribution of a newly characterized receptor for advanced glycation end products in tissues. *The American journal of pathology* **143**, 1699-1712

342. Wan, H., Luo, F., Wert, S. E., Zhang, L., Xu, Y., Ikegami, M., Maeda, Y., Bell, S. M., and Whitsett, J. A. (2008) Kruppel-like factor 5 is required for perinatal lung morphogenesis and function. *Development* **135**, 2563-2572

343. Xu, H., Wan, H., Sandor, M., Qi, S., Ervin, F., Harper, J. R., Silverman, R. P., and McQuillan, D. J. (2008) Host response to human acellular dermal matrix transplantation in a primate model of abdominal wall repair. *Tissue Eng Part A* **14**, 2009-2019

344. Baeck, C., Wei, X., Bartneck, M., Fech, V., Heymann, F., Gassler, N., Hittatiya, K., Eulberg, D., Luedde, T., Trautwein, C., and Tacke, F. (2014) Pharmacological inhibition of the chemokine C-C motif chemokine ligand 2 (monocyte chemoattractant protein 1) accelerates liver fibrosis regression by suppressing Ly-6C(+) macrophage infiltration in mice. *Hepatology* **59**, 1060-1072

345. Bialkowska, A. B., Crisp, M., Bannister, T., He, Y., Chowdhury, S., Schurer, S., Chase, P., Spicer, T., Madoux, F., Tian, C., Hodder, P., Zaharevitz, D., and Yang, V. W. (2011) Identification of small-molecule inhibitors of the colorectal cancer oncogene Kruppel-like factor 5 expression by ultrahigh-throughput screening. *Molecular cancer therapeutics* **10**, 2043-2051

346. Yang, Y., Goldstein, B. G., Nakagawa, H., and Katz, J. P. (2007) Kruppel-like factor 5 activates MEK/ERK signaling via EGFR in primary squamous epithelial cells. *FASEB J* **21**, 543-550

347. Morris, V. A., Cummings, C. L., Korb, B., Boaglio, S., and Oehler, V. G. (2016) Deregulated KLF4 Expression in Myeloid Leukemias Alters Cell Proliferation and Differentiation through MicroRNA and Gene Targets. *Molecular and cellular biology* **36**, 559-573

348. Degos, L., and Wang, Z. Y. (2001) All trans retinoic acid in acute promyelocytic leukemia. *Oncogene* **20**, 7140-7145

349. Chanchevalap, S., Nandan, M. O., Merlin, D., and Yang, V. W. (2004) All-trans retinoic acid inhibits proliferation of intestinal epithelial cells by inhibiting expression of the gene encoding Krüppel-like factor 5. *FEBS letters* **578**, 99-105

350. Lafferty, M. J., Bradford, K. C., Erie, D. A., and Neher, S. B. (2013) Angiopoietin-like protein 4 inhibition of lipoprotein lipase: evidence for reversible complex formation. *The Journal of biological chemistry* **288**, 28524-28534

351. Doege, H., Baillie, R. A., Ortegon, A. M., Tsang, B., Wu, Q., Punreddy, S., Hirsch, D., Watson, N., Gimeno, R. E., and Stahl, A. (2006) Targeted deletion of FATP5 reveals multiple functions in liver metabolism: alterations in hepatic lipid homeostasis. *Gastroenterology* **130**, 1245-1258

352. Li, S., Nagothu, K., Ranganathan, G., Ali, S. M., Shank, B., Gokden, N., Ayyadevara, S., Megyesi, J., Olivecrona, G., Chugh, S. S., Kersten, S., and Portilla, D. (2012) Reduced kidney lipoprotein lipase and renal tubule triglyceride accumulation in cisplatin-mediated acute kidney injury. *American journal of physiology. Renal physiology* **303**, F437-448

353. Tan, N. Y., and Khachigian, L. M. (2009) Sp1 phosphorylation and its regulation of gene transcription. *Molecular and cellular biology* **29**, 2483-2488

354. Hu, P., Lai, D., Lu, P., Gao, J., and He, H. (2012) ERK and Akt signaling pathways are involved in advanced glycation end product-induced autophagy in rat vascular smooth muscle cells. *International journal of molecular medicine* **29**, 613-618

355. Avanzas, P., Arroyo-Espliguero, R., Cosin-Sales, J., Quiles, J., Zouridakis, E., and Kaski, J. C. (2004) Multiple complex stenoses, high neutrophil count and C-reactive protein levels in patients with chronic stable angina. *Atherosclerosis* **175**, 151-157

356. Rotzius, P., Thams, S., Soehnlein, O., Kenne, E., Tseng, C.-N., Björkström, N. K., Malmberg, K.-J., Lindbom, L., and Eriksson, E. E. (2010) Distinct Infiltration of Neutrophils in Lesion Shoulders in ApoE(−/−) Mice. *The American journal of pathology* **177**, 493-500

357. Mirigian, M., Mukherjee, K., Bane, S. L., and Sackett, D. L. (2013) Measurement of in vitro microtubule polymerization by turbidity and fluorescence. *Methods in cell biology* **115**, 215-229

358. Davidson, D., and Patel, H. (2014) Cytokine-induced neutrophil chemotaxis assay. *Methods Mol Biol* **1172**, 107-113

359. Dai, Y., Kennedy-Darling, J., Shortreed, M. R., Scalf, M., Gasch, A. P., and Smith, L. M. (2017) Multiplexed Sequence-Specific Capture of Chromatin and Mass Spectrometric Discovery of Associated Proteins. *Analytical chemistry* **89**, 7841-7846